NASA CR 174938

(NASA-CR-174938) DETAILED STUDIES OF AVIATION FUEL FLOWABILITY Final Report (Boeing Commercial Airplane Co.) 95 p HC A05/MF A01 CSCL 21D N85-31308 Unclas G3/28 21895

Detailed Studies of Aviation Fuel Flowability

Final Report

H. K. Mehta and R. S. Armstrong

Boeing Commercial Airplane Company
Seattle, Washington

Prepared for
NASA-Lewis Research Center
Under Contract NAS3-24081

NASA
National Aeronautics and Space Administration

1985

NASA CR 174938

Detailed Studies of Aviation Fuel Flowability

Final Report

H. K. Mehta and R. S. Armstrong

Boeing Commercial Airplane Company
Seattle, Washington

TABLE OF CONTENTS

PRECEDING PAGE BLANK NOT FILMED

LIST OF TABLES

LIST OF FIGURES

LIST OF FIGURES (CONCLUDED)

1.0 SUMMARY

An experimental program was conducted under NASA Contract NAS3-24081 to study the fuel flowability behavior at low temperatures, near or below the fuel freezing point, for several aviation fuels of various composition. The main objective of the study was to extend previously gained knowledge and correlate the effects of heat transfer rates, fuel temperature profiles, and dynamic conditions on the fuel flowability.

The tests were conducted in a simulator tank that modeled a section of a wing tank of a wide-body commercial airplane. The tank, with a 190L fuel capacity, was cooled by circulating coolants in the upper and lower chambers to emulate aerodynamic cooling of aircraft wing tanks. During and after the tests, visual observations of the fuel cooling process were made through view windows on two sides of the insulated tank. Provisions for a controlled withdrawal of fuel, slosh, vibration, and external heating and recirculation were made to study various aspects of the flowability characteristics. Six fuels with varying composition and flowability characteristics were tested, all of which met the commercial Jet A freezing point specification. The most useful data included vertical temperature profile histories from five different racks, the unpumpable fuel or holdup measured at the end of each test, and recirculating fuel temperatures under a variety of test conditions. In addition, the performance of several flow improver additives was also evaluated.

In tests called static holdup tests, each fuel was chilled with the tank skin temperatures maintained at 10°C below the fuel freezing point for varying periods of time. At the end of chilling period, the fuel was withdrawn and the unpumpable fuel quantity or holdup was determined. The holdup ranged from 0 to 13.5% depending on fuel type and chill period. Holdup was correlated to the boundary layer fuel temperature measured at 0.6 cm above the bottom skin. These tests showed that the flowability of fuel at low temperature depends on its composition. The behavior of the six fuels fell into three distinct groups when the fuel freezing point was included in the correlations.

Tests with a combination of dynamic conditions showed that tank vibration, slosh, or rate of fuel pumpout had minor, if any, effects on either the thermal profiles or the holdup.

In flight simulation tests, the tank skin temperatures were programmed in accordance with temperature histories for extreme cold day flights. Holdup with any fuel did not exceed 5% in these tests. Holdup was further reduced when there was an ullage space and the tank upper skin was unwetted. No holdup occurred when the last phase of the flight simulation had skin temperatures increasing to simulate the descent warmup.

External fuel heating and recirculation tests were intended to evaluate the effectiveness of this method in improving the flowability. Results showed that a moderate heat input reduced holdup by modifying the thermal boundary layer. Fuel heating was equally effective when delayed, that is, initiated later in flight after the fuel attained a minimum temperature.

The addition of flow improvers to the fuel is an alternative to fuel heating. Tests showed that the additives reduced holdup. However, the additives were not optimized for jet fuel improvement, and the percentage reduction in holdup for the two additives tested was less than in moderate external heat input tests.

In general, this experimental program provided extensive data and useful correlations that will add to the understanding of aviation fuel flowability in cold environments similar to those experienced in practice.

2.0 INTRODUCTION

In this report, results of an experimental investigation performed by the Boeing Commercial Airplane Company, under the NASA Contract NAS3-24081, titled "Detailed Studies of Aviation Fuel Flowability at Low Temperatures," are presented. This investigation was aimed at providing a wider data base on fuel flowability at low temperatures near the freezing point in simulated aircraft-operational conditions.

The uncertainty of the world supply of hydrocarbon fuel, coupled with the increased demand for the middle distillates from which jet fuel is derived and crude oil price increases of the past years, made it necessary to consider the methods of increasing the yield of jet fuel from middle distillates. Even though the petroleum crude supply situation presently has eased, there is a continuing concern to maximize fuel availability in the face of limited choice of crude type. Refining jet fuels with broader boiling range and compositional tolerances may become advantageous. Jet fuel is a blend of hydrocarbons that can be manufactured from any of the available fossil sources, including shale oil and coal liquids as well as petroleum. If the boiling range of this blend is broadened to reduce processing cost and complexity, the result may be a fuel with a higher freezing point than the current standard.

High-freezing-point fuels pose problems such as potential line blockage and poor pumpability, especially for long-range flight over polar routes, because of severity of aerodynamic cooling of the fuel. Hydrocarbon fuels change phase from liquid to solid over a range of temperatures. As the fuel temperature decreases, fine particles of solidified wax crystals appear, which increase in size and concentration with further cooling. Fuel systems do not perform reliably when required to move this semisolid slurry from the tank to the engine. The NASA-Lewis Research Center has sponsored a number of studies to determine this low temperature fuel flowability and its effects on the fuel system performance. The loss in the performance of the fuel system can be conveniently determined by measuring the holdup, or the unpumpable fuel retained in the tank upon otherwise complete withdrawal (refs. 1 to 3).

In previous studies, a general approach has been to use a scale model of a wide-body aircraft outboard wing tank. A variety of fuels having differing compositions and freezing points have been subjected to various thermodynamic simulations to develop a data base and a set of correlations. Boeing conducted a test program to study fuels near or below their freezing point (ref. 3) in which Jet A and No. 2 diesel fuels were used in the fuel tank thermal simulator. It was found that hydrocarbon fuels cooled to temperatures near or just below the ASTM D2386 freezing point flowed readily. Significant free-floating and precipitated solid wax particles were observed under quiescent cooling conditions, but they did not inhibit fuel flow. There also was considerable thermal stratification of fuel, depending upon cooling rate and wetted-area geometry. Fuel recirculation with heating superimposed on tank cooling resulted in significantly higher bulk fuel temperature and little or no wax formation. A similar Lockheed study sponsored by NASA-LeRC (refs. 4 and 5) concluded that suspended solids do not clog the pump screen. It was also found that in high holdup tests, liquid fuel was trapped in the matrix of frozen fuel crystals and could not be dislodged by manual sloshing. A second study by Lockheed for NASA-LeRC (refs. 6 and 7) employed external fuel heating and recirculation and found bulk fuel temperature elevation as anticipated. However, heating had a small effect on the fuel temperature within the thermal boundary layer. Holdup was lower in these tests than in comparable unheated tests. The effect of flow improver additives as an alternative to fuel heating was found to be more significant in reducing holdup in fuels that would otherwise produce medium to large holdups than those that would produce small holdup without the additives.

In this investigation, the data bases of the previous studies were expanded to cover a realistic range of conditions. The study fuels all met the Jet A freezing-point specification, but the fuels differed in composition and implied flowability behavior. Tests evaluated holdup at static conditions, the effects of dynamic conditions such as slosh and vibration, the effects of extreme cold day flight simulations with and without the last warmup leg, the holdup reduction and thermal boundary layer modification due to external heating and recirculation, and the flowability improvement due to additives. It is believed that the extensive data base created by this investigation will add to the understanding of fuel flowability for existing aviation fuels and for fuels derived from sources other than petroleum, viz., oil shale, coal, and tar sand.

This report encompasses detailed descriptions of the test apparatus, procedures, and presentations of typical data and photographs, followed by interpretations and discussions of results and conclusions.

3.0 APPARATUS

This section describes the test facilities and equipment used in this investigation, located in the Propulsion Laboratory at Boeing Field in Seattle.

3.1 FUEL TANK SIMULATOR

A photograph of the overall setup is shown in Figure 1, and a schematic is shown in Figure 2. The simulator models a wing fuel tank in a commercial wide-body airplane. Such fuel tanks have large lateral dimensions compared to vertical dimensions. Heat transfer to the fuel tank is thus almost exclusively in the vertical dimension. This is modeled in the simulator tank by insulating the sidewalls heavily and controlling the upper and lower skin temperatures. Fuel cooling or heating on the horizontal surfaces of the tank is obtained by passing a water-methanol solution through two flat-plate heat exchangers, the inner surfaces of which form the top and bottom surfaces of the tank. The outer surfaces of the heat exchangers are insulated to minimize heat transfer to the surroundings. The water-methanol solution may be either chilled by liquid nitrogen or heated by a steam heat exchanger.

3.1.1 Test Tank

Figure 3 is a sketch of the test tank in plan view, and Figure 4 shows a crosssection looking from one of the view window sides. Figure 5 is a photograph showing the internal construction and thermocouple installations. The basic apparatus has been used for the previous studies described in References 3, 8, and 9, but for this investigation the tank was modified by removal of an internal boost pump, tubing, and a baffle. The internal dimensions of the 6061-T6 aluminum alloy tank are 53-cm high by 76-cm wide by 51-cm deep, resulting in a volume of 190L (50 gal). Modeling of important vertical dimensions of the inboard section of the 747 outboard main tank is full scale.

Upper and lower stringers are constructed from two aluminum alloy angle extensions bolted together to form Z sections 7.6-cm (3.0-in) high. These stringers are heat transfer paths and are essential to proper simulation. Each Z stringer has a 1.9- by 4.5-cm elliptical fuel transfer opening ("limber hole") to allow fuel flow to the boost pump inlet.

The tank bottom has two drain holes as shown in Figure 3, one leading to the external boost pump, the other to a gravity drain. A 2.54-cm (1-in)-dia tank vent tube with an inlet near the tank upper skin is routed through the side of the tank to a point above the highest fuel level of the tank. The tube is terminated at a fitting connected to the liquid nitrogen heat exchanger vapor discharge duct to reduce moisture intake during fuel withdrawal. Two doublepane viewing ports made of Lexan are located on opposite vertical sides of the tank. Dry nitrogen gas is circulated between the outer and inner panes of the viewing surfaces, thereby minimizing vapor or ice formation on the windows.

3.1.2 Test Tank Cooling and Heating System

As discussed above, the top and bottom surfaces of the tank simulator are heat exchangers through which a water-methanol mixture is pumped. A schematic of the cooling system is shown in Figure 6. The flow rate through each skin, controlled by valves, is measured by turbine flowmeters. An air-driven vane-type pump circulates the water-methanol

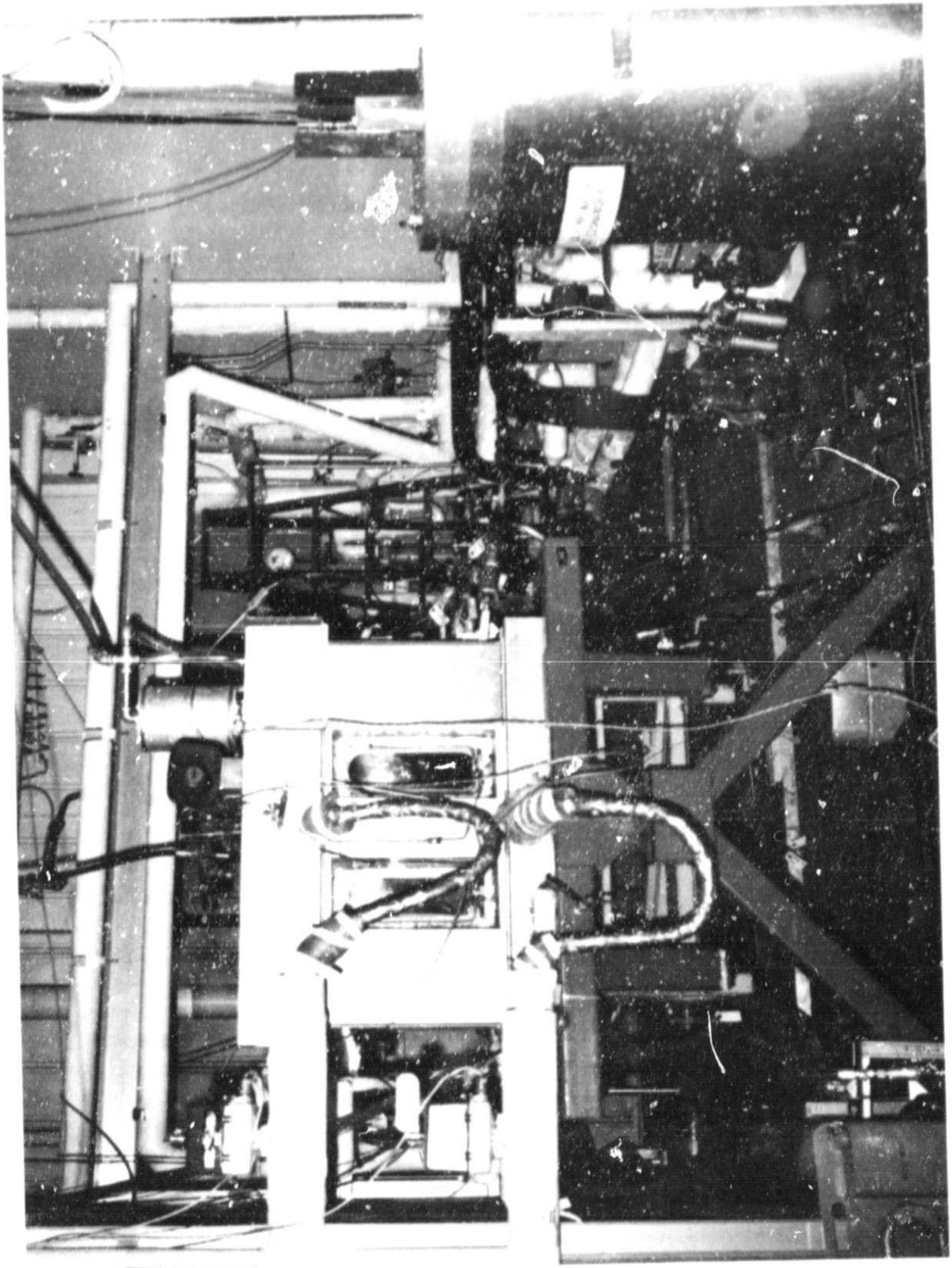

Figure 1. Fuel Tank Thermal Simulator

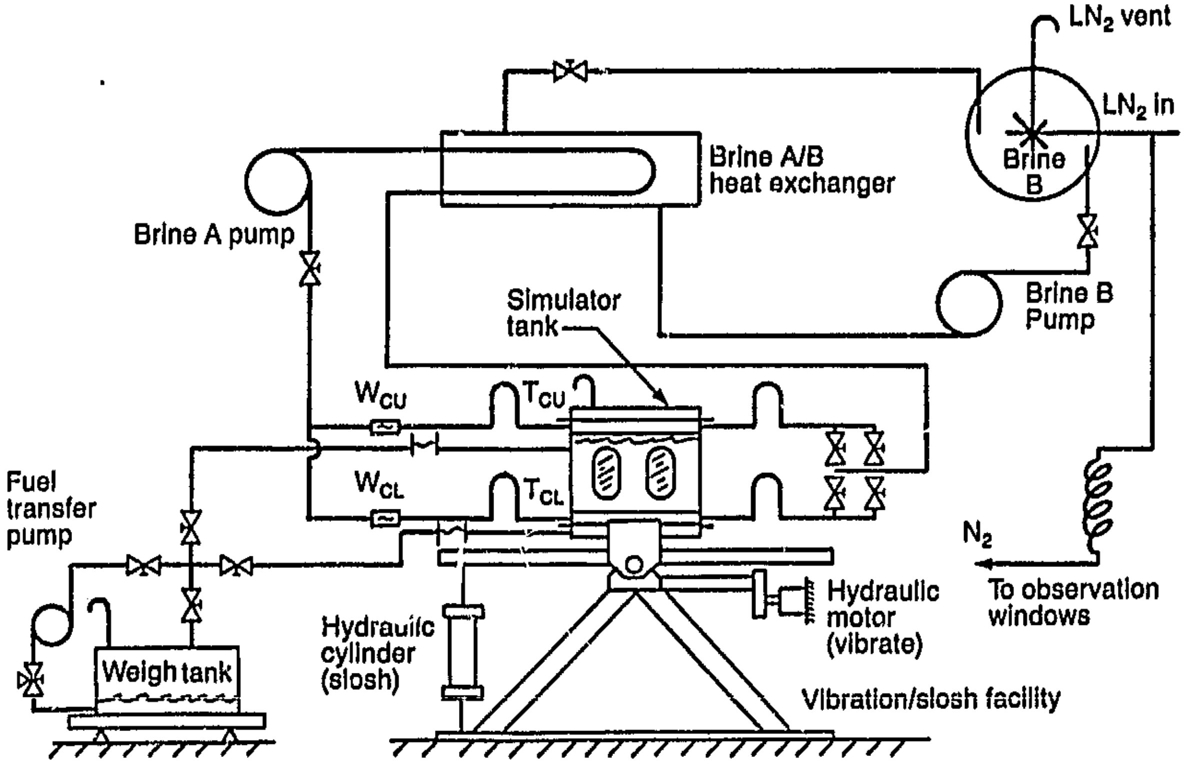

Notes: Brine refers to water/methanol solution

W_{CU} = Flow to upper coolant plate

W_{CL} = Flow to lower coolant plate

T_{CU} = Upper coolant temperature

T_{CL} = Lower coolant temperature

Figure 2. Fuel Tank Thermal Simulator Schematic

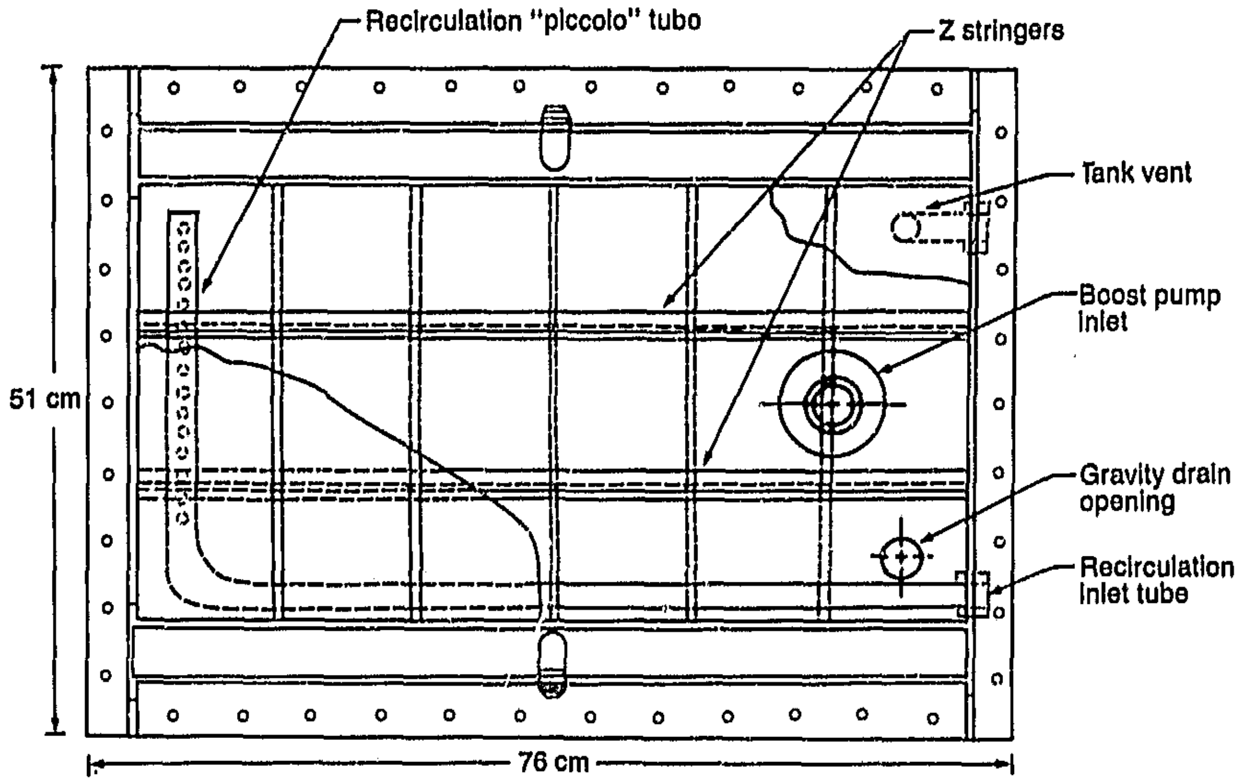

Figure 3. Thermal Simulator Tank Plan View

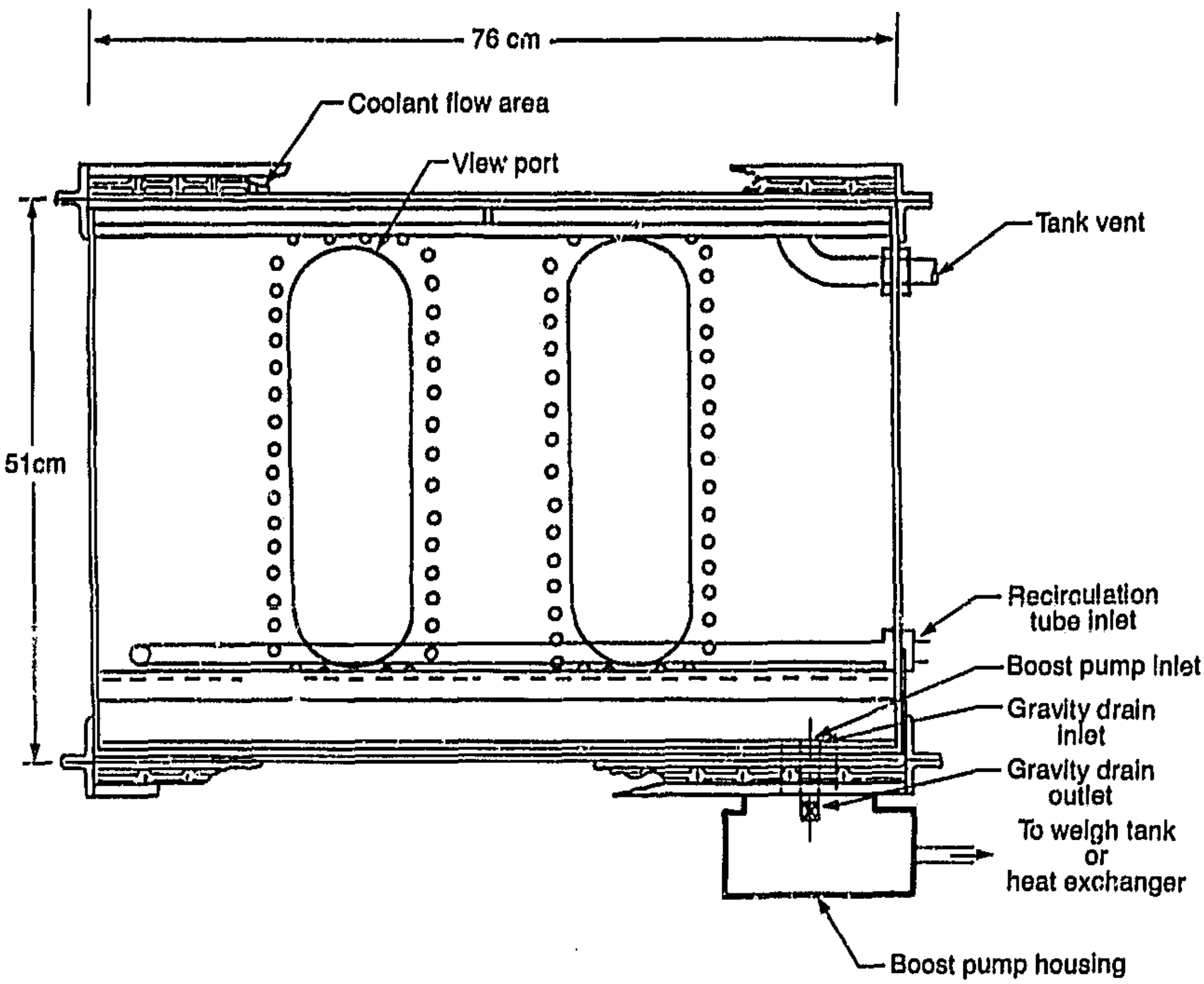

Figure 4. Cross-Sectional Front View of the Thermal Simulator Tank

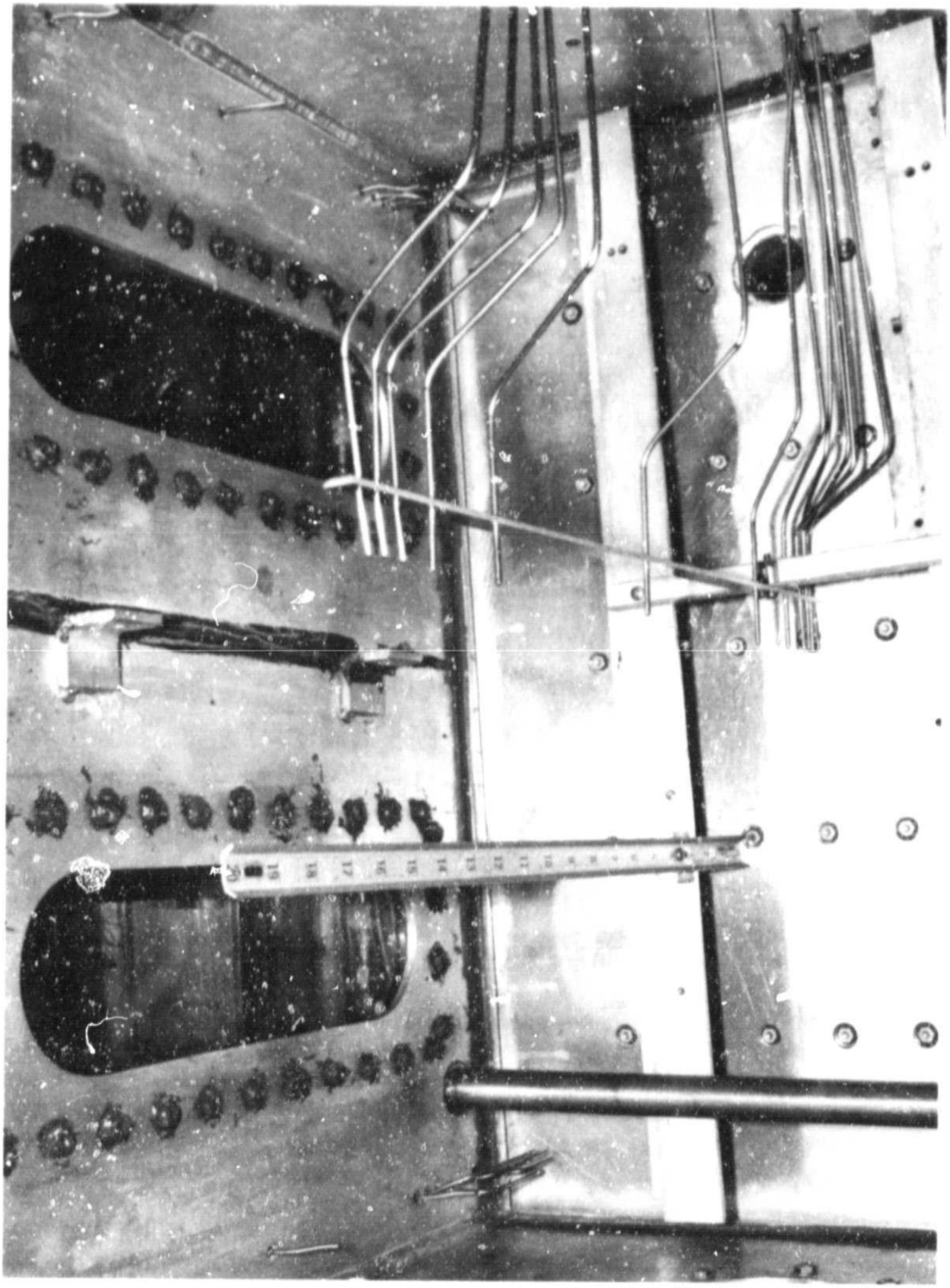

Figure 5. Internal View of the Simulator Tank

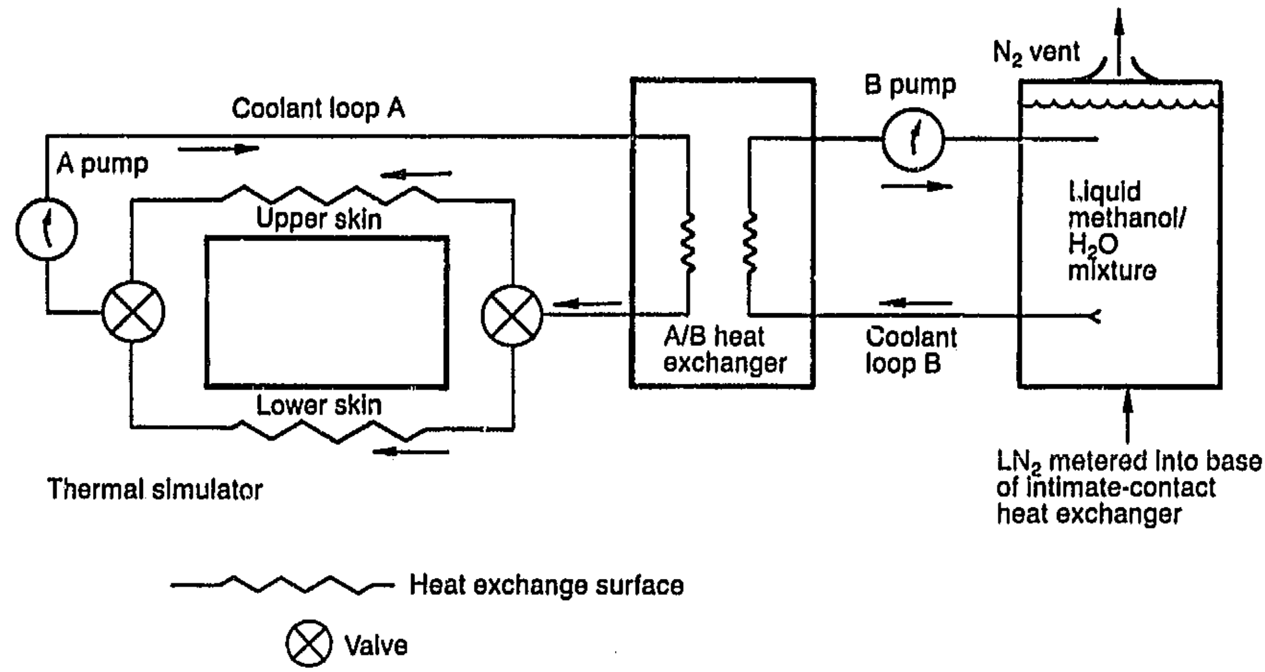

Figure 6. Fuel Tank Thermal Simulator Coolant Flow Schematic

mixture in closed loop A over the upper and lower outside tank surfaces and then through a conventional double-pass stainless-steel shell-and-tube heat exchanger. Coolant in loop B flows through the same double-pass heat exchanger and is cooled by a controlled flow of liquid nitrogen in an intimate-contact vat-type heat exchanger. The liquid nitrogen is introduced directly into the coolant, where it absorbs energy as it changes phase. The nitrogen vapor then passes out of the heat exchanger to the atmosphere.

The fuel tank thermal simulator features automatic control of upper and lower skin temperatures. Control is achieved by a probe that senses skin temperature for comparison with the desired temperature versus time schedule. Constant or varying schedules up to 11.5-hr long may be specified. A steam heat exchanger is incorporated in loop A for controlled warming of the tank skin in certain flight simulations.

3.1.3 Slosh and Vibration Table

The test tank is mounted on a slosh and vibration table as shown in Figure 1. Figures 7 and 8 show the vibrator hydraulic drive motor and the slosh hydraulic actuator. The vibrator eccentric weights are set to displace the simulator approximately ±0.05 mm at 53 Hz (1.5 g acceleration). The slosh table has a maximum travel of ±15 deg at 0.33 Hz.

3.1.4 Fuel Withdrawal Pump

An electrically operated boost pump capable of delivering fuel at rates between 0 and 30 L/min is housed in a small insulated chamber outside the simulator tank, as shown in Figures 4 and 9. A large-area 4-mesh/in screen is used to cover the inlet to the pump. The discharge of the pump is routed in such a way that it can be either collected into a weigh tank or recirculated back into the simulator tank. Instrumentation in the discharge system provides measurement of electrical power input to the pump, flow discharge pressure, and fuel withdrawal rate. A weigh tank mounted on a load cell also can provide data to calculate fuel withdrawal rate.

3.2 EXTERNAL FUEL HEATING AND RECIRCULATION SYSTEM

An external fuel heating system was designed for the heated fuel tests. The main component of this system is a lubricating oil-to-fuel, shell-and-tube heat exchanger, a schematic of which is shown in Figure 10. A secondary heat exchanger is used to heat the engine lubricating oil through electrical cartridge elements. For heated fuel tests, the boost pump withdraws fuel from the simulator tank and circulates it through the oil-fuel heat exchanger. Recirculated fuel is evenly distributed across the tank through a perforated "piccolo" tube with holes facing downward. Fuel and oil flow rates are measured by venturi flowmeters and governed by control valves. The electrical heat input rate is maintained at desired level by a variable transformer (variac).

Measurements include temperatures of fuel leaving and entering the test tank and oil temperatures. The system is designed so that the regulated heat input can vary up to 1500W. The fuel and oil flow rates through the system are variable in the range 0 to 5 L/min.

Figure 7. Vibrator Hydraulic Drive Motor

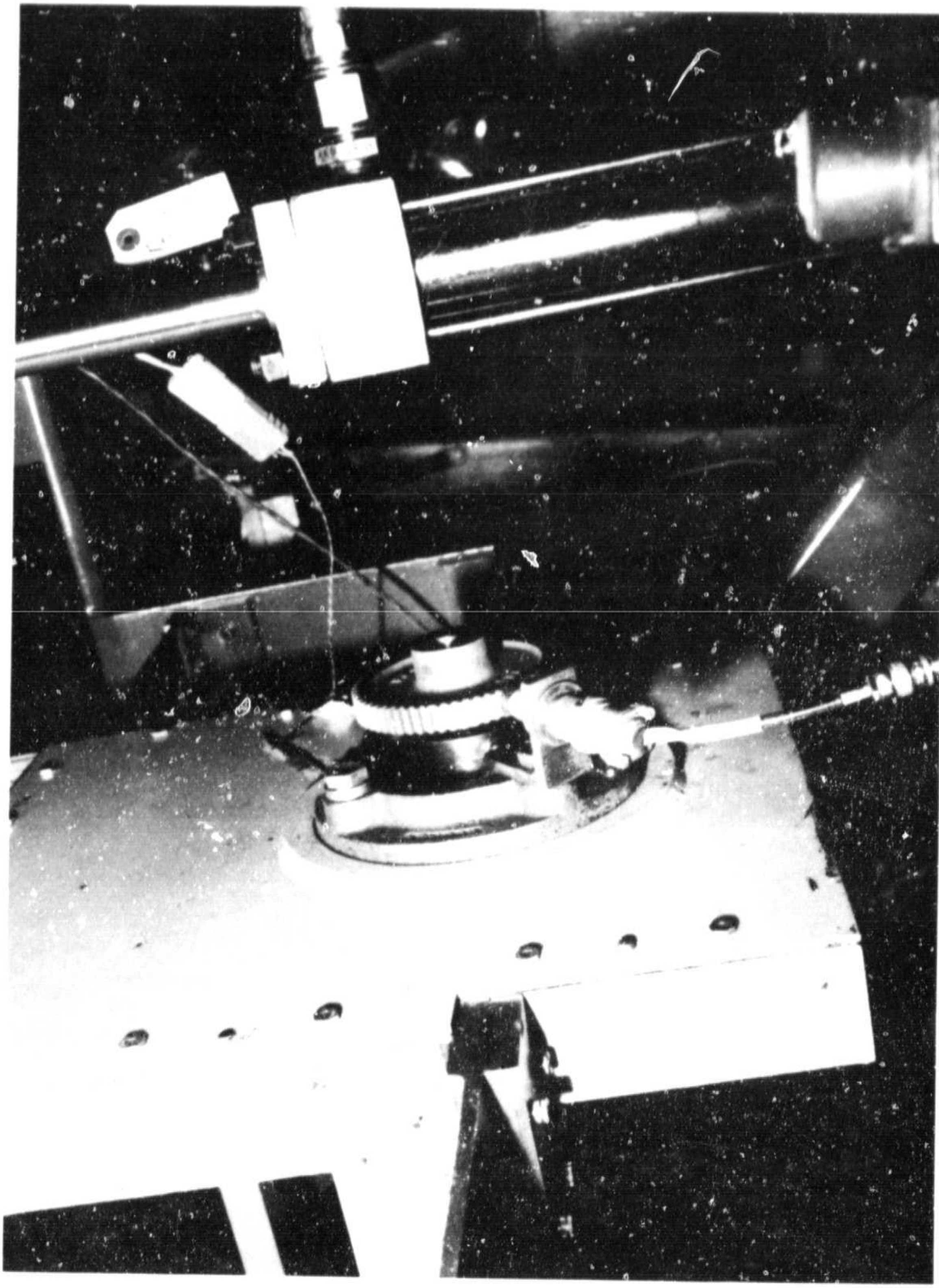

Figure 8. Slosh Hydraulic Actuator

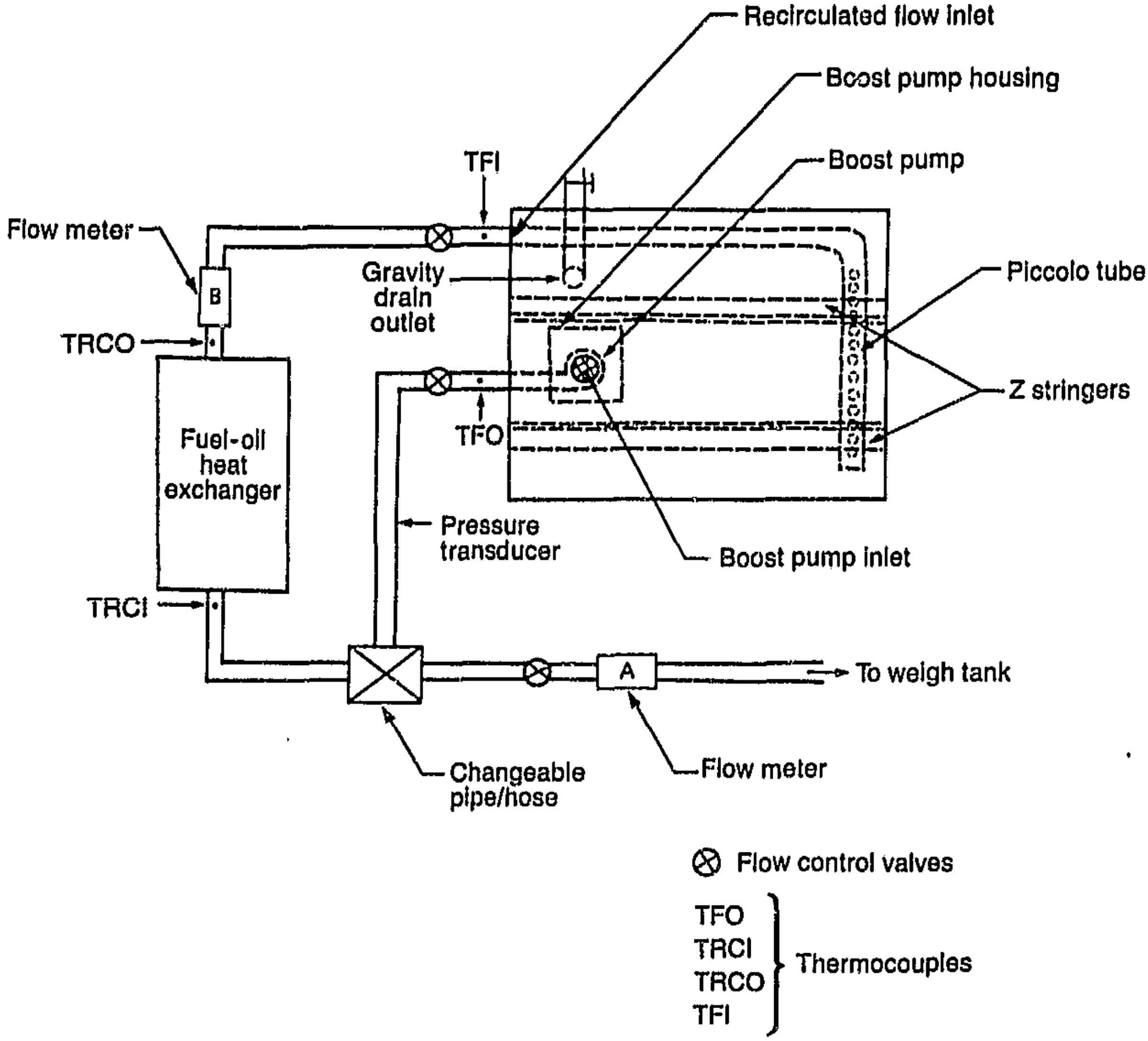

Figure 9. Tank Discharge System Schematic

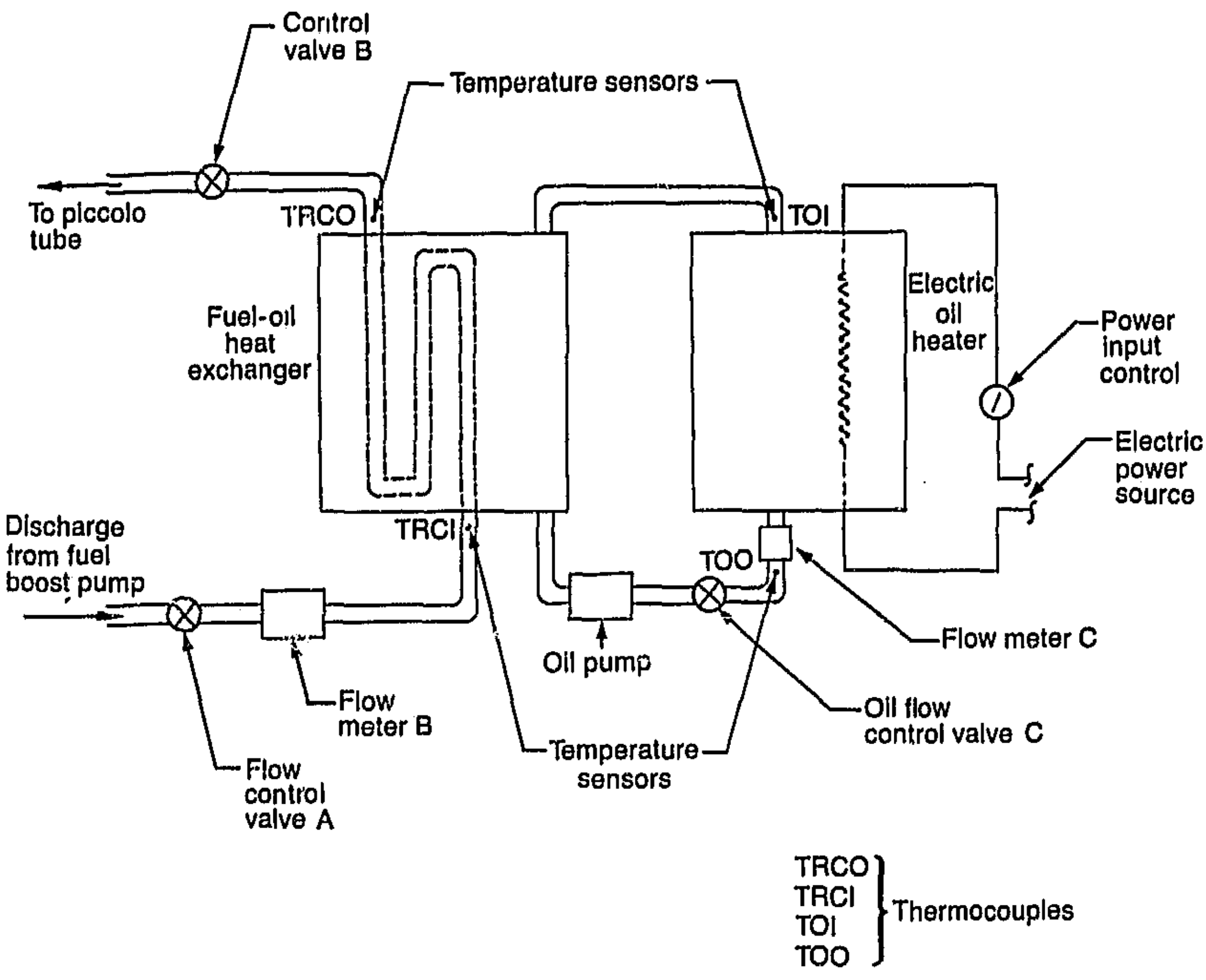

Figure 10. External Fuel Heating System Schematic

3.3 INSTRUMENTATION

The vertical fuel temperature profiles and mass holdup were the important measurements throughout the test program. Other measurements included fuel recirculation and withdrawal rates, chilling rates, external heat input to fuel, and slosh and vibration amplitude and frequencies.

3.3.1 Temperature Measurement

An array of 48 thermocouple probes is used for determination of fuel temperature profiles. These are distributed in five vertical racks, one in the center of the test tank and one in each corner as shown in Figure 11. All thermocouples are type K (chromel/alumel) with premium-grade wire, certified accurate within ±1°C by the Boeing Flight Test Instrumentation Laboratory. Two more thermocouples are provided to measure tank top and bottom skin temperatures. In addition, the simulator cooling system includes a temperature sensor in each of the lines supplying coolant to the top and bottom surfaces of the tank, a third sensor located in the line connecting the liquid nitrogen (LN_2)-coolant heat exchanger to the double-pan heat exchanger, and a fourth sensor immersed directly into the LN_2-coolant mixture in the heat sink. The external heating and recirculation system has six temperature probes as shown in Figure 10.

3.3.2 Fuel Mass Holdup Measurement

The fuel mass holdup is determined from initial, final, and postpumpout mass measurements in the weigh tank suspended from a load cell. The load cell is a strain gage type with an accuracy of ±0.454 kg (1 lb). The weigh tank-load cell system can be elevated in a guide rail assembly by a hydraulic drive for gravity fueling of the test tank.

3.3.3 Other Measurements

Three flowmeters are indicated in Figures 9 and 10, and there are, in addition, three others in the simulator chilling system. The flowmeters are turbine-type with a stated accuracy of ±1% of full scale. They are calibrated on a Propulsion Laboratory flow bench with accuracy traceable to the National Bureau of Standards.

Four accelerometers are placed on the outside of the fuel tank, as shown in Figure 12, to monitor vibration displacement. A CEC 117 vibration meter measures the vibration level.

3.4 DATA ACQUISITION SYSTEM

The essential component of the data acquisition system is a scanner with 60 channels of low-level relay actuators and 10 programmable relay actuators for control applications. Other components include a desktop computer, recorders, data storage, and conditioners. Research, Inc., Model FGE5510 drum programmers are used to generate signals for simulating a mission schedule. These are connected to motor-operated valves controlling the flow of coolant or steam by inhouse-fabricated interfaces.

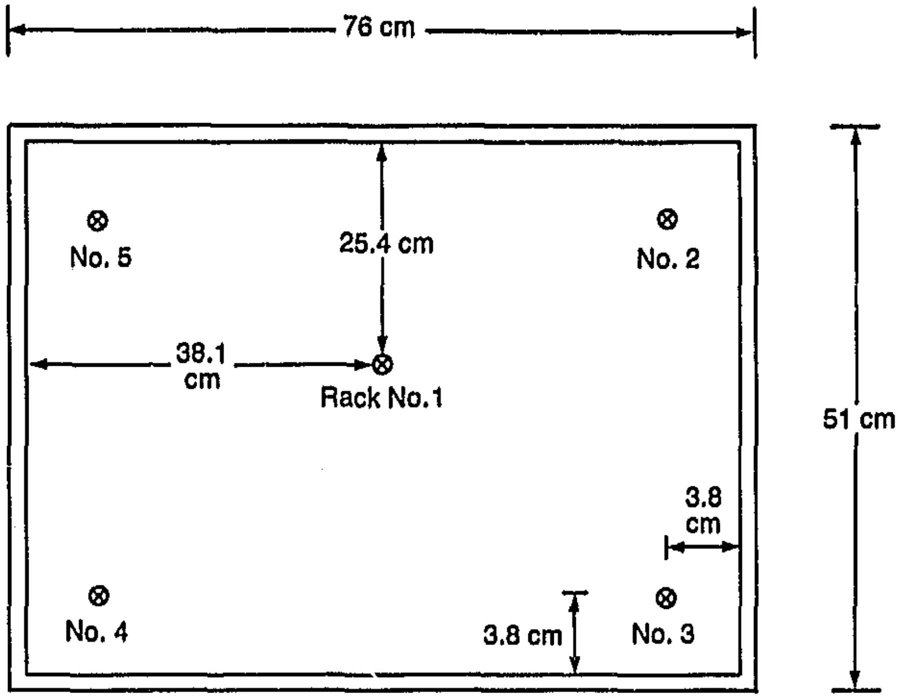

Plan view

Thermocouple locations Height above bottom (cm)	(in)	Thermocouple identifiers Rack 1	Rack 2	Rack 3	Rack 4	Rack 5
0	0	1	13	21	29	39
0.60	0.25	2			30	40
1.27	0.50	3	14	22	31	41
2.54	1.00	4	15	23	32	42
5.08	2.00	5				
10.16	4.00	6	16	24	33	43
25.40	10.00	7	17	25	34	44
40.64	16.00	8	18	26	35	45
45.72	18.00	9				
48.26	19.00	10	19	27	36	46
49.53	19.50	11			37	47
50.80	20.00	12	20	28	38	48

Identification

Figure 11. Fuel Tank Thermocouple Locations

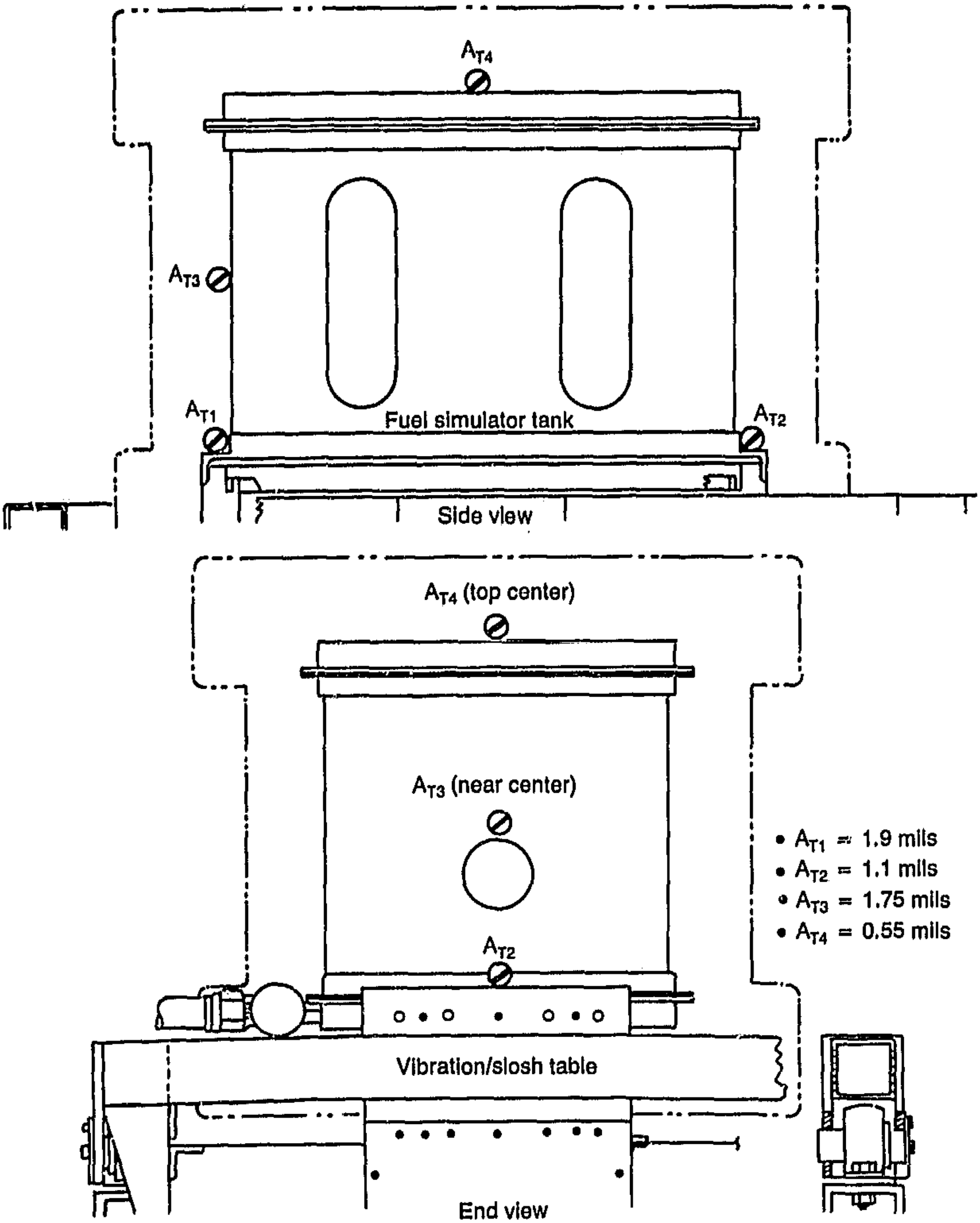

Figure 12. Accelerometer Locations

4.0 TEST PROCEDURES

This section describes the fuels used in the investigation and the procedures used for the tests.

4.1 TEST FUELS

Table 1 lists the main characteristics of the six fuels used in this study. Four fuels, designated LFPA-1 through LFPA-4, were experimental fuels purchased by NASA for this study. These fuels were each blended from the same base kerosene stock with additions of varying amounts of normal paraffin (wax) components. Figure 13 shows the distillation characteristics of all fuels. LFPA-1 through LFPA-4 have nearly identical distillation curves; their different characteristics are the result of the wax contents. The other two fuels, LFP-9 (ref. 4) and LFP-11 (refs. 5 and 6) are lower-wax kerosene fuels used in previous low-temperature studies.

The following characterization tests were performed on the fuels by the Fuels and Lubricants division of the Boeing Materials Technology Laboratory, Renton, WA.

1. Specific gravity at 15.5° and 0°C - ASTM D 1298
2. Viscosity at -20°C - ASTM D 445-74
3. Freezing point - ASTM D 2386
4. Pour point - ASTM D 97 modified to 1°C interval of measurement
5. Distillation - ASTM D 86
6. Water content - (Karl Fischer) ASTM D 1744-64

LFPA-3 was selected as the reference fuel for the first series of tests. All six fuels meet the ASTM D 1655 Jet A freezing point limit of -40°C. The fuels differ in their normal paraffin (wax) contents. The data for n-paraffin contents listed in Table 1 were determined by gas chromatography at the NASA-Lewis Research Center. The n-paraffin content of LFP-9 was reported as 20.6% in an earlier independent measurement shown in the appendix of Reference 4. Discrepancies of several percent may be typical of the reproducibility of these measurements.

4.2 STATIC TESTS

In these tests, the fuel was cooled in the simulator tank under static conditions. The fuel was first loaded in the weigh tank, an initial mass reading was recorded, and then the simulator tank was loaded by gravity flow from the elevated weigh tank. The difference between the weigh tank readings before and after fueling ascertained the initial fuel quantity in the test tank. During the chilldown, the upper surface of the simulator tank was kept wetted through a four-liter overflow tube above the top surface of the tank. This tube itself was kept full by filling it from the weigh tank whenever necessary. In most static tests the simulator skin temperatures were controlled automatically to reach predetermined values (usually 10°C below the freezing point of the fuel) as fast as possible and to maintain them for the remaining cooling phase. The fuel bulk temperature was thus determined by the duration of the cooling phase. At the end of the cooling phase, another mass reading was recorded to

Table 1. Characteristics of Test Fuels

Test method	LFPA-1	LFPA-2	LFPA-3	LFPA-4	LFP-9	LFP-11
Distillation ASTM D 86						
IBP	154.4°C	153.3	160.0	160.0	172.2	160.0
Volume recovered 10%	189.4	187.8	186.7	187.8	188.9	184.4
20%	192.8	192.8	192.8	193.3	195.0	195.6
50%	202.2	202.2	202.2	204.4	211.1	224.4
90%	225.6	224.4	225.6	228.3	238.9	262.8
FBP	243.9	245.6	246.7	248.9	257.8	277.8
Specific gravity ASTM D 1298-67 15.6°C/15.6°C	0.8060	0.8023	0.7967	0.7957	0.8010	0.8328
ASTM D 941-55 0°C/0°C	0.8180	0.8130	0.8010	0.8050	0.8089	0.8405
Viscosity ASTM D 445-74 at 20°C	4.57 cs	4.65 cs	4.57 cs	4.68 cs	5.09 cs	7.09 cs
Freezing point ASTM D 2386	–46.1°C	–44.7°C	–42.8°C	–41.1°C	–45.0°C	–47.0°C
Pour point ASTM D 97	–51°C	–51°C	–43°C	–42°C	–46°C	–59°C
Water content ASTM D1744-64	30 ppm	29 ppm	22 ppm	25 ppm	26.6 ppm	27.5 ppm
Normal paraffins by gas chromatography	19.4 wgt %	20.8 wgt %	32.7 wgt %	43.8 wgt %	15.5 wgt %	7.5 wgt %

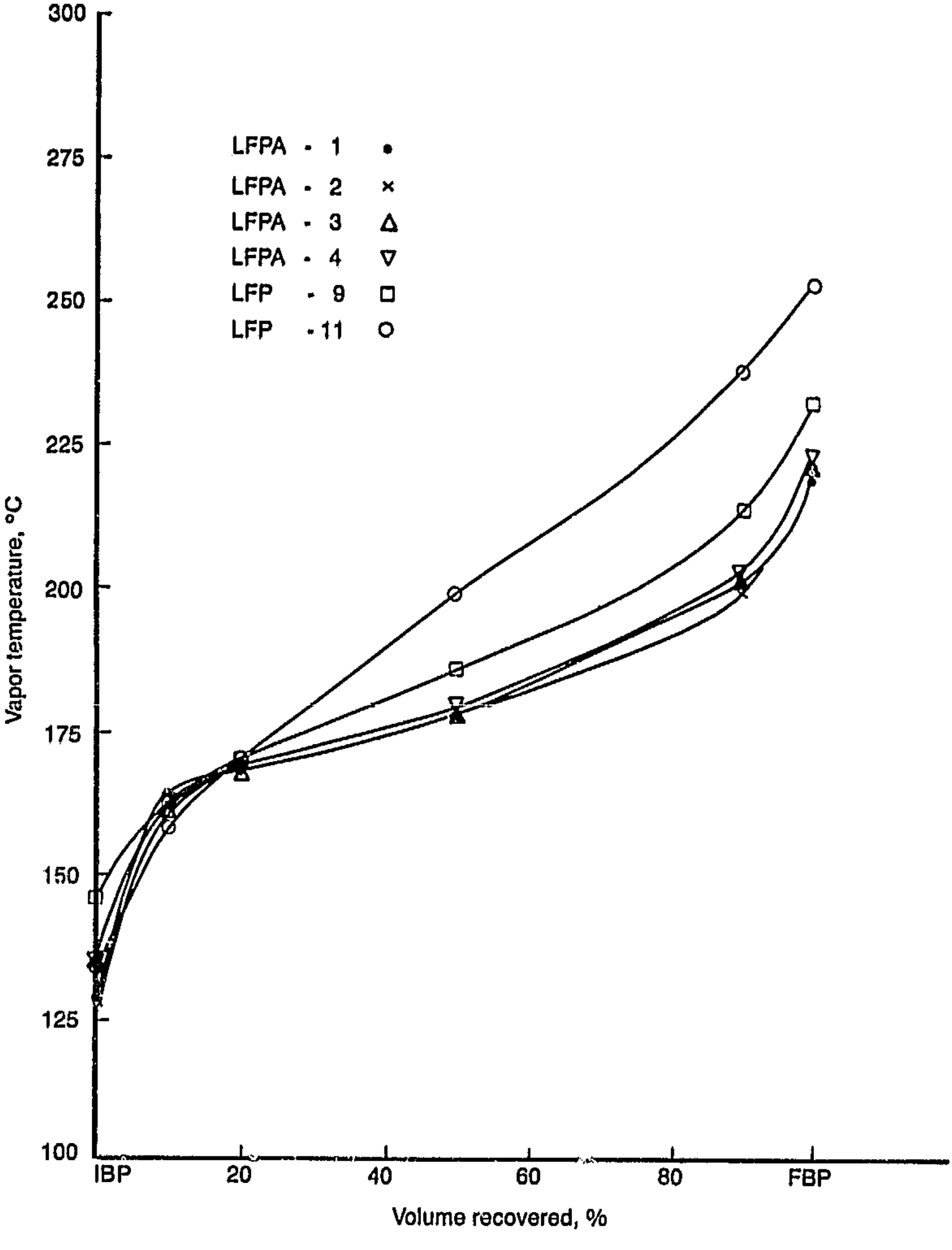

Figure 13. Distillation Characteristics of Test Fuels ASTM D 86

calculate the final quantity of fuel in the tank. The fuel was then pumped out into the weigh tank. After the pumpout, any fuel remaining in the tank was drained using the gravity drain outlet and returned to the weigh tank. The final mass of the weigh tank enabled determination of the mass holdup. The holdup consisted of frozen fuel and liquid slurry that could not flow to the pump inlet or gravity drain. This fuel thawed and was collected the next day, weighed separately on a balance, and then returned to the weigh tank. After each test, photographs of the interior of the test tank were taken to document holdup details. Notes of visual observations were also kept. Data were recorded automatically every 15 min during the chilldown phase and every 5 min during the pump out.

4.3 DYNAMIC TESTS

In these tests, either vibrations or slosh were superimposed upon the tank during the cooling phase. The vibration frequency was maintained at 53 Hz with amplitudes of about 0.03 mm. The slosh simulation followed the cycle shown in Figure 14. This was based on flight data typical of large transport airplanes. For slosh simulations, the tests were conducted with the upper surface unwetted. The remaining dynamic test procedures were similar to those of the static tests.

4.4 FLIGHT SIMULATION TESTS

In these tests, the skin temperatures, instead of being held constant, were varied according to schedules representing conditions for extreme cold day commercial flights. In most tests, upper and lower skin temperatures were identical and these temperatures were controlled automatically. In a few tests with separate upper and lower temperature schedules, the upper skin was controlled by the automatic system and the lower one was manually controlled. The other test procedures were similar to those for the static tests.

4.5 EXTERNAL HEATING AND RECIRCULATION TESTS

In these tests, fuel was withdrawn from the simulator tank, circulated through an external heat exchanger, and returned to the simulator tank where normal cooling or flight simulation proceeded. The recirculation was started either at the beginning of the cooling cycle or after a specified time interval in the cooling cycle, depending upon the test conditions. The flow rate of recirculated fuel was varied between 1.9 and 3.8 L/min, and the oil flow in the heat exchanger was varied between 3.0 and 4.2 L/min. The electrical heat input to the oil heater ranged from 0 to 1200W.

Since the same boost pump was used for discharge and recirculation, it was necessary to change a hose connection back to the weigh tank prior to pumpout. External heating and recirculation was thus terminated about 15 min before the end of the cooling cycle. To ensure correct measurement of holdup, the entire recirculation loop was kept filled with the fuel throughout the test, and care was taken not to spill any fuel during hose connection alterations. The rest of the procedure was similar to that of static or dynamic tests.

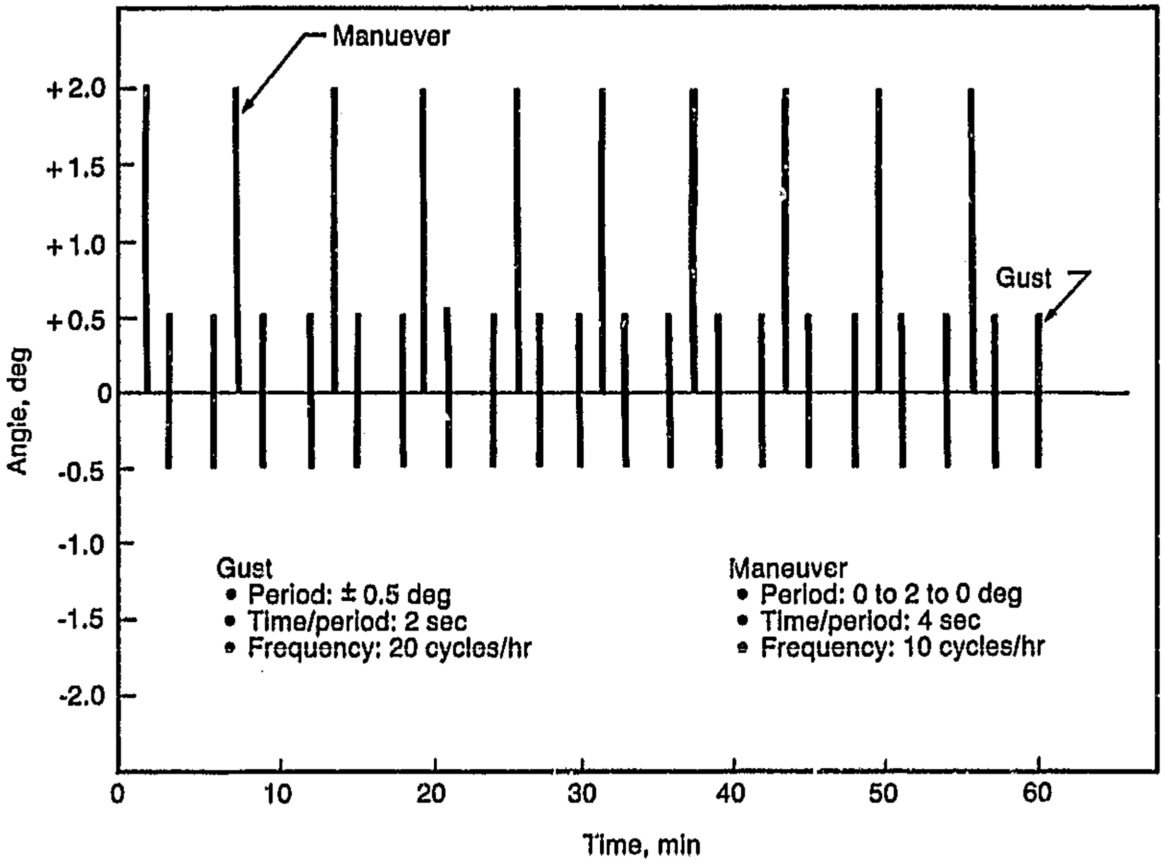

Figure 14. Gust and Maneuver Cycles for Slosh Simulation

4.6 MODIFIED FUEL TESTS

In these tests, selected test fuels were modified by the addition of flow improver additives. To produce a proper blend, first the required amount of additive was measured and mixed with about 10L of fuel. This was added to the weigh tank containing the balance of the fuel to be modified. The mixture was then circulated for 1 hr at 10 L/min through the test tank and back to the weigh tank in a closed loop to produce a thoroughly blended flow-improved fuel.

The modified fuels were investigated in a limited series of static, dynamic, flight simulation, and heated fuel tests.

5.0 RESULTS AND DISCUSSION

This section describes results of tests in various categories with different test fuels. A summary of all tests is given in Appendix A. In all there were 103 test runs useful for reporting. The first series of tests, discussed in section 5.1, was called reference fuel tests. These tests established long-period cooling characteristics of a reference jet fuel under static and dynamic conditions to measure holdup for different periods of cooling. Test conditions evaluated the effects of vibration, changes in heat transfer rate, changes in fuel withdrawal rate, unwetted upper surface, and slosh, at constant skin and flight simulation schedules.

The second series of tests, discussed in section 5.2, was the experimental fuel tests in which flowability characteristics of five different fuels were studied. The test conditions were similar to the reference fuel tests, with the objective to make performance comparisons and develop correlations.

The third series of tests, discussed in section 5.3, were the heated fuel tests, in which the effectiveness of external heating and recirculation of fuel to improve the flowability was studied. These tests included constant skin temperatures as well as flight simulations, plus vibration, slosh, and unwetted upper surface conditions.

The last series of tests, discussed in section 5.4, was modified or flow-improved fuel tests. The objective of these tests was to evaluate the improvement in flowability achieved by mixing flow-improver additives in selected fuels. The modified fuel tests were primarily static holdup tests with constant skin temperatures, but one test each was performed with unwetted upper surface and external heating.

5.1 REFERENCE FUEL TESTS

This series of tests was conducted with the LFPA-3 reference fuel to establish a base of flowability performance for comparison to other fuels. Table 2 is a summary of the test conditions and holdup results for this series.

5.1.1 Static Holdup Tests

The objective of these tests was to determine the relationship of unpumpable holdup to fuel temperature under static constant skin-temperature conditions. In the first tests, a standard chilling rate was maintained by keeping the skin temperatures at 10°C below the fuel freezing point of -42.8°C, that is, at -53°C. Table 2 shows that for tests 401 to 404, holdup increased from near zero to 12.3% as test times increased from 39 min to 5.5 hr. Corresponding bulk temperatures at the end of each test ranged from -4.9 to -44.1°C (Appendix A). Bulk temperature was measured by TF6, the thermocouple 10 cm above the tank bottom. This reading generally agreed with a calculated volume average of the fuel temperature strata within the tank. Moreover, the thermocouple corresponds very closely to the relative location of the fuel temperature probe in commercial airplane fuel tanks. The near-zero holdup (test 404) is regarded as an incipient freezing limit even though the load cell measurements showed some holdup (0.38%).[1]

[1]Due to the uncertainty of the load cell measurement, a practice of weighing thawed fuel collected from the gravity drain outlet on the morning after the test was initiated. The comparisons confirmed that in most tests, the uncertainty in holdup result was less than 0.4%. In the presentation of results, therefore, the holdup corresponds to load cell measurement with .4% uncertainty except in those cases where the difference between two measurements was larger than 1 kg. In later cases, holdup result was adjusted to correspond to a mean value. See Appendix B for a comparison of these results, starting with test 411.

Table 2. List of Tests Using Reference Fuel (LFPA-3)

Test no.	Test conditions	Chill time, hr.:min.	Holdup, %	Remarks
401	Static, standard fuel withdrawal rate, skin temperatures at −52.8°C	5:30	12.27	
402		4:30	8.34	
403		3:08	4.80	
404		0:39	0.38	Zero holdup
405	Static, slower fuel withdrawal rate, skin temperature at −52.8°C	3:14	3.97	
406		5:27	11.86	
407		4:31	9.32	
408	Static, faster fuel withdrawal rate, skin temperatures at −52.8°C	4:30	9.43	
409		3:10	4.91	
410		5:33	13.06	
411	Dynamic (vibrations), skin temperatures at −52.8°C	4:30	10.31	
412		5:31	11.97	
415	Extreme cold day flight simulation, static	7:28	1.33	
416	Above with prechilling	7:30	1.50	
417	Extreme cold day simulation with vibrations	7:30	1.19	
418	Above with prechilling	7:30	1.32	
419	Extended cold day simulation, static	10:37	1.50	
420	Above with vibrations	10:42	0.66	
421	Above with prechilling	10:40	1.05	
422	Static, skin temperatures at −47.8°C (Intermediate chilling rate)	4:30	2.04	
423		5.31	2.78	
424		3:10	0.97	
425	Dynamic (vibrations) skin temperatures at −47.8°C (Intermediate chilling rate)	5:30	1.34	
426		4:30	1.10	
427	Static, unwetted upper surface (70% full tank), skin temperatures at −52.8°C	5:31	8.84	
428	Above with skin temperatures at −74.8°C	5:30	1.02	

Table 2. List of Tests Using Reference Fuel (LFPA-3) (Continued)

Test no.	Test conditions	Chill time, hr.:min.	Holdup, %	Remarks
429	Unwetted upper surface (70% full tank) with slosh, skin temperatures at −52.8°C	5:30	8.24	
430	Above with skin temperatures at −47.8°C	5:30	1.07	
431	Extreme cold day simulation including warmup phase	10:31	0.16	No holdup
450	Static, unwetted upper surface (97% full tank), skin temperatures at −52.8°C	5:30	8.29	
451	Above with slosh	5:30	8.54	
461	Static, modified extreme cold day profile (with 5°C lower temperature in the minimum temperature phase)	7:30	6.05	

Total number of tests: 32

The static holdup test at the standard withdrawal rate of 10 L/min was repeated at a slower rate of 5 L/min (tests 405 to 407) and at a higher rate of 20 L/min (tests 408 to 410). Figure 15 compares the mass holdup for the different withdrawal rates on the basis of corresponding chilling time (equal bulk fuel temperatures). Holdup appears to increase slightly for the higher rate of withdrawal, due possibly to increased blockage by an agglomeration of fuel crystals. The effect of withdrawal rate is quite small, nevertheless.

The windows in the simulator tank permitted observations during the tests. Initially, the LFPA-3 fuel is clear, with a brownish-yellow tint. As fuel temperatures decrease with chilling time, the fuel becomes cloudy, obscuring the view of the tank interior. This phenomenon has been attributed to water particles in previous studies (ref. 3), but similar behavior with water-dry fuels (ref. 4) suggests that the cloudiness is largely the condensation of microparticles of wax from the fuel.

Figures 16 through 19 are photographs showing the frozen fuel, or holdup, remaining in the tank after completion of pumpout. Figure 16 is a view of the interior of the tank after test 403, with 4.8% holdup. The orientation is the left side of the tank, toward rack no. 5 as drawn in Figure 11. The recirculation distributor is seen at the left. The unpumpable fuel covers the bottom of the tank to a depth of about 3 cm (shown as 1.2 in on the scale). There is a slight coating of crystals on the stringers and sidewalls above this depth. Figure 17 is a view of the interior of the tank after the same test, oriented toward the right side and rack no. 2. Note that the solid fuel layer is tilted toward the outlet port due to the action of draining the tank. Figure 18 is a view at the same location as Figure 16 after test 401, with 12% holdup. The unpumpable fuel in this case covers the bottom of the tank to a depth of about 5 cm (shown as 2 in on the scale). The fuel layer appears liquid, indicating that an appreciable fraction of liquid is trapped with the solid crystals, since the limber holes in the stringers are plugged with solid fuel. A heavy coating of fuel crystals covers the top of the stringers and some of the vertical surfaces. In the right-side view (fig. 19), the near bay with the discharge port appears dry, while far bay has the wet holdup layer seen in Figure 18.

These observations are consistent with previous descriptions of unpumpable fuel in wing-tank simulators (ref. 5). When there is a small amount of frozen fuel (illustrated by the 4.8% holdup test), nearly complete drainage of the liquid fuel is possible. The residue is a layer of solid fuel at the bottom of the tank. At colder conditions (illustrated by the 12% holdup test), the heavier deposition of solid fuel can interfere with tank discharge. In this case, the unusable fuel includes trapped liquids as well as solids.

Temperature histories during static holdup tests are illustrated in Figure 20. Bulk temperature is again assumed to be that of TF6, the center thermocouple locted 10 cm above the tank bottom. The three histories illustrated are for tests with the same chilling times and skin temperatures. Differences in loading temperature and control settings at the beginnings of the three tests cause variations in bulk temperatures during the first 2 to 3 hr of testing. However, the temperatures after 3-hr elapsed time to the end of the chilling period are almost identical. Long-range flight calculations (ref. 10) have predicted that, for given atmospheric conditions (skin temperatures in the simulator), bulk fuel temperatures after several hours of flight time are no longer influenced by the initial temperatures.

Examples of the internal temperature profiles with the tank are shown in Figures 21 and 22. The complete set of thermocouple readings within the tank is plotted in Figure 21. Temperatures are constant throughout most of the tank, from the 10-cm location to the top. In this portion of the tank, the temperatures are lowest for the center rack, no. 1, although differences between this rack and the corner racks, nos. 2 to 5, are less than a degree. Heat

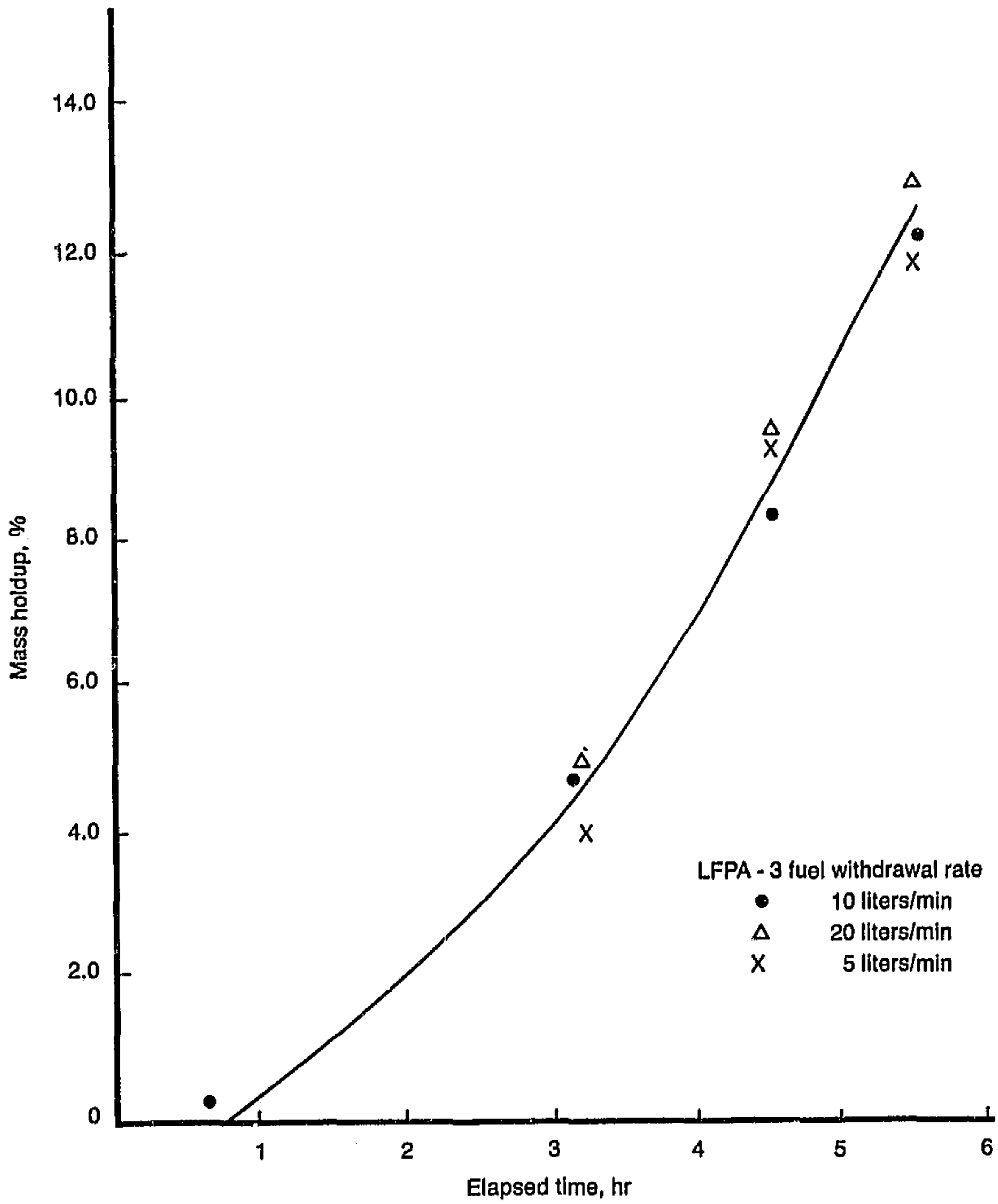

Figure 15. Effects of Fuel Withdrawal Rates on Holdup

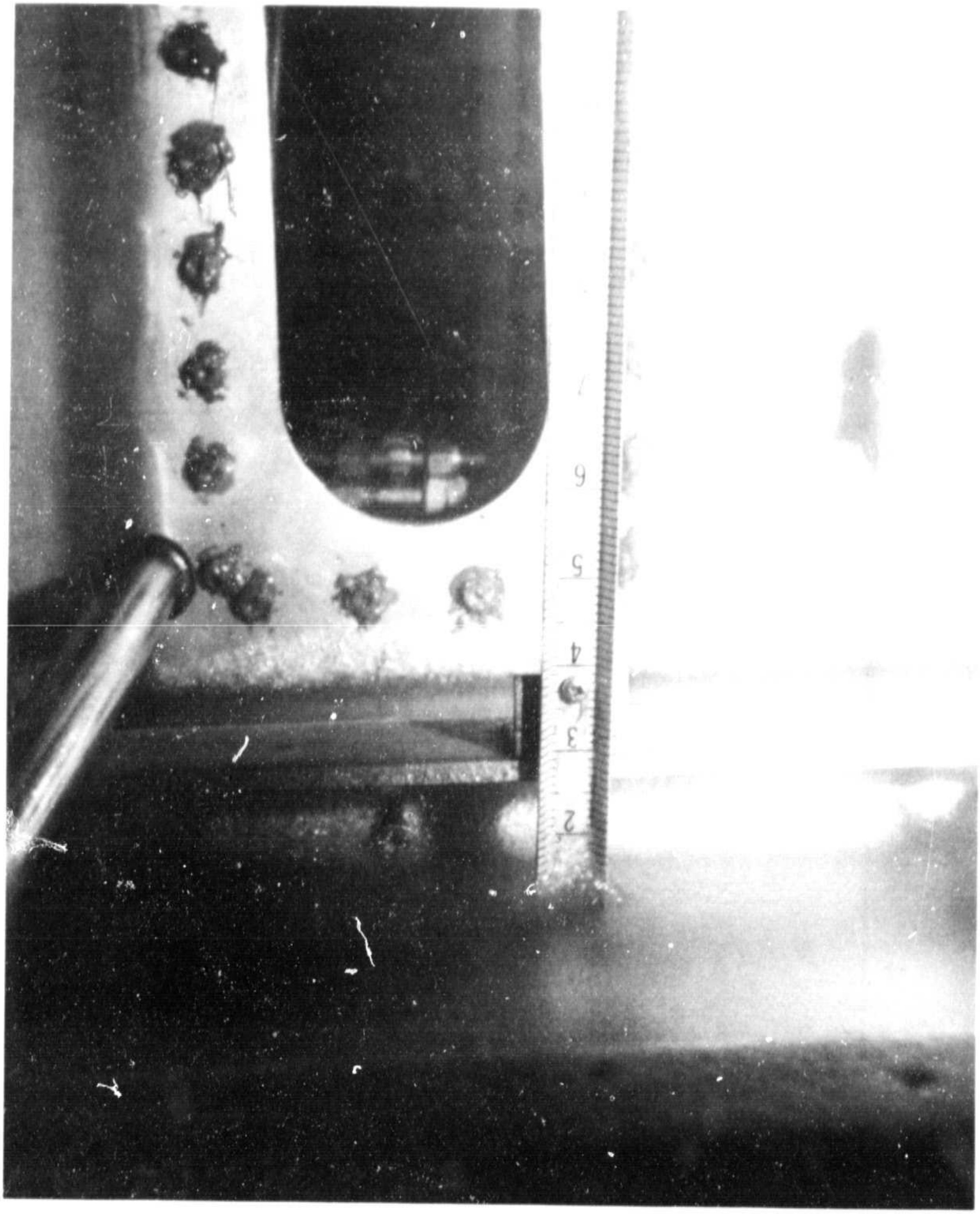

Figure 16. Interior of Tank, Left Side, After Pumpout With 4.8% Holdup (Test No. 403)

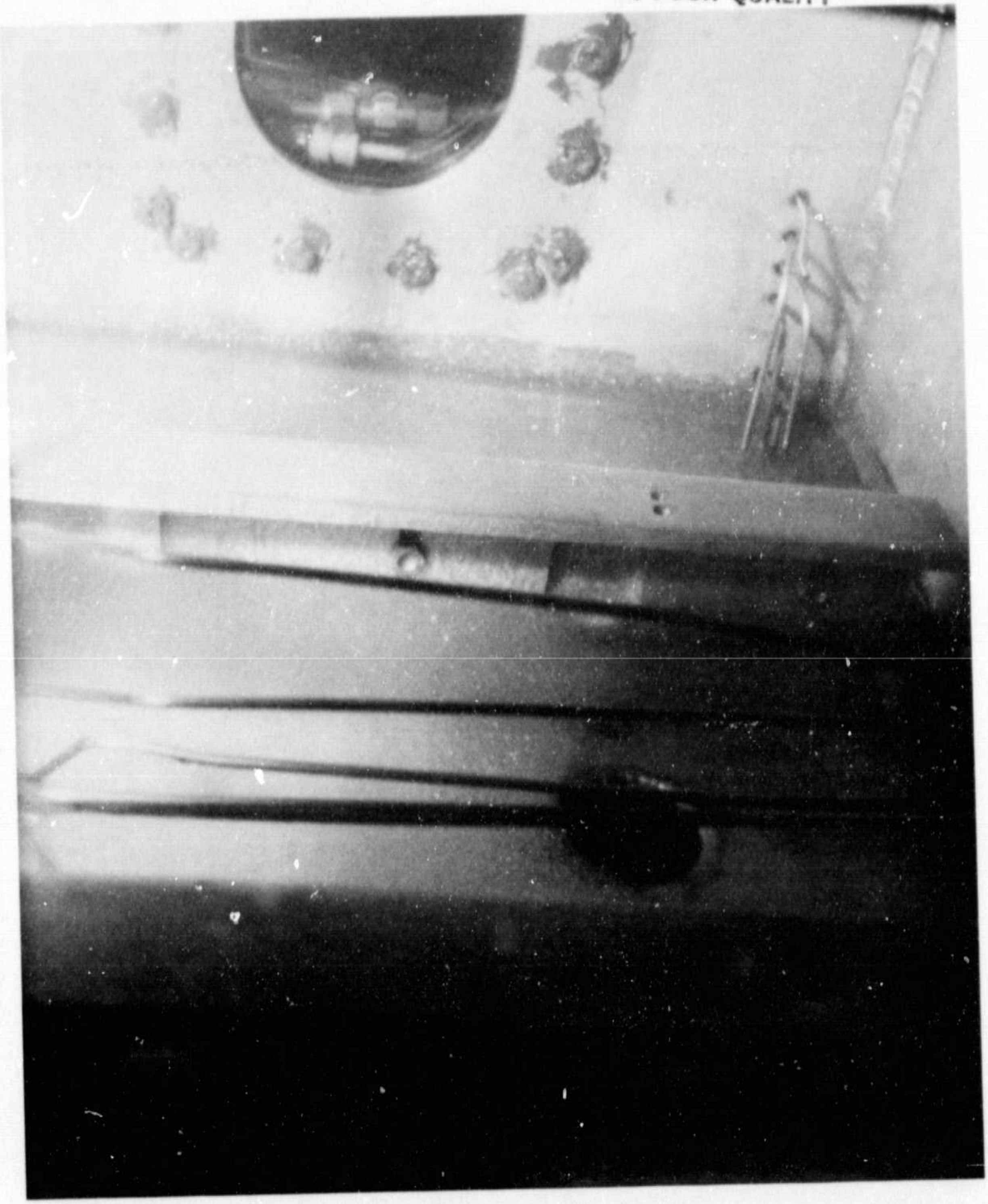

Figure 17. Interior of Tank, Right Side, After Pumpout With 4.8% Holdup (Test No. 403)

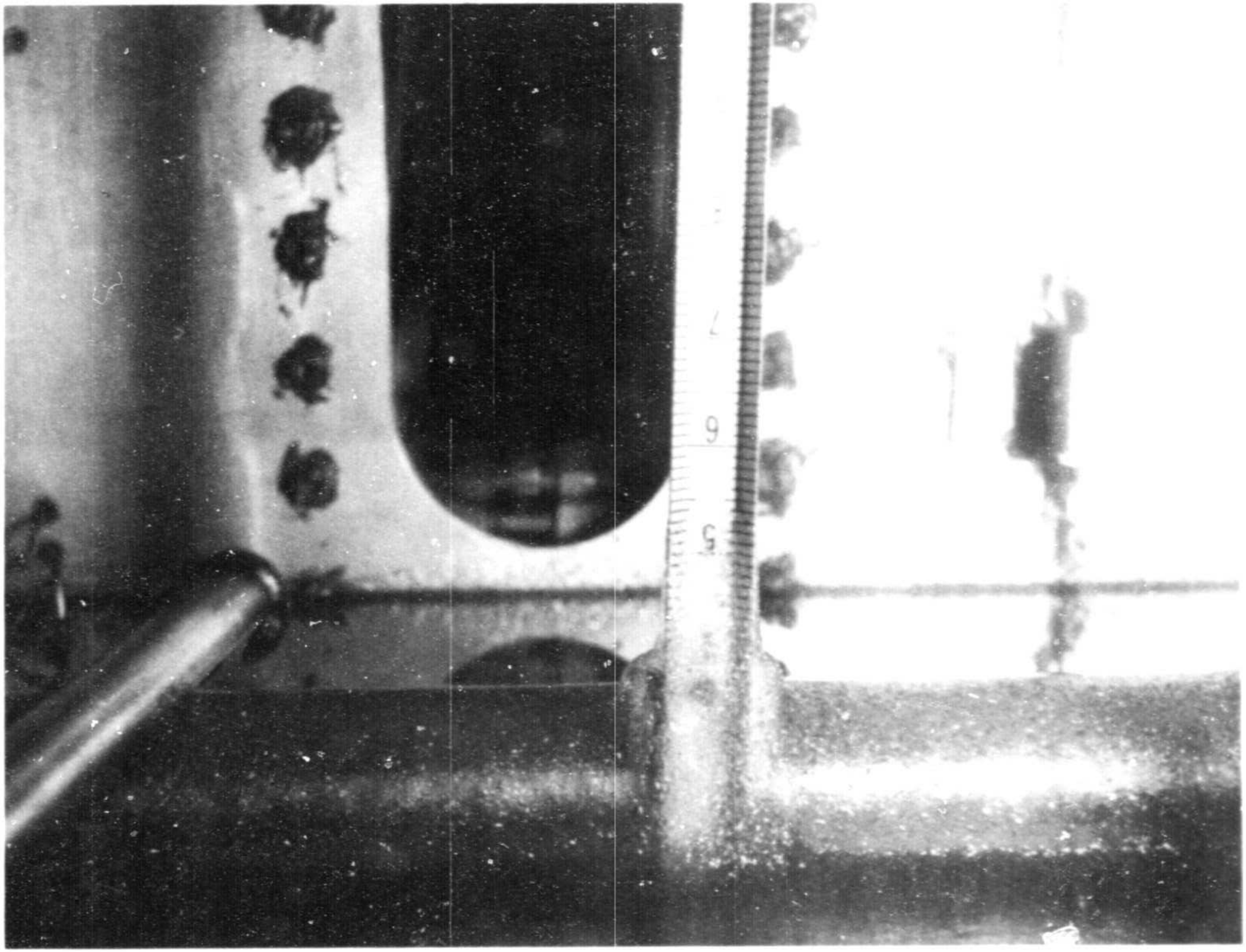

Figure 18. Interior of Tank, Left Side, After Pumpout With 12% Holdup (Test 401)

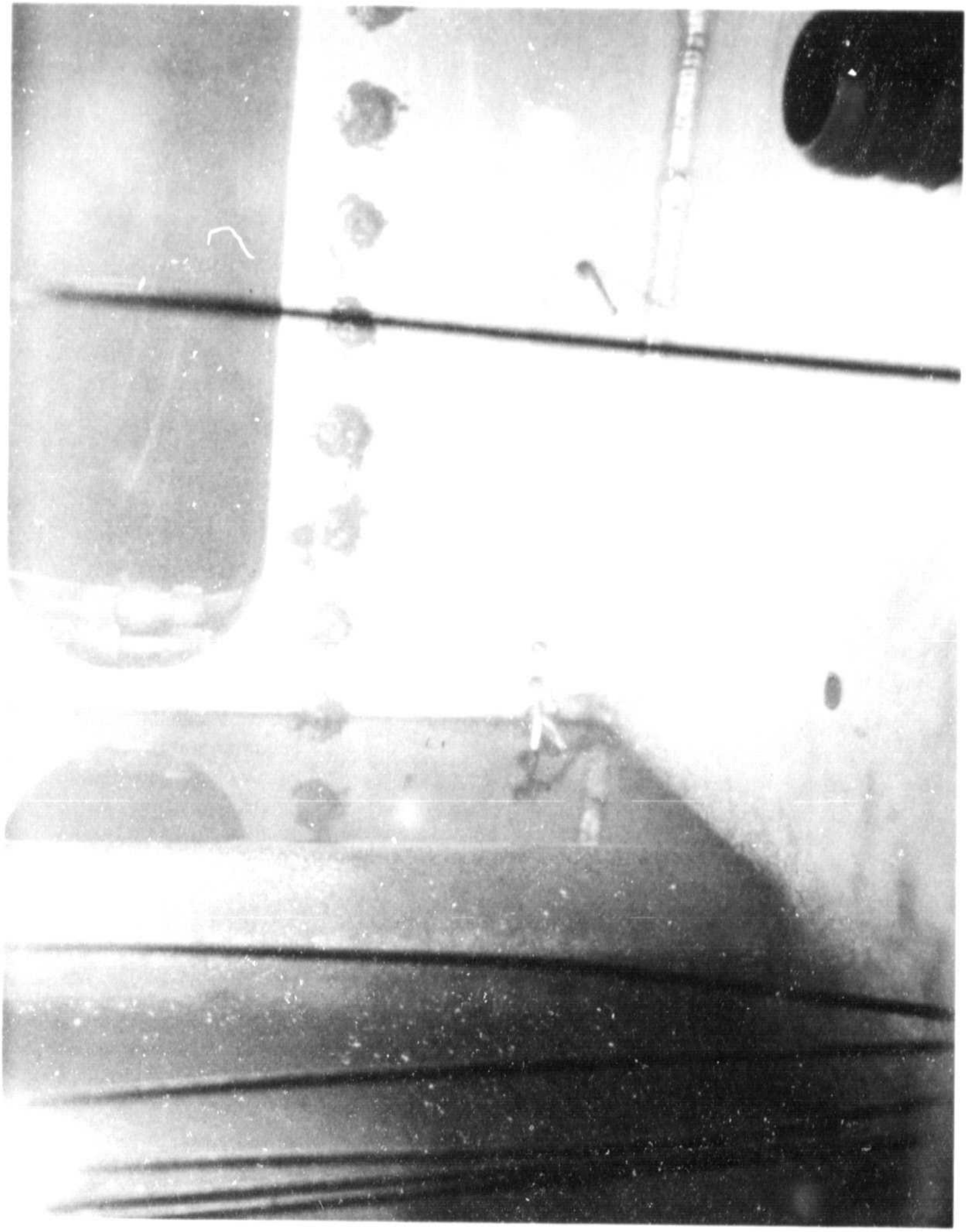

Figure 19. Interior of Tank, Right Side, After Pumpout With 12% Holdup (Test 401)

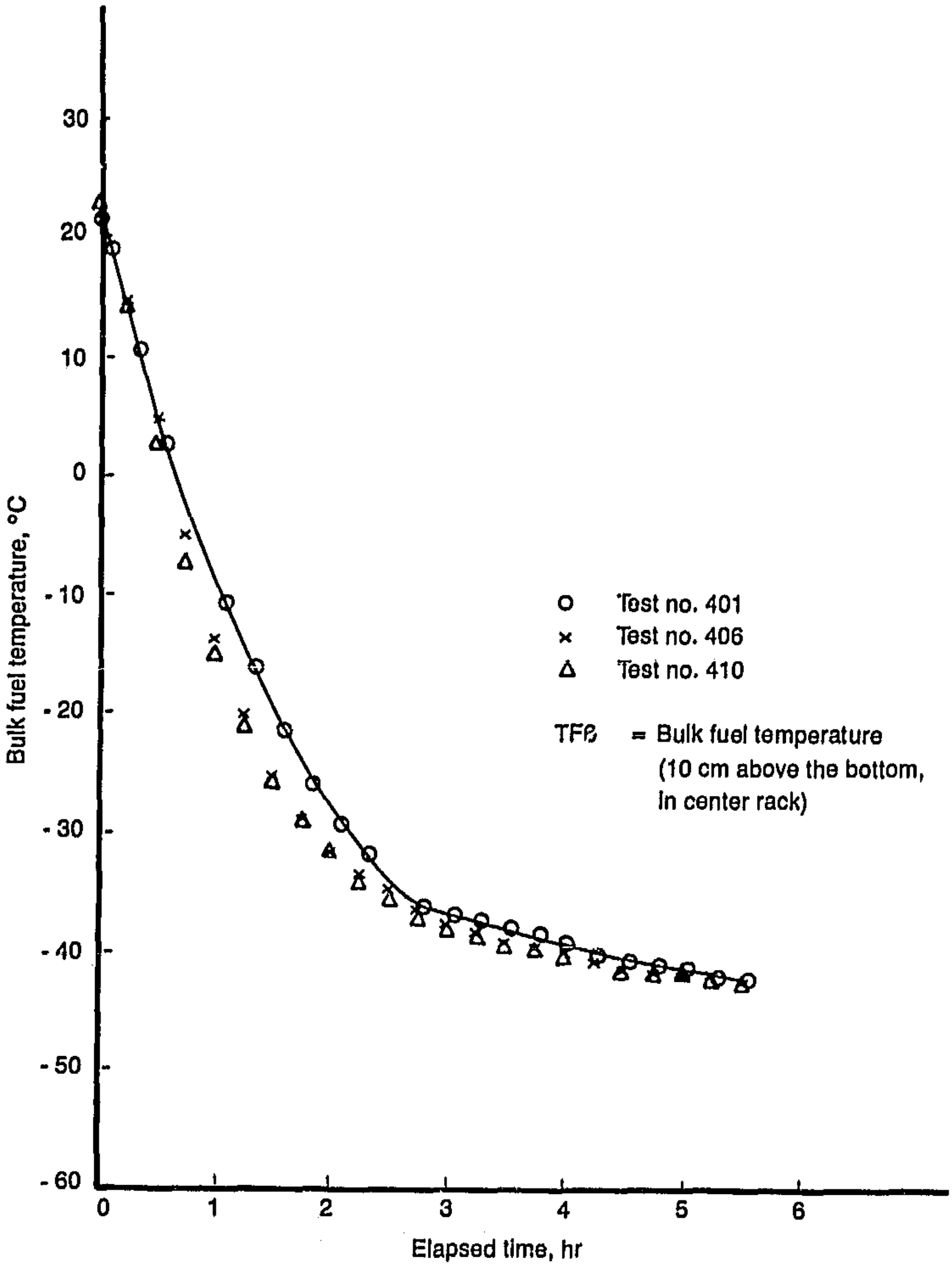

Figure 20. Bulk Fuel Temperature History From Reference Fuel Static Holdup Tests

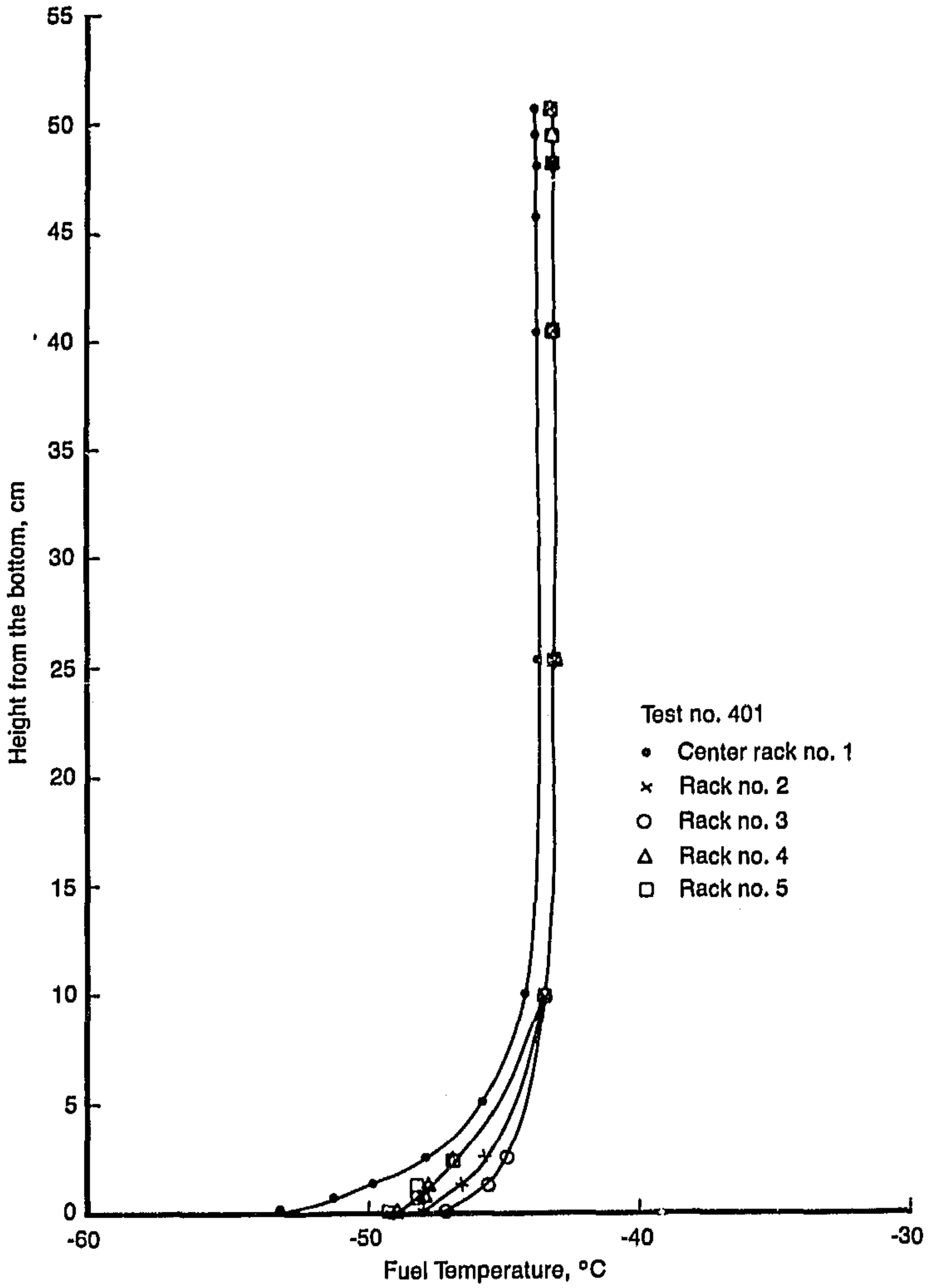

Figure 21. Temperature Profiles at the End of a Typical Static Holdup Test

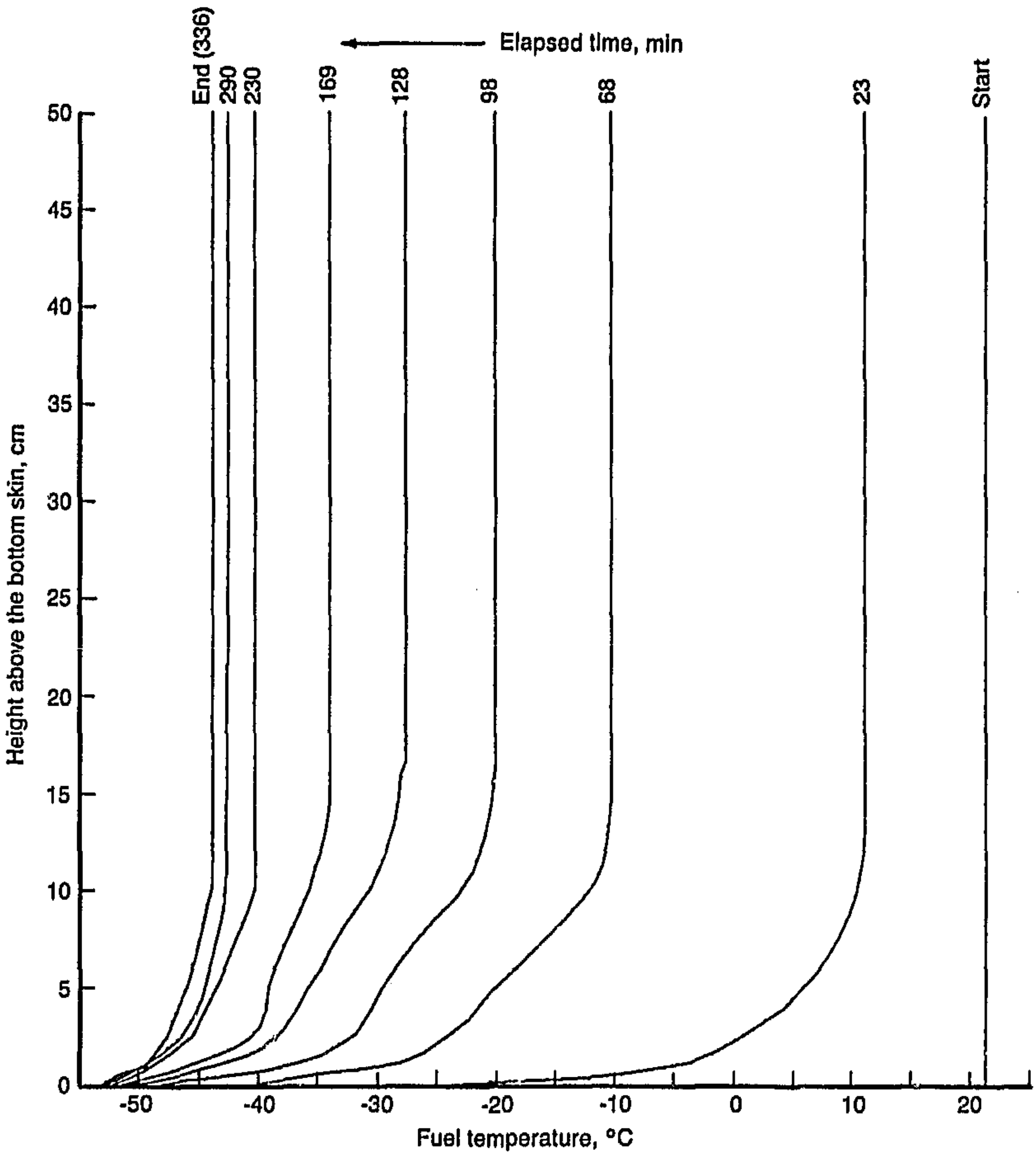

Figure 22. Typical Fuel Temperature Profile History at Center Rack, Test No. 401

leakage through the insulated sidewalls is thus very small, except possibly at the corners, represented by the bottom thermocouples on racks no. 2 to 5.

A history of the center temperature profiles for the test illustrated in Figure 21 is most interesting. The profiles in Figure 22 show the typical shape of a uniform bulk temperature with a consistent conduction-layer gradient at the bottom. The profiles resemble those measured in the same apparatus with an internal boost pump (refs. 8 and 9), and, to some extent, those measured in another simulator (refs. 4 and 5) and in an instrumented airplane tank (refs. 11 and 12). The major difference between the profiles recorded in different facilities is the presence or absence of a gradient at the upper boundary of the tank, representing the convection layer. In Figure 22, no upper boundary layer is seen. The boundary layer is apparently thinner than the spacing of the thermocouples between the upper skin and the fuel. This upper surface boundary layer is seen in the reported profiles of previous testing, and in many cases the appreciable upper gradient is the result of incomplete wetting of the upper surface of the tank by the fuel. The Figure 22 profiles also show a "wiggle" in the gradients in the vicinity of 5 cm above the bottom. This nonuniformity may be caused by the complex interaction of conduction layer and the mixing (bulk) region. It is reproducible and does not seem to be instrumentation related.

5.1.2 Dynamic and Other Holdup Tests

Figure 23 compares holdup on the basis of elapsed time for a variety of tests with the reference fuel. In addition to the static tests at standard chilling rates just described, there were static tests at an intermediate rate, with the skin temperatures maintained 5°C rather than 10°C below the fuel freezing point. For the same chilling times, fuel bulk temperatures were 3°C higher for the intermediate chilling rate tests and holdup was reduced appreciably.

The dynamic tests were conducted with continuous vibrations throughout the chilling phase. In comparison to the static tests at the standard chilling rate, one vibration test showed 2% more holdup, the other 0.3% less holdup (fig. 23). Temperature profiles, however, were nearly identical, varying by less than 0.5°C. For the intermediate-chilling-rate tests, vibration reduced holdup slightly. The effect of vibrations appears to be minor for the most part.

Additional tests were conducted with unwetted upper tank surfaces, with and without superimposed slosh. The holdup results are included in Figure 23. In most unwetted upper surface tests, the tank was only 70% full. Two tests, one static and one with slosh, were conducted with the tank 97% full. Figure 24 presents bulk and boundary-layer temperature histories for these tests. As expected, the unwetted upper surface reduced the heat transfer rate, resulting in higher bulk fuel temperatures throughout and reducing holdup. However, insignificant differences are seen between the results with the 70% filled tank and the 97% filled tank tests. Likewise, slosh has a negligible influence on the flowability. The effect of unwetted upper tank surfaces on heat transfer has been calculated and discussed in previous studies (refs. 8 and 9). This influence of the reduced convection resulting from unwetted upper surface on fuel temperature and holdup is significant, because in actual practice, there is always an ullage in airplane fuel tanks.

5.1.3 Flight Simulation Tests

The flight simulation tests differed from the static and dynamic tests in that the skin temperatures, instead of being constant with time, were varied to simulate the temperature history associated with an extreme cold day commercial flight. Previously reported flight

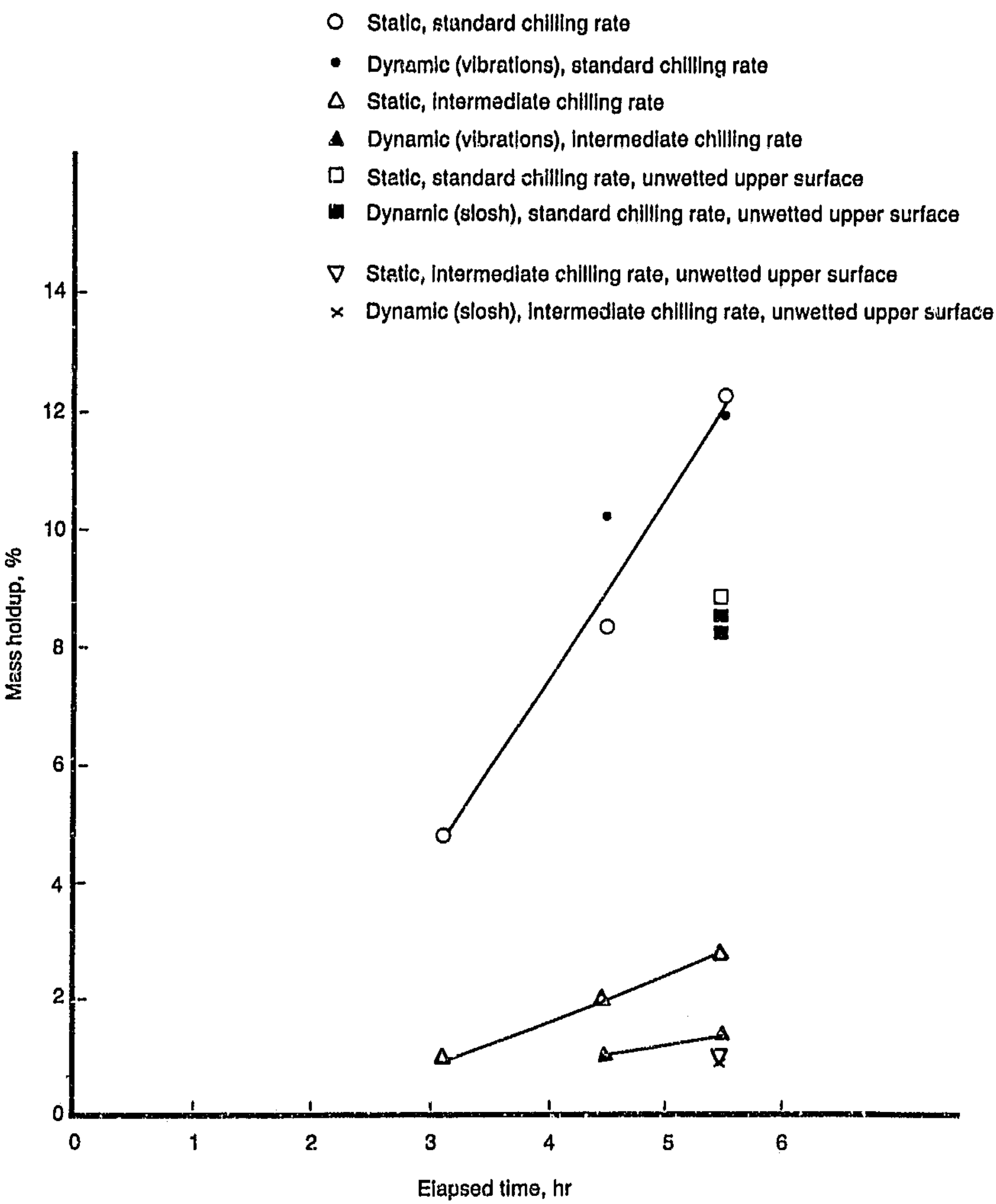

Figure 23. Comparison of Holdup Results From Various Reference Fuel Static and Dynamic Tests

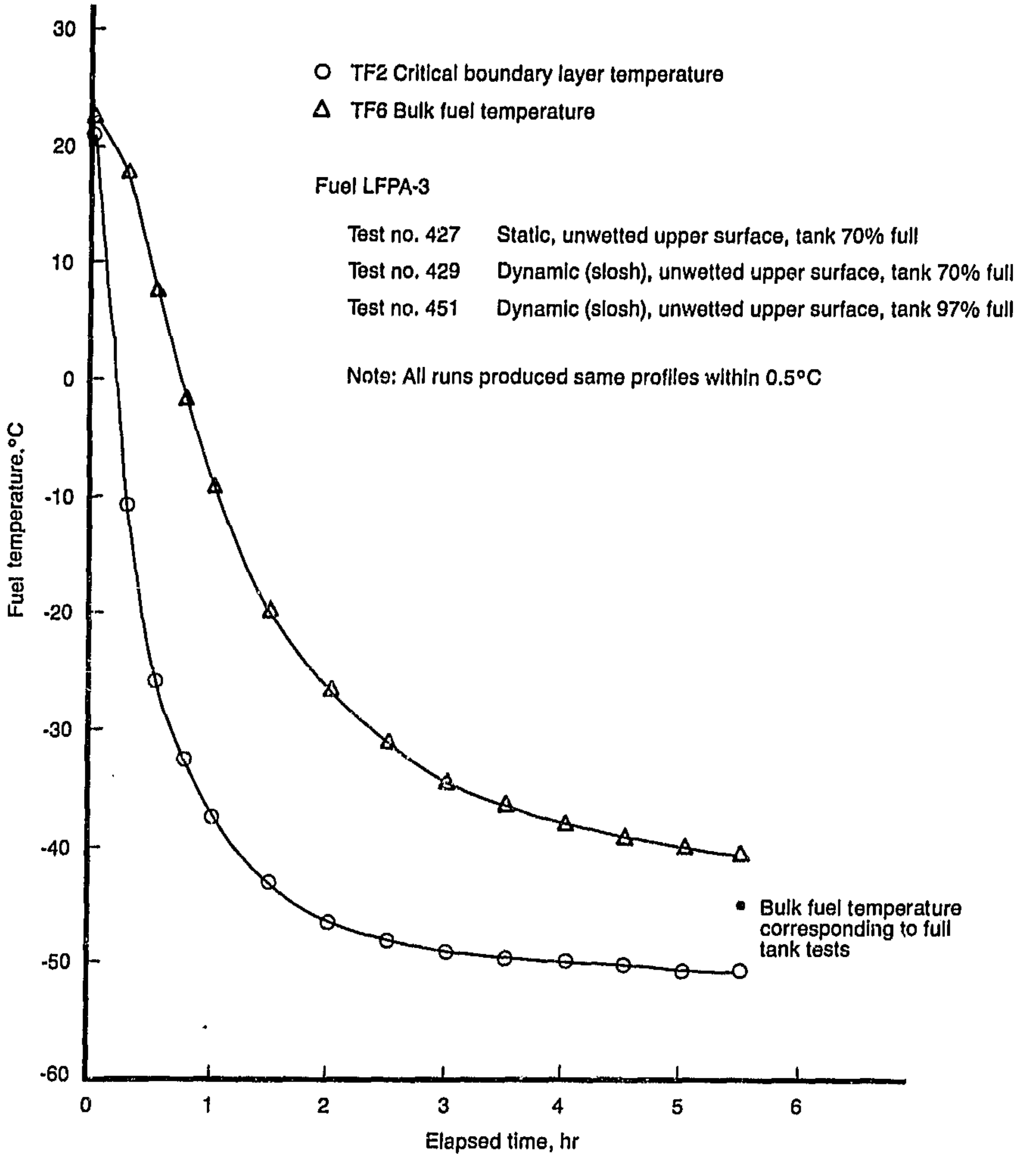

Figure 24. Bulk and Critical Fuel Temperature Histories From Reference Fuel Unwetted Upper Surface Tests

simulation tests were based on meteorological statistics (refs. 8 and 9). In the present study, the flight simulation was based on an actual flight history for a cold day flight of a 747 from Bahrain to New York (ref. 13). Figure 25 shows the simplified flight temperature history (BAH-JFK) and three flight simulation schedules derived from the flight history. To determine the holdup at the coldest condition, it was necessary to terminate the simulation after 7.5 hr, at point D. This schedule was called the extreme cold day simulation. The extended cold day simulation was created by cooling at constant skin temperature up to point F, or an elapsed time of 10.7 hr. A third schedule was defined by lowering the minimum skin temperature, that is, segment CD, by 5°C. This was termed the modified extreme cold day simulation. The flight simulation tests also included conditions such as prechilling of fuel to simulate cold fuel that would be available at some airports during winter and the imposition of tank vibrations to represent the flight environment.

Bulk temperature results for the extreme cold day flight simulation tests are shown in Figure 26. After 4 to 5 hr, the bulk temperatures for the several tests are identical, even when the fuel is prechilled. This again confirms the heat transfer analyses of long-range flight fuel temperatures (refs. 10 and 14). Holdup results for these tests are compared as bar graphs in Figure 27. For LFPA-3, a fuel which meets Jet A specifications, the extreme cold day flight simulations produce small holdups of 1 to 1.5%. The reference flight probably used Jet A-1 fuel with a specification freezing pont of -47°C, at least 4.5° lower than that of LFPA-3. Vibrations reduced the extreme cold day flight simulation holdup very slightly. Prechilling the fuel or the use of the extended cold day simulation increased holdup very slightly, compared to that for the extreme cold day baseline test (test 415). One flight simulation test (test 431, not included in fig. 27) was conducted with a simulation of the complete reference flight history (ABCDE in fig. 25). There was practically zero holdup for this test, showing that the small holdups of the order of 1 to 2% occurring at the end of minimum temperature segments would disappear with warmer skin conditions in the last portion (descent) of the flight.

5.2 EXPERIMENTAL FUEL TESTS

The fuels LFPA-1, LFPA-2, LFPA-4, LFP-9, and LFP-11 varied in composition mainly in their n-paraffin content. All of these fuels were subjected to static tests to determine the variation in flowability, compared to the reference fuel, LFPA3. The dynamic and flight simulation tests were restricted to LFPA-1, LFPA-4, and LFP-11. Table 3 is a summary of the test conditions and holdup results for this series of tests.

5.2.1 Static Holdup Tests

For each fuel, the skin temperatures for the static holdup tests were maintained at 10°C below the respective freezing points. During the pumpout, the flow rate was 10 L/min in all tests. Two examples of the temperature history results for the experimental fuels are included here. Figure 28 presents the temperatures at several locations in the center of the tank for a test with LFPA-4, the fuel with the highest freezing point, -41°C, and the greatest n-paraffin content. The 3.8-hr test produced 11% holdup. Figure 29 is a similar plot for LFP-11, the fuel with the lowest freezing point, -47°C, and the least n-paraffin content. The 7-hr test produced 7.6% holdup. The histories for all the static tests with the experimental fuels were similar to that for the reference fuel (fig. 20). There were differences in the nature of the solid fuel deposits observed after pumpout. Figure 30 shows the left side of the tank interior after test 457 with LFPA-4, which produced 5.8% holdup. This is comparable to the reference fuel test

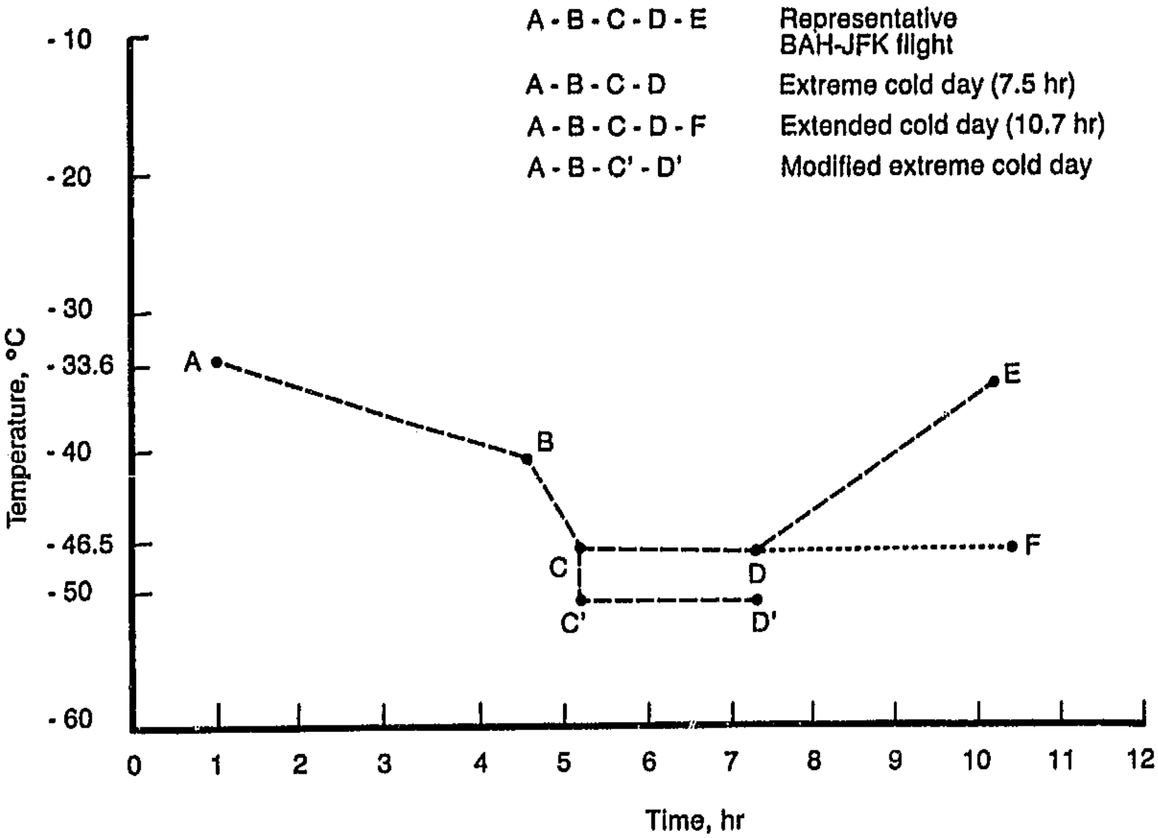

Figure 25. Skin Temperature Schedules for Flight Simulation Tests

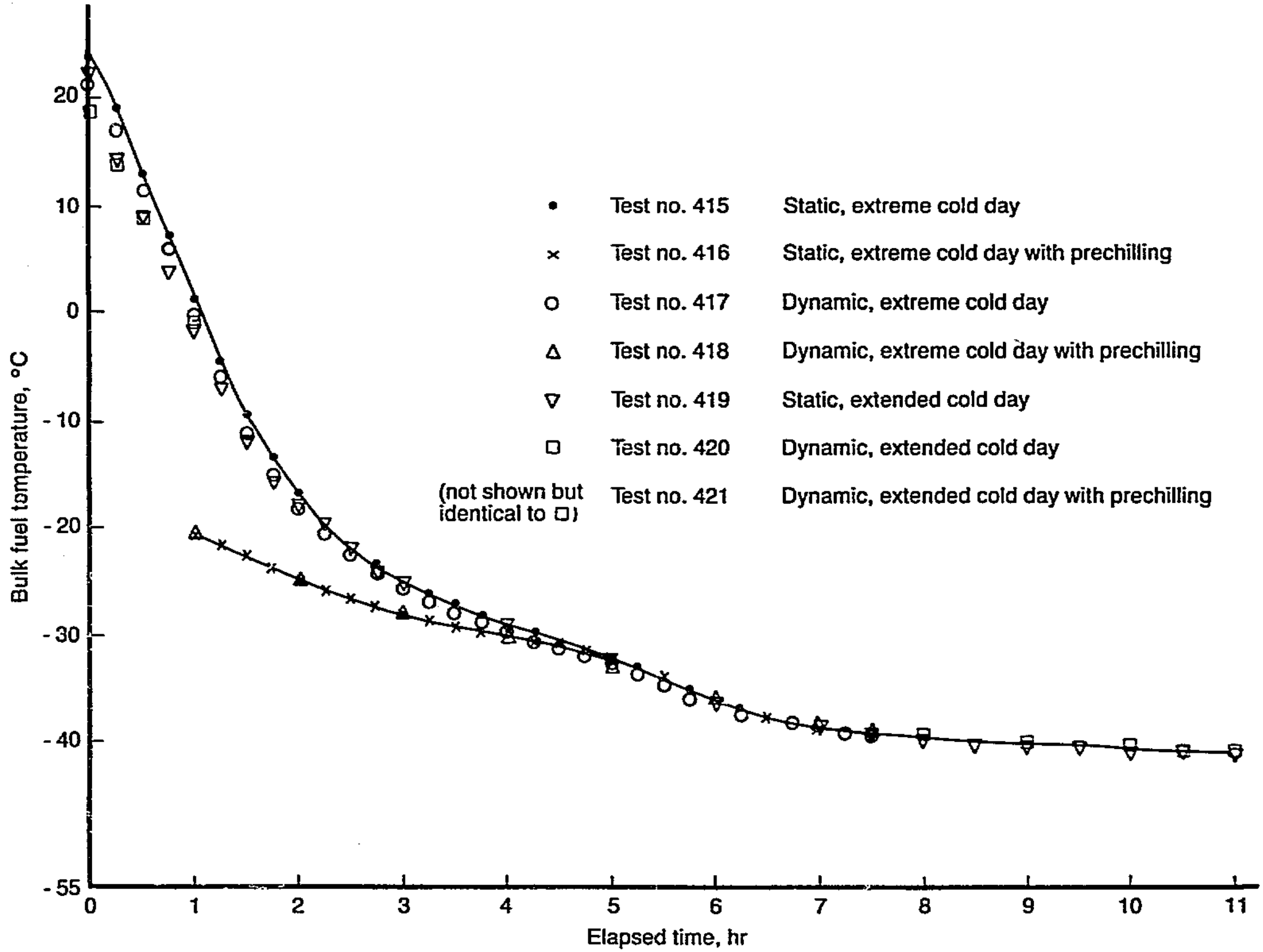

Figure 26. Bulk Fuel Temperature Histories From Reference Fuel Flight Simulation Tests

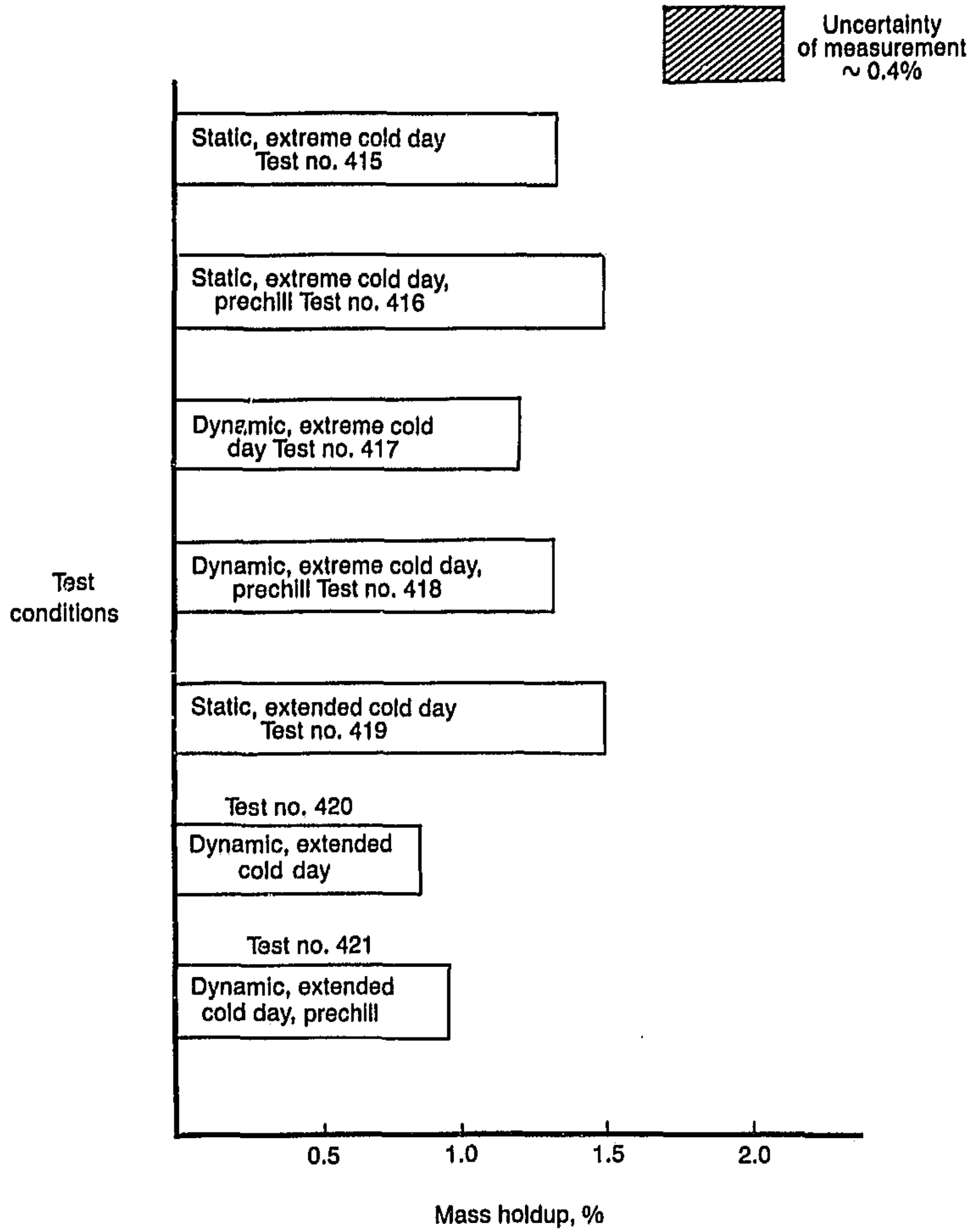

Figure 27. Comparison of Holdup Results From Reference Fuel Flight Simulation Tests

Table 3. List of Tests Using Experimental Fuels (LFPA-1, LFPA-2, LFPA-4, LFP-9 and LFP-11)
(No External Heating or Flow Improvers)

Fuel	Test no.	Test conditions	Chill time, hr.:min.	Holdup, %	Remarks
LFPA-2	434	Static, skin temperature	3:00	2.61	
	435	at −54.7°C	5:01	6.17	
	436		6:30	8.29	
	437		1:40	0.25	No holdup
LFP-9	442	Static, skin temperatures	3:00	4.62	
	443	at −55°C	5:00	13.50	
	444		4:00	9.16	
	445		1:20	0.90	
LFPA-1	452		4:00	3.98	
	453	Static, constant skin	7:00	6.93	
	454	temperatures at −57°C	1:45	0.93	
	455		9:00	9.86	
	456	Static, skin temperatures at −49°C	4:00	0.41	No holdup
	458	Static, extreme cold day profile	7:30	0.69 0.33	Slight holdup
	460	Static, modified extreme cold day profile (with 5°C lower minimum temperature)	7:30	0.47	
	486	Static, constant skin temperatures at −55°C	6:00	2.50	
LFPA-4	438	Static, skin temperatures	3:00	6.72	
	439	at −51.1°C	3.45	11.00	
	440		0:55	0.14	No holdup
	441		2:00	2.37	
	457	Static, skin temperatures at −49°C	4:00	5.83	
	459	Static, extreme cold day schedule	7:30	4.98	
	465	TriStar flight simulation	5:60	0.44	No holdup
	466	Static, above schedule with 90% tank full	6:50	0.40	No holdup
	467	Above with slosh	6:50	0.58	No holdup
	468	TriStar flight upper skin temperature schedule on both skins, 90% full tank and slosh	6:50	0.10	No holdup
	469	Static, modified TriStar flight schedule with warmup between 2nd and 3rd hours	6:50	0.30	No holdup
	490	Static, skin temperatures at −51.1°C	3:30	9.58	
	494	Static, constant coolant flow rates and inlet temperature	3:30	8.58	
	499	Static, prechilled fuel, TriStar flight simulation	6:50	0.86 0.20	No holdup

Table 3. List of Tests Using Experimental Fuels (LFPA-1, LFPA-2, LFPA-4, LFP-9 and LFP-11) (Continued) (No External Heating or Flow Improvers)

Fuel	Test no.	Test conditions	Chill time, hr.:min.	Holdup, %	Remarks
LFP-11	446	Static, skin temperatures at −57°C	3:00	1.95	
	447		5:00	5.83	
	448		7:00	7.59	
	449		1:45	0.39	No holdup
	462	TriStar flight simulation, upper skin temperature schedule	6:50	0.38	No holdup
	463	As above with lower skin temperature schedule	6:50	0.36	No holdup
	464	As above, both skins on separate schedules	6:50	0.15	No holdup

Total number of tests: 37

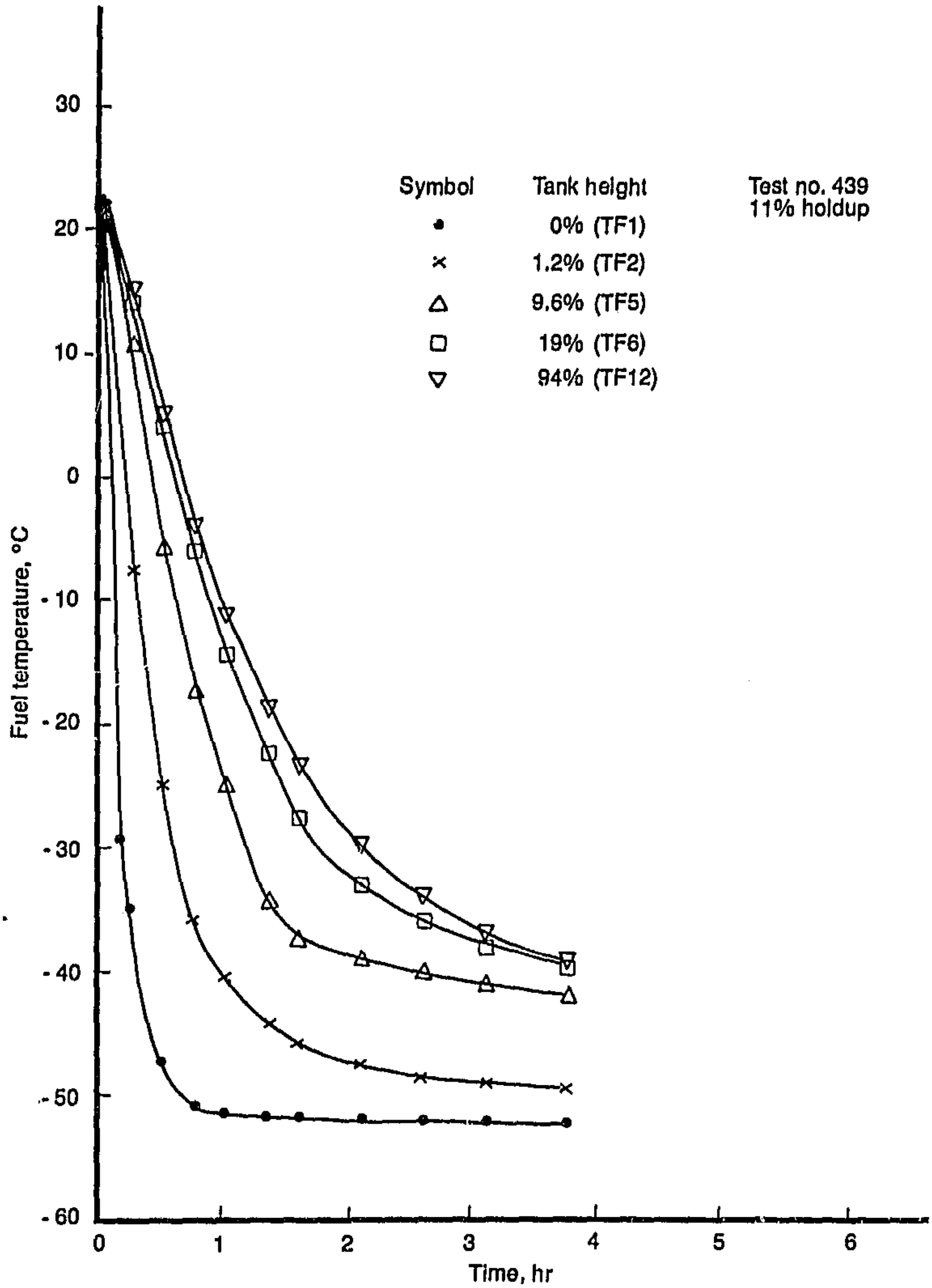

Figure 28. Typical Temperature Histories From LFPA-4 Fuel Static Test

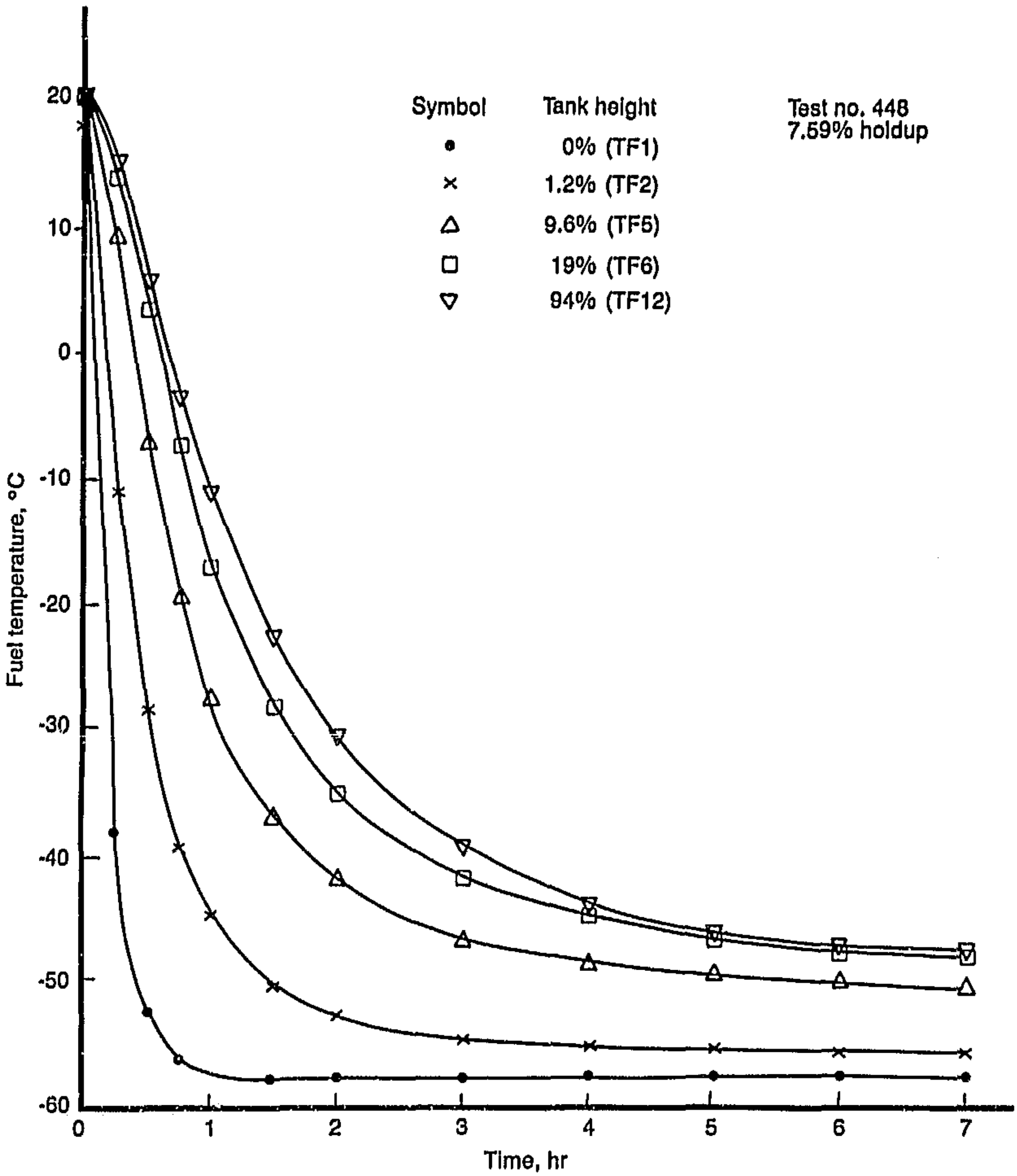

Figure 29. Typical Temperature Histories From LFP-11 Fuel Static Test

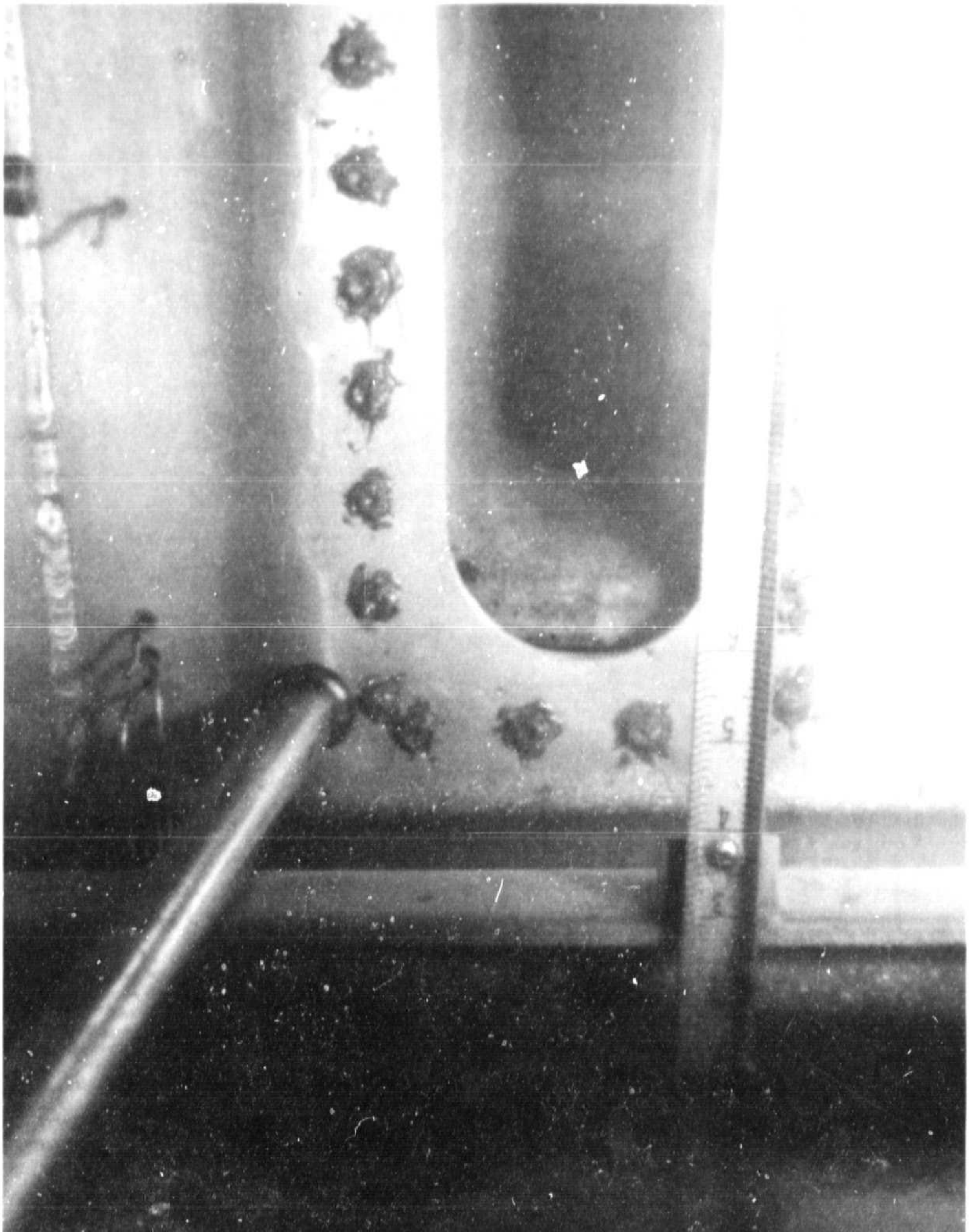

Figure 30. Interior of Tank, Left Side, After Pumpout With LFPA-4, 5.8% Holdup (Test No. 457)

illustrated in Figure 16. As before, with this moderate holdup, almost all of the solid fuel is deposited in the bottom of the tank. Figure 31 shows the tank interior after test 447 with LFP-11, which produced approximately the same holdup as the test shown in Figure 30. For the LFP-11 test, large, rough crystals adhere to the stringers and sidewalls. The difference in appearance between Figures 30 and 31 may come partly from the different compositions of the fuels and partly from the different test times. The longer chill time of test 447 favors large crystal growth.

Figure 32 shows a comparison of holdup results for the experimental and reference fuels. While the different fuels showed similar temperature profiles during the chilldown phase, the amount of holdup varied with fuel type for the same chill periods. In general, LFPA-3, LFPA-4, and LFP-9, the fuels with the highest pour points (table 1), produced higher holdups than LFPA-1, LFPA-2, and LFP-11.

A different method to compare results of holdup is to correlate the data with the critical boundary layer temperature, TF2, measured 0.6 cm from the lower skin. Figure 33 shows such a correlation. The zero holdup limit for the critical boundary layer temperature is very close to the freezing point. At decreasing values of the critical boundary layer temperature, holdup increases 2 or 3% at temperatures 4 to 6°C below the freezing point. Holdup then increases rapidly at further decreases in the critical boundary layer temperature. In these tests, the small changes in the boundary layer temperature as it approaches the skin temperature are accompanied by greater changes in the bulk temperature. In addition, it is likely that crystal buildup accelerates rapidly, increasing holdup greatly, as the boundary layer approaches the pour point. The holdup curves in Figure 33 resemble holdup measurements in the isothermal "shell" tester (refs. 8 and 9).

A better correlation of the holdup characteristics of the different fuels may be obtained by plotting (freezing point-TF2) versus holdup as in Figure 34. The data fall into three separate curves. The three fuels, LFPA-3, LFPA-4, and LFP-9, show the same correlation. Similarly, LFPA-2 and LFP-11 show another correlation, while LFPA-1 has a third, unique correlation. It appears that the groupings have some relation to pour point or n-paraffin content, but the data were not sufficient to explore this possibility any further. A holdup correlation related to a function of both freezing point and pour point has been suggested by previous investigators (refs. 15 and 16). It should be noted that only data from static holdup tests with constant skin temperatures 10°C below the fuel freezing point have been used in these correlations. Data from other static tests may or may not fit these plots as different skin temperature profiles and chill periods affect the boundary layer temperature history differently.

5.2.2 Dynamic and Flight Simulation Tests

Since the reference fuel tests showed that dynamic conditions have a minor influence on flowability, only two tests, one each with slosh (upper surface unwetted) and vibration were conducted, and these were combined into the flight simulation tests. Three fuels, namely LFPA-1, LFPA-4, and LFP-11, were tested. LFPA-1 and LFP-11 were representatives of the lowest holdup producing fuels. LFPA-4, on the other extreme, was representative of the highest holdup producing fuels. In addition to the extreme and modified extreme cold day schedules (fig. 25), a new set of flight simulation schedules was employed. These schedules, shown in Figure 35, were based upon the coldest of a set of actual flight data obtained by NASA from a TriStar wing tank (ref. 12). These simulations are called the TriStar simulations. The airplane measurements showed that the upper and lower skin temperatures deviated from each other during flight by as much as 5°C. Thus, four simulations were

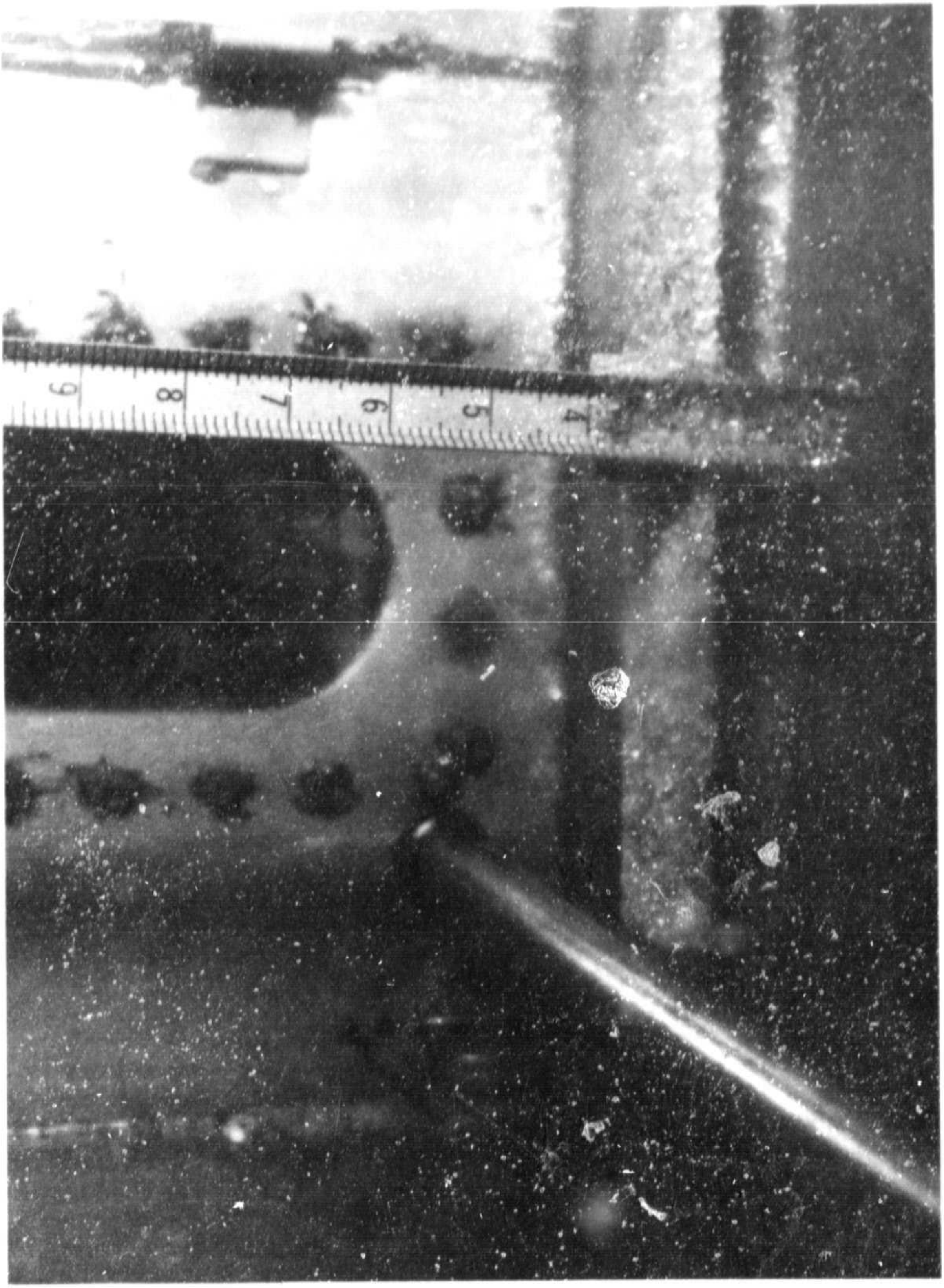

Figure 31. Interior of Tank, Left Side, After Pumpout With LFP-11, 5.8% Holdup (Test No. 447)

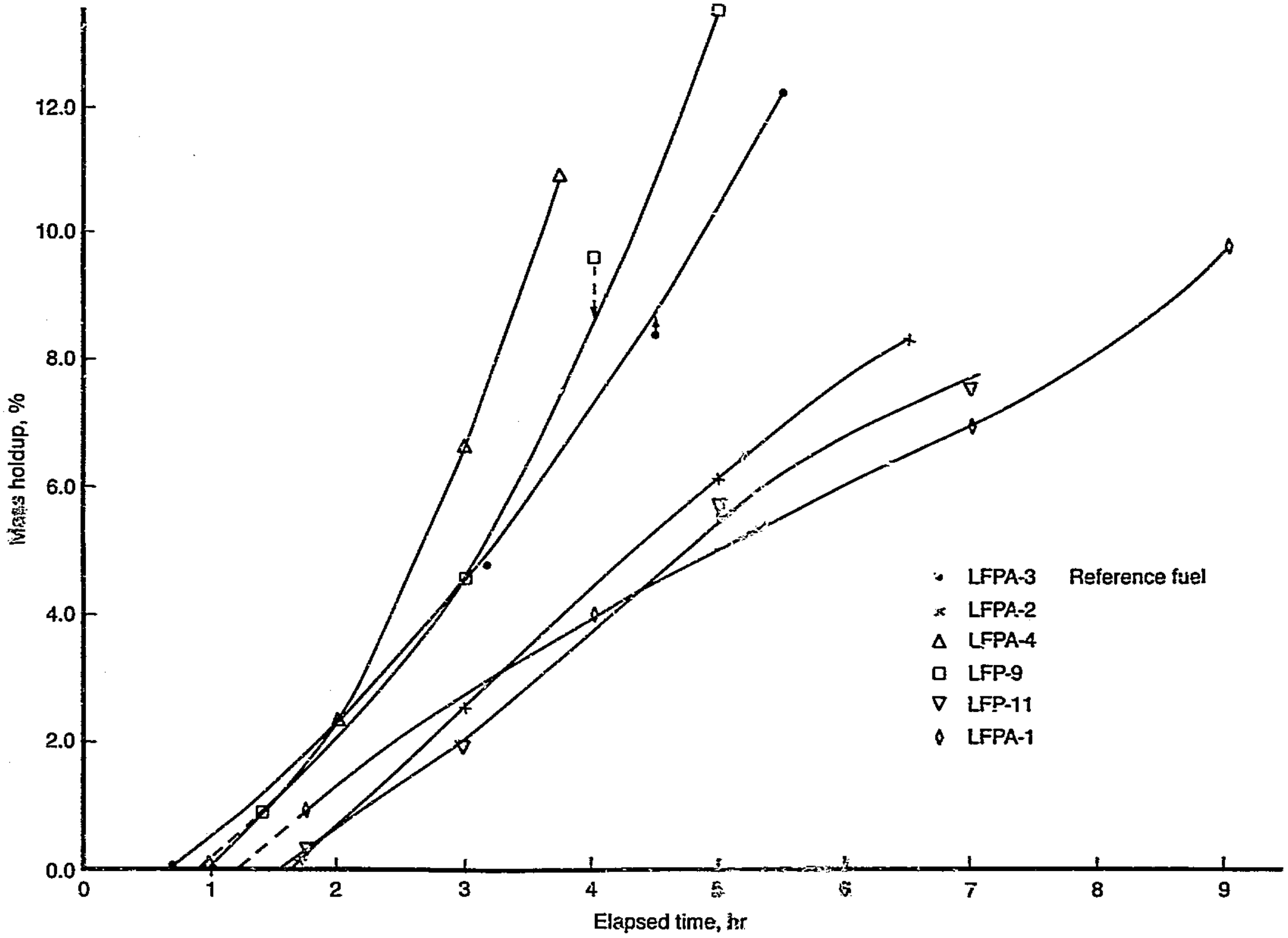

Figure 32. Comparison of Holdup Characteristics of Reference and Experimental Fuels

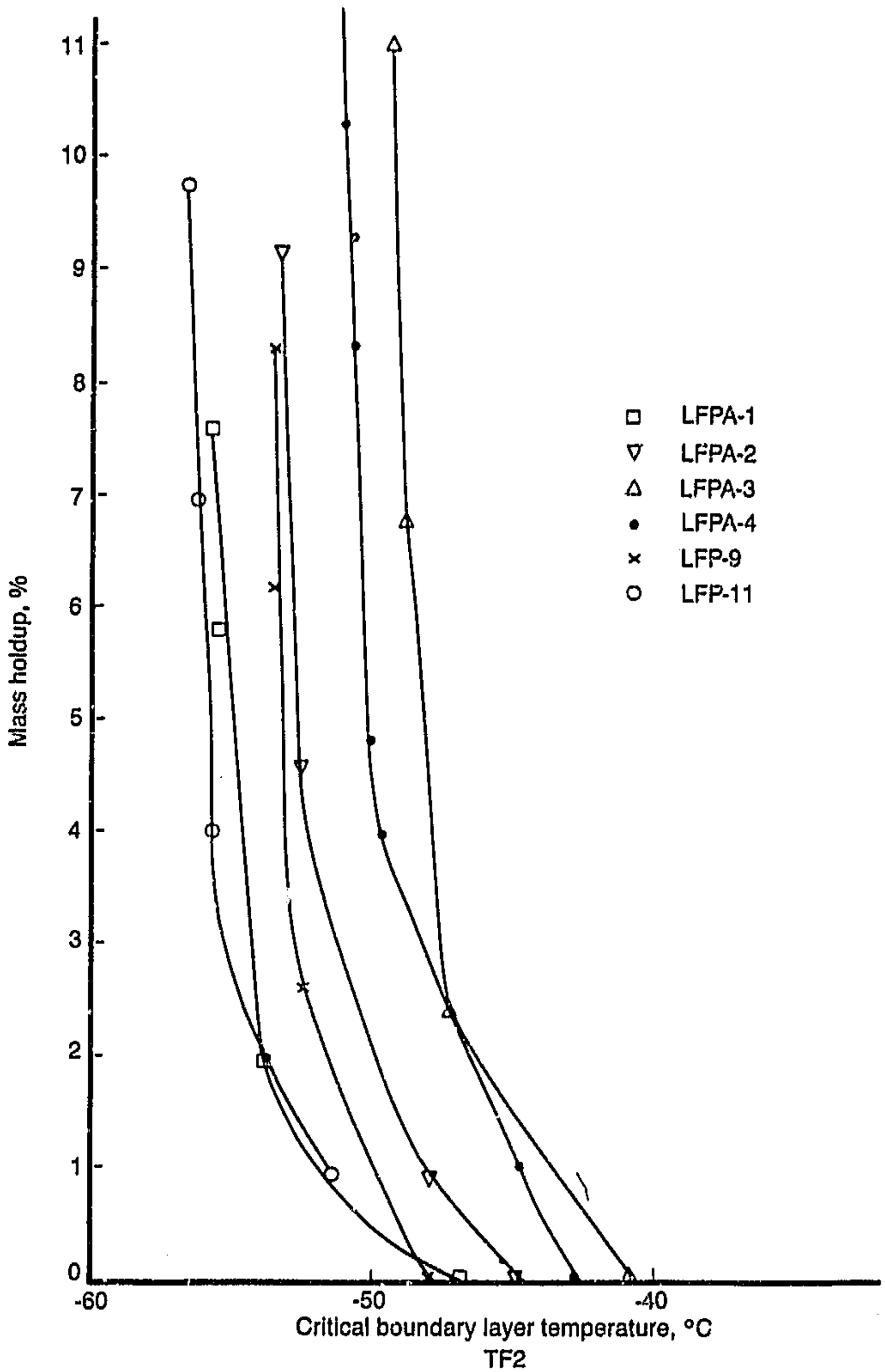

Figure 33. Correlation of Holdup With Critical Boundary Layer Temperature in Static Tests

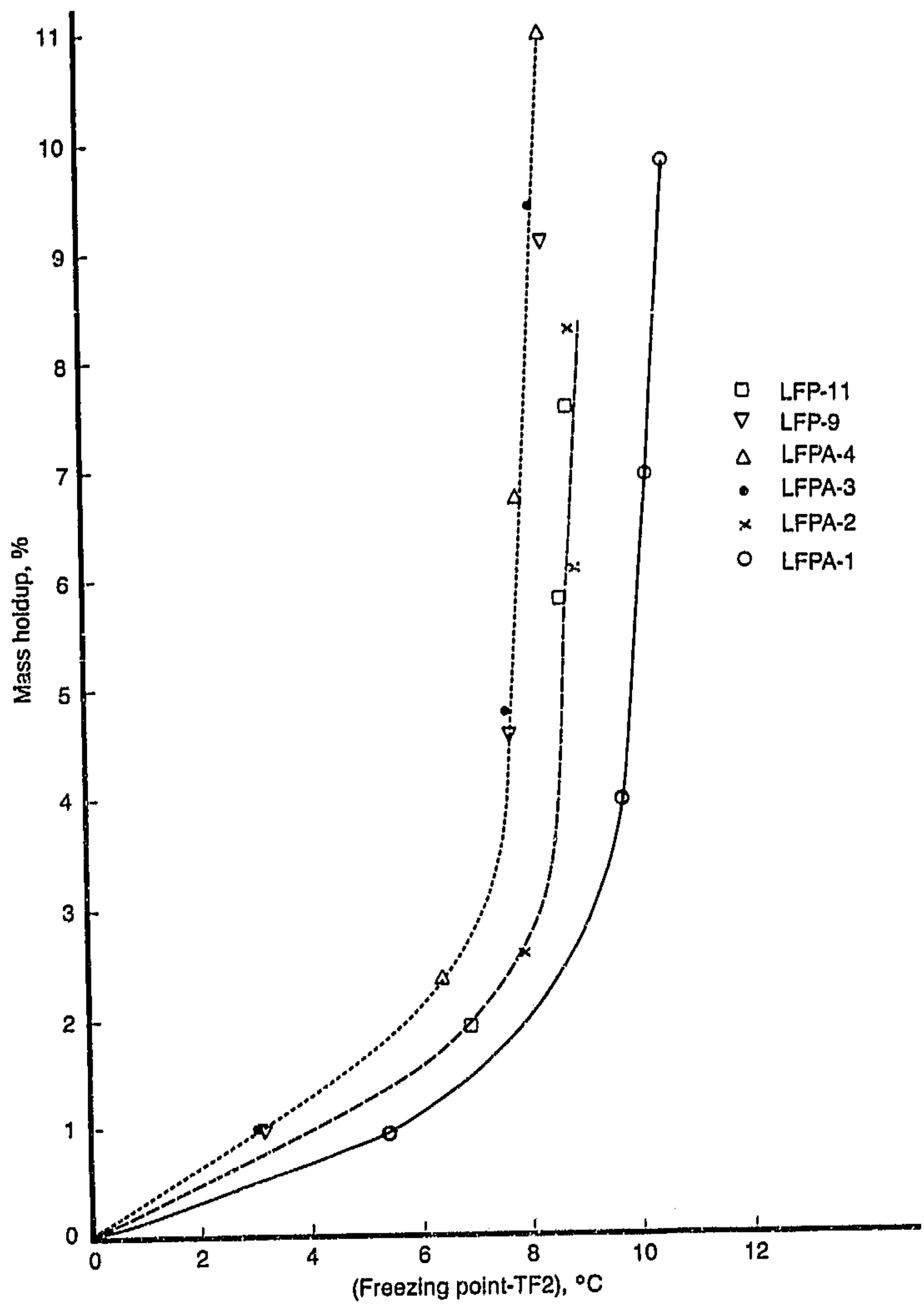

Figure 34. Correlation of Holdup With Normalized Critical Boundary Layer Temperature in Static Tests

defined: (1) both simulator skins programmed according to the airplane upper-skin history, (2) both simulator skins programmed according to the airplane lower-skin history, (3) upper and lower simulator skins programmed independently to duplicate the airplane history, and (4) both skins programmed to a modified schedule with an 8°C warming during the central 3 hr of flight (ABCDE in fig. 35). Figure 36 presents the holdup results for the flight simulation tests in bar graph form. For all variations of the TriStar simulations with both LFPA-4 and LFP-11, holdup was less than 0.5%. The effect of dynamic conditions appeared to be negligible. When tested over the extreme cold day simulation used in the reference fuel series (test 459), LFPA-4 did produce 5% holdup, appreciably greater than the corresponding results for the reference fuel (test 415, fig. 27).

Figure 37 represents the bulk temperature histories for two of the TriStar simulation tests. The final temperature was approximately -30°C for either LFPA-4 or LFP-11. For the airplane flight (the March 9, 1983 flight cited in ref. 12), the final bulk temperature was -34°C. The simulation tests produced bulk temperatures no colder than -31°C for any mode of simulation or dynamic conditions (fig. 38). While there is some resemblance between the internal temperature gradients in the flight wing tank and the simulator, the airplane obviously had higher heat transfer rates. This difference cannot be satisfactorily explained at this time, although one possibility is that the airplane tank had appreciable span and chordwise heat transfer, modes assumed negligible in the design of the simulator.

5.3 EXTERNAL FUEL HEATING AND RECIRCULATION TESTS

These tests were designed to evaluate the effectiveness of external fuel heating in improving the flowability of fuels near their freezing point temperatures. Heat transfer predictions as well as flight simulations confirm that initial fuel temperatures have insignificant impact on temperatures toward the end of the flight. Hence, the tests also assessed the effectiveness of external heating when delayed to later elapsed time, instead of continuous heating. Two fuels, LFPA-1 and LFPA-4, with marked differences in flowability characteristics, were selected for this part of the test program. Table 4 shows the list of tests conducted in this series.

5.3.1 Continuous Heating Tests

In these tests, skin temperature profiles were maintained as in similar unheated tests, and fuel was recirculated throughout the chilling phase (except the last 15 min) for heating. The fuel recirculation rate was nominally 3 L/min. Three different heat input conditions were defined. The lowest heat input corresponded to fuel recirculation through the fuel-oil heat exchanger circuit without any electrical heat addition on the oil side of the heat exchanger. The recirculated fuel gained heat due to the temperature difference between the plumbing and the ambient air as well as due to the work done by the electrical boost pump, which consumed about 250-275W during its operation. The maximum heat input was nominally 1200W, a value based on the estimates of a previous study (ref. 6) that modeled a 1/100-scale wing tank. An intermediate heat input was defined between the two extremes. For the minimum heat input, typical heat gains were calculated to be 357W (table 5). The intermediate rate was calculated to be typically 800W heating for 900W input (table 6). The maximum heating rate was calculated to be typically 1012W for 1200W input (table 7).

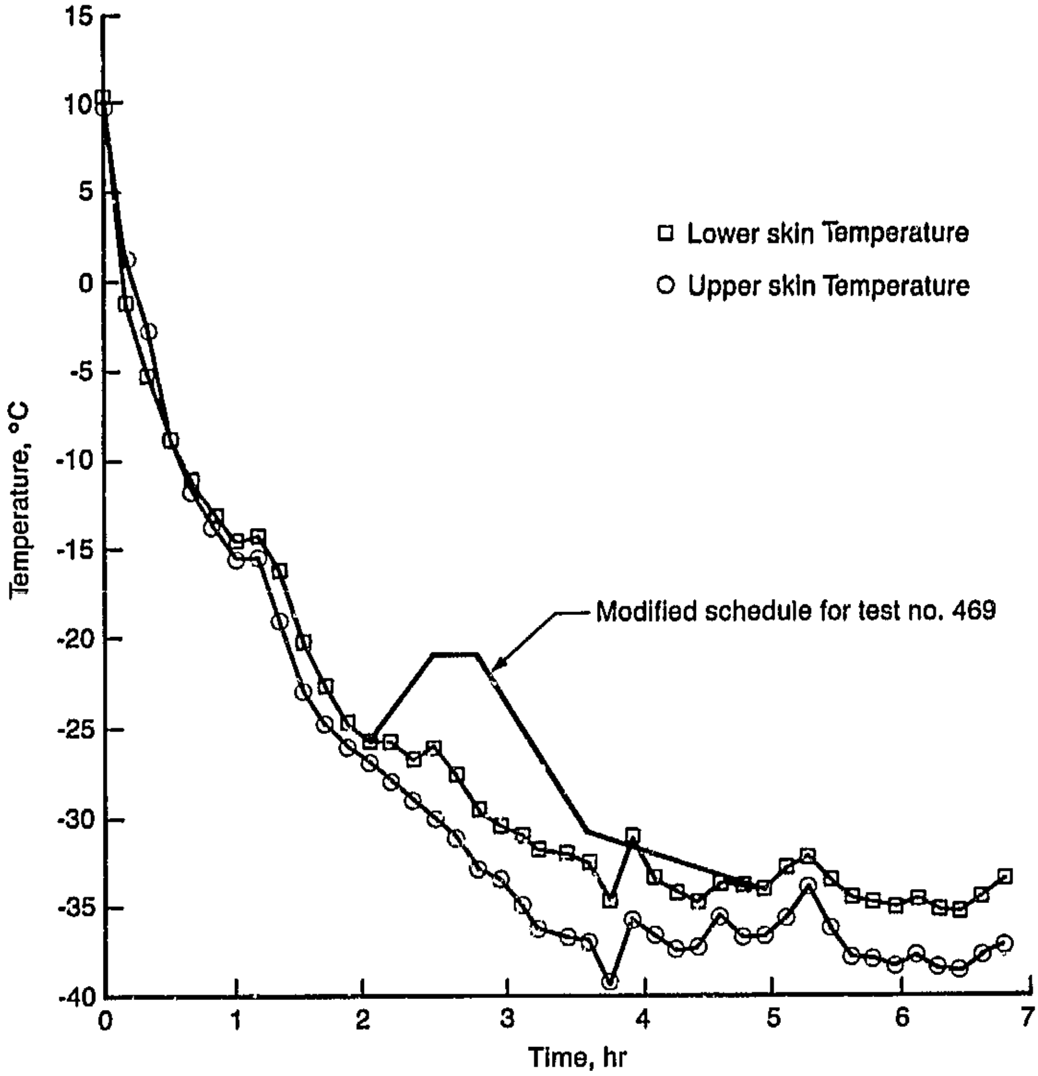

Figure 35. Skin Temperature Histories for TriStar Flight Simulation Tests

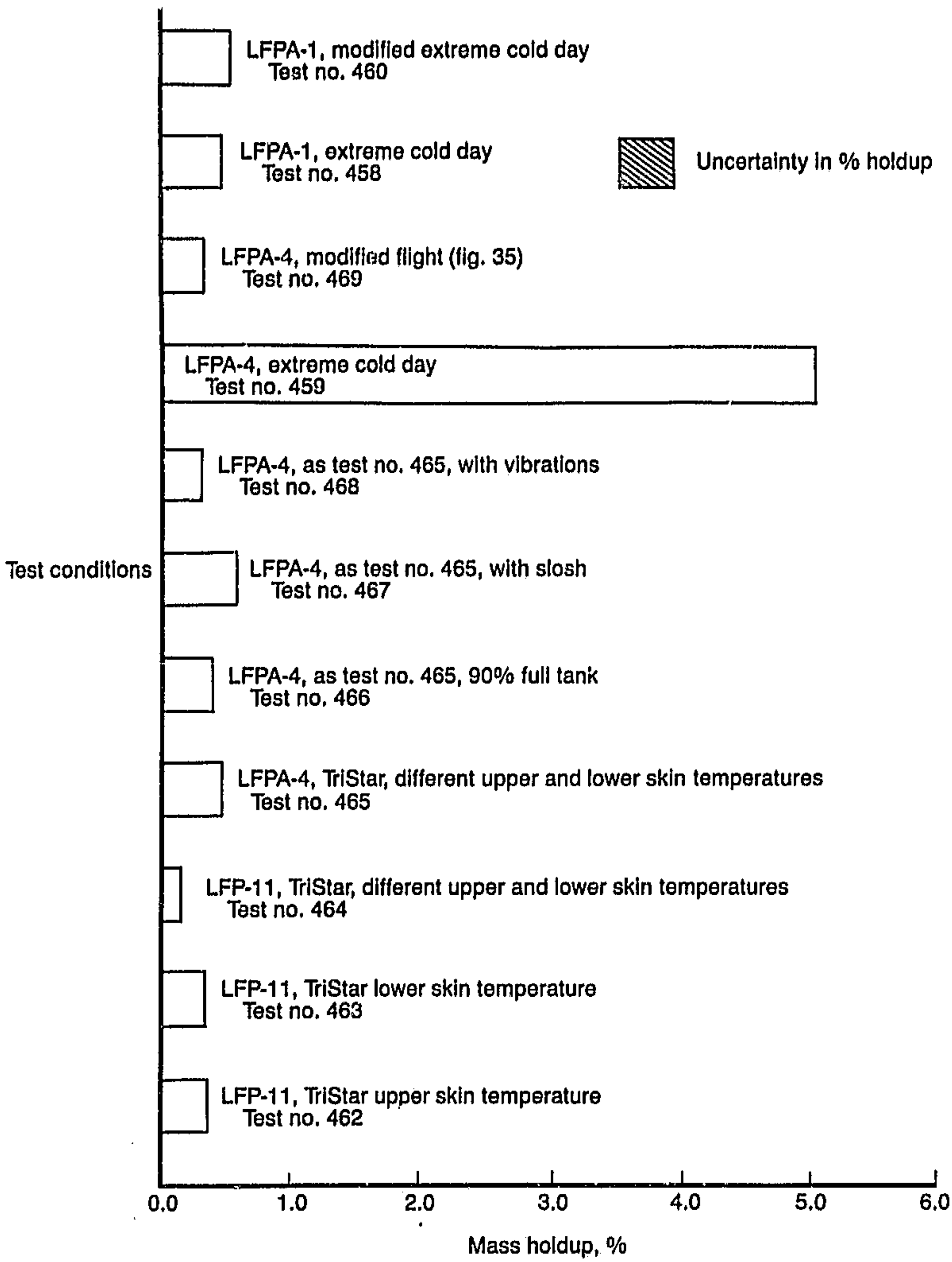

Figure 36. Comparison of Holdup Results From Flight Simulation Tests Using Experimental Fuels

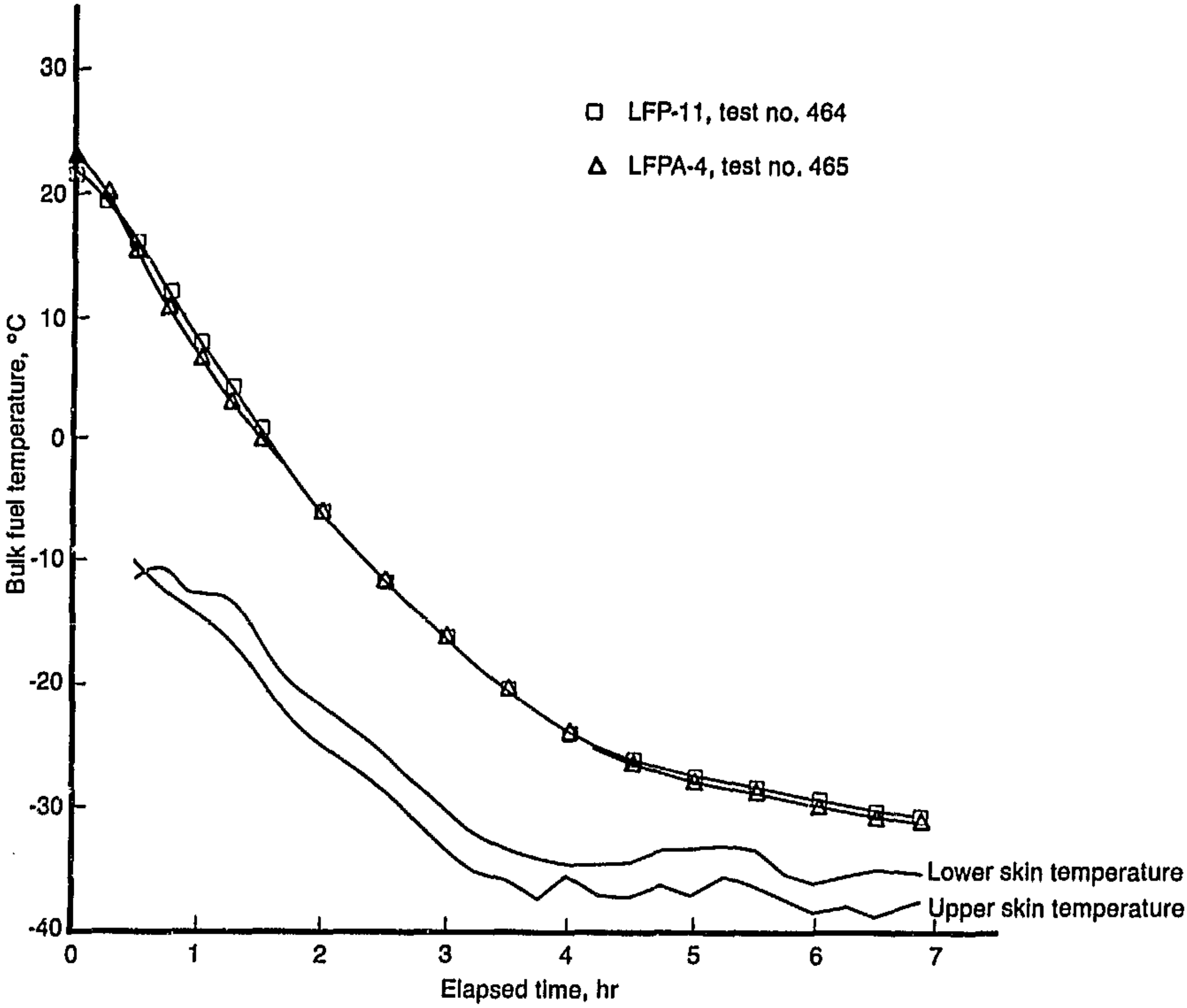

Figure 37. Bulk Fuel Temperature Histories From Flight Simulation Tests With Separate Upper and Lower Skin Temperatures

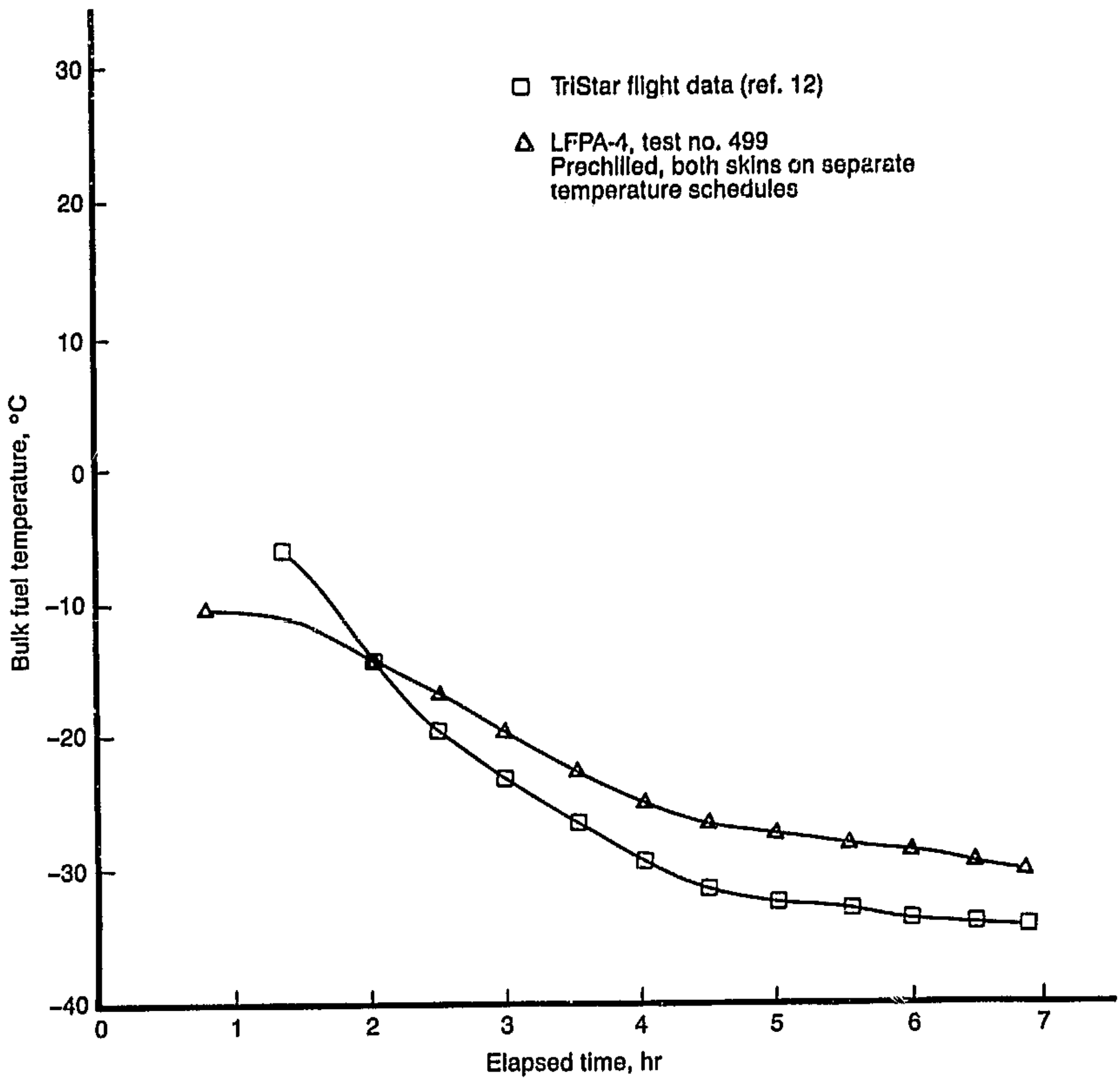

Figure 38. Comparison of Experimental and Actual Flight Bulk Fuel Temperature Histories

Table 4. List of Tests With External Heating and Recirculation

Fuel	Test no.	Test conditions	Chill time, hr.:min.	Holdup, %	Remarks
LFPA-4	474	Static, extreme cold day simulation with continuous recirculation (lowest heat rate)	7:30	1.25	
	476	As above with intermediate heat rate, 800-900W	7:30	1.07	
	477	As above with highest heat rate, 1200W	7:30	0.67	
	482	Static, extreme cold day simulation with 3-hr delayed recirculation	7:30	1.28	
	483	As above with highest heat rate, 1200W	7:30	0.50	
	484	Static, extreme cold day simulation with 5-hr delayed recirculation	7:30	1.69	
	485	As above with highest heat rate, 1200W	7:30	0.83	
	491	Static, continuous heating, highest heat rate, 1200W with skin temperatures at −51.1°C	3:30	1.28	
	492	As above with recirculation only	3:30	1.73	
	493	As above with intermediate heat rate, 900W	3:30	1.40	
	495	Static, constant coolant flow rates and inlet temperature with highest heat rate after 1-hr delay	3:30	1.07	
LFPA-4	496	Static, 2.5-hr delayed intermediate heat rate, 900W with skin temperatures at −51.1°C	3:30	2.00	
	497	Dynamic (vibrations), continuous intermediate heat rate 900W with skin temperatures at −51.1°C	3:30	1.50	
	498	As above with 97%-full tank and slosh	3:30	0.40	
LFPA-1	478	Static, extreme cold day simulation, continuous recirculation	7:30	0.39	No holdup
	479	As above with 3-hr delayed recirculation	7:30	0.49	Slight holdup
	480	As above with 5-hr delayed recirculation	7:30	0.48	Slight holdup
	487	Static, continuous highest heat rate, 1200W with skin temperatures at −55°C	6:00	0.78 / 0.69	
	488	As above without heat input (recirculation only)	6:00	0.95 / 0.80	
	489	As above with intermediate heat rate, 900W	6:00	0.97 / 0.70	

Total number of tests: 20

Table 5. Typical Fuel External Heat Gain Estimate for Recirculation Only

Test	Condition no.	Elapsed time, hr:min	Fuel flow rate, L/min	Fuel temperatures, °C (see figs. 9 and 10 for definition)				Nominal heat input, W	Actual heat gain by fuel, W
				T_{FO}	T_{RCI}	T_{RCO}	T_{FI}		
Test no. 492,	5	0:30	2.87	5.5	6.8	7.0	8.2	0	198
10-18-84,	7	1:00	1.73	–10.9	–7.4	–6.8	–4.2	0	297
LFPA-4,	9	1:30	1.08	–19.0	–13.3	–11.9	–7.8	0	309
constant skin temperatures	11	2:00	3.31	–23.8	–20.8	–20.9	–18.7	0	433
	13	2:30	3.16	–26.7	–23.9	–23.6	–21.3	0	438
	15	3:00	3.29	–28.8	–25.6	–25.7	–23.2	0	472

Average heat gain rate 357W
(For 3 hr 15 min)

Table 6. Typical Fuel External Heat Gain Estimate for Intermediate Rate

Test	Condition no.	Elapsed time, hr:min	Fuel flow rate, L/min	Fuel temperatures, °C (see figs. 9 and 10 for definition)				Nominal heat input, W	Actual heat gain by fuel, W
				T_{FO}	T_{RCI}	T_{RCO}	T_{FI}		
Test no. 493,	5	0:30	3.03	4.6	5.5	11.1	11.5	900	536
10-19-84,	7	1:00	2.96	−9.0	−6.9	0.6	1.6	900	804
LFPA-4,	8	1:15	3.11	−13.4	−11.0	−3.1	−1.9	900	917
constant skin temperatures	10	1:45	3.02	−19.3	−16.4	−9.4	−6.4	900	998
	12	2:15	2.26	−22.0	−18.2	−7.8	−7.0	900	869
	16	3:15	3.20	−24.9	−22.0	−12.9	−11.8	900	1074

Average heat gain rate 800W
(For 3 hr 15 min)

Table 7. Typical Fuel External Heat Gain Estimate for Highest Rate

Test	Condition no.	Elapsed time, hr:min	Fuel flow rate, L/min	Fuel temperatures, °C (see figs. 9 and 10 for definition)				Nominal heat input, W	Actual heat gain by fuel, W
				T_{FO}	T_{RCI}	T_{RCO}	T_{FI}		
Test no. 491,	5	0:30	2.80	−1.6	−.3	6.2	6.6	1200	586
9-28-84,	7	1:00	2.90	−14.0	−11.4	0.0	−0.7	1200	988
LFPA-4,	9	1:30	2.85	−20.1	−17.5	−6.7	−5.5	1200	1068
constant skin temperatures	11	2:00	3.20	−22.3	−19.7	−10.3	−8.6	1200	1125
	13	2:30	2.83	−24.0	−20.9	−8.5	−8.9	1200	1095
	15	3:00	2.92	−25.1	−21.8	−8.2	−8.9	1200	1212

Average heat gain rate 1012W
(For 3 hr 15 min)

Figure 39 compares the temperature profile history for a heated fuel test to a corresponding unheated test. The most remarkable feature in the plots is the reduction of the lower thermal boundary layer. In the unheated tests the fully developed boundary layer was 10-cm thick (19% of the tank height)[1]. In the heated test it was 5-cm thick (9.5% of the tank height), giving a 9.5% tank height reduction or 50% boundary layer reduction.

The figure also shows that the bulk fuel temperature at the end of the test was 10.8°C higher. This temperature increase corresponds to about 344W heat input over 195 min into 178 kg of fuel in the tank. This is about 34% of the maximum 1012W of heat input to the fuel and indicates that a large portion (66%) of heat gained by fuel due to recirculation and external heat input was lost through various transfer mechanisms, including chilling of upper and lower skins.

Figure 40 compares bulk temperature histories for a static, unheated test with LFPA-4 to those for tests with three levels of heating. Minimum recirculation heating increased the final bulk temperature by 6.5°C. Intermediate heating increased the final bulk temperature by 10°C compared to the unheated test, but maximum heating produced no further increase in bulk temperature. Holdup results are also shown on the figure. Minimum heating reduced holdup substantially, but there were little further improvements with increased heating rates.

Since a high percentage of externally added heat is shown to be lost from the fuel through skin chilling, a special test was conducted in which the coolant flow rates rather than skin temperatures were duplicated in unheated and heated tests. The final bulk fuel temperatures differed by insignificant amounts in the comparison tests. The intention here was to determine, if, by removing approximately the same amount of heat through the tank upper and lower skins, more externally added heat could be retained in the heated test compared to the reference unheated test. A comparison of results showed some improvement in this regard, since the bulk temperature difference of 11.0°C in 135 min of external heating corresponds to 506W which is 50% of average heat gain by fuel through recirculation and heating. The remainder of the external heat input was presumed lost to the chilling system. The exact amount of heat removed through the skins could not be calculated due to the lack of continuous and precise coolant temperature data and also due to unavailability of precise methods to determine the fraction lost through the supporting structure. From another point of view, the higher fuel temperature decreases the temperature difference beween the ambient and the fuel. Thus, relatively less heat is gained from the ambient compared to the unheated test. In any case, it is safe to assume that in external heating cases, only 35 to 50% of actual heat acquired by the fuel could be expected to be useful in improving flowability (a view in qualitative agreement with that of ref. 16).

Two of the heated tests were performed to evaluate effects of dynamic conditions and heating. Again, as in the unheated tests, vibrations had a negligible effect on flowability as shown by holdup. Slosh with heating produced practically zero holdup as expected, since cooling from the upper skin was reduced by the unwetted upper surface.

Several fuel heating tests were conducted with LFPA-4 fuel using the extreme cold day flight schedule. The bulk temperature histories are plotted in Figure 41. Minimum heating increased the final bulk temperature, compared to the unheated test, by 6°C. Intermediate heating increased bulk temperatures by 10°C; maximum heating increased bulk temperatures by 13°C. As in the static heating tests, most of the holdup reduction occurred with minimum heating, but there were some further improvements at the higher heating rates.

---

[1] The thermal boundary layer thickness was determined from the criterion that the fuel temperature at the location marking the end of boundary layer should be within 0.5°C of the bulk fuel temperature.

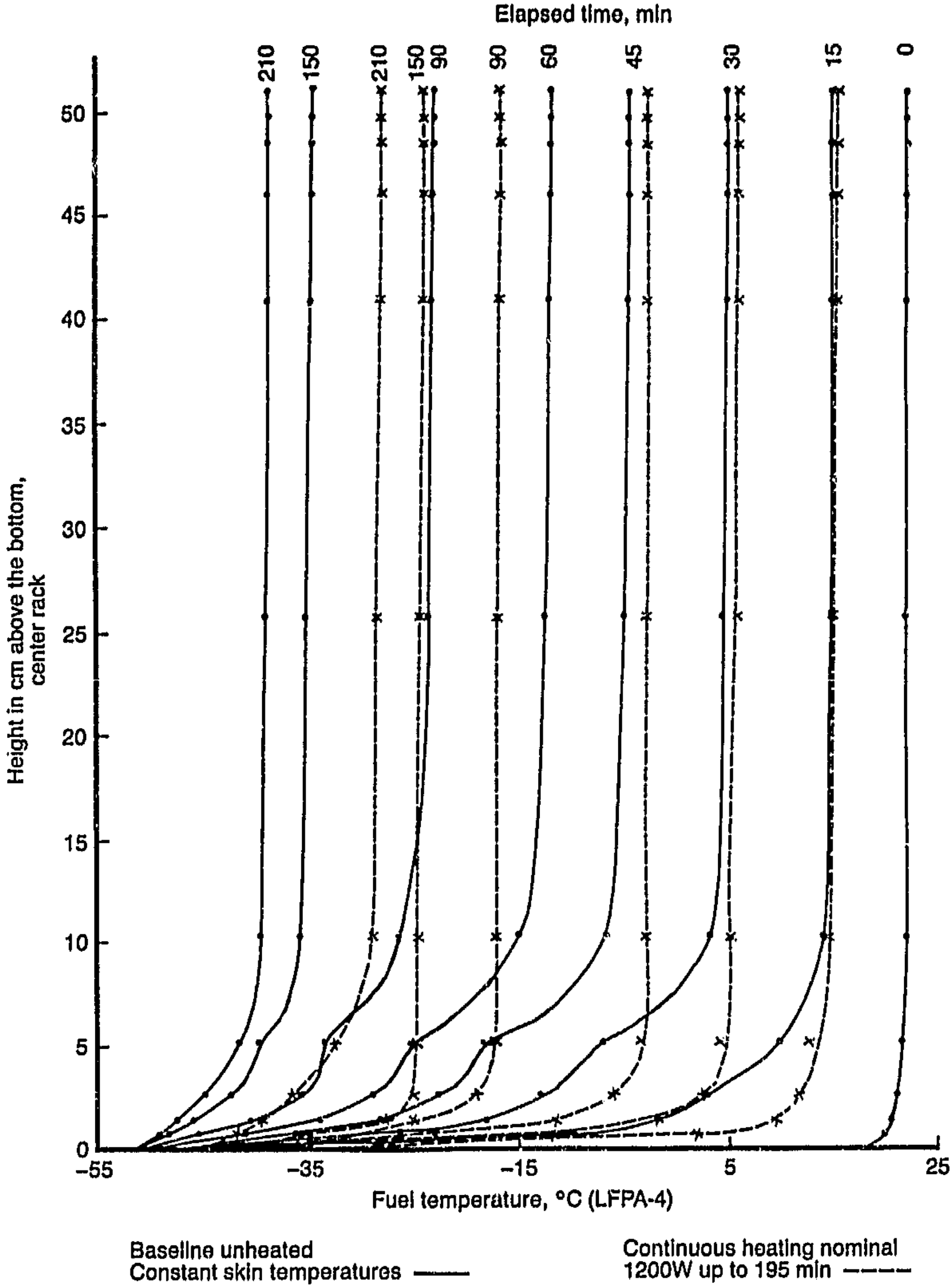

Figure 39. Thermal Boundary Layer Reduction and Fuel Temperature Gain Due to External Heating

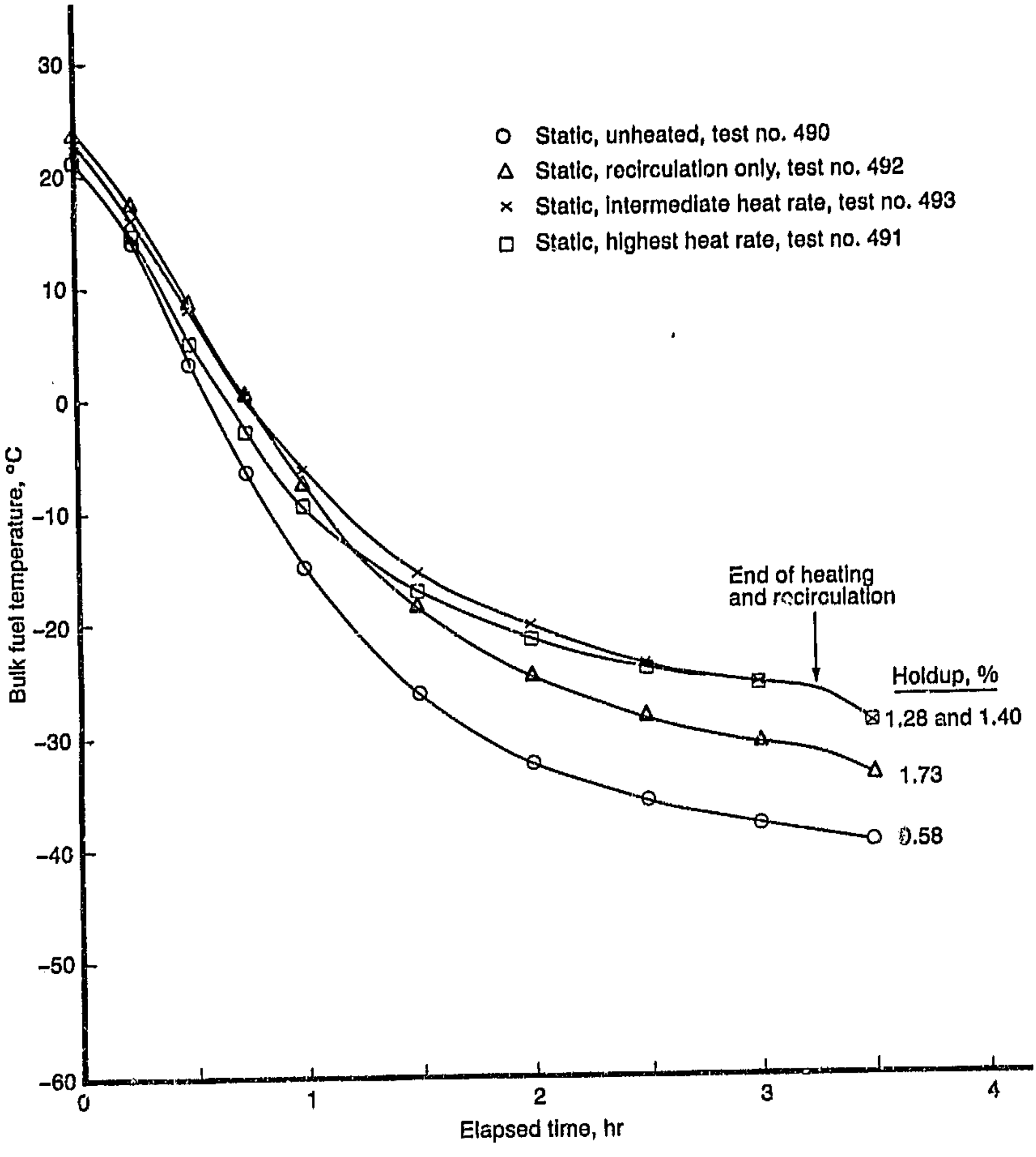

Figure 40. Bulk Fuel Temperature Histories for Unheated and Heated Tests, LFPA-4

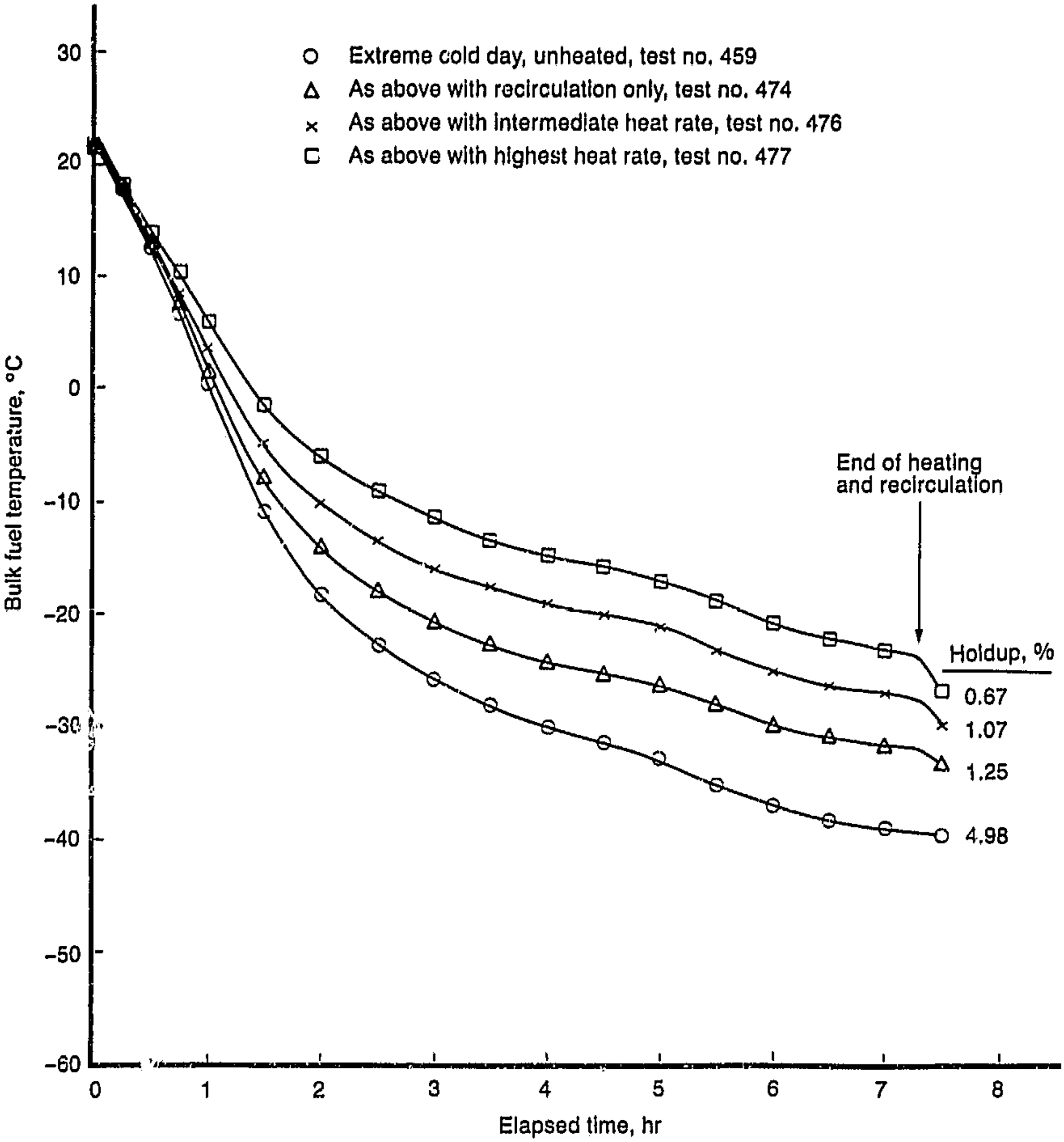

Figure 41. Bulk Fuel Temperature Histories in Flight Simulation With External Heat, LFPA-4

Static heating tests with LFPA-1 fuel showed bulk temperature and holdup results similar to those with LFPA-4, although the holdup reductions for this smallholdup fuel were not as dramatic.

5.3.2 Delayed Heating Tests

Most delayed heating tests were performed with the extreme cold day profile. Figure 42 presents holdup results, comparing delayed and continuous heating. For the minimum heating (recirculation only), the 3-hr delay had no effect on holdup, while the 5-hr delay increased holdup slightly. For the maximum heating, the 3-hr delay test even showed a small improvement in holdup, but there is generally little difference in the results. Bulk temperature histories are compared in Figure 43. The effect of heating is apparent as an immediate increase in bulk temperature. Final temperatures are within a degree for the same rate of heating, whether continuous (not shown in fig. 43), delayed 3 hr, or delayed 5 hr. Figure 44 is the same comparison for the critical boundary layer temperature histories. Because heating time has a greater effect on the temperature gradients and the boundary layer temperatures, the final temperatures differ for the different onsets of delayed heating. Delayed heating tests were also conducted with LFPA-1 fuel. In all cases holdups were small, within the uncertainty of the measurements, and comparisons of delayed and continuous heating for this fuel were inappropriate.

The holdup results and temperature profiles indicate that external heating is as effective in the delayed mode as in the continuous mode if the heating is initiated after the skin temperatures fall to within 5°C of the fuel freezing point. The heated fuel test results also indicate that even the minimum rate of heating is effective in a fuel that would normally produce a high holdup.

The simulator tank represents approximately a 1/100-scale model of a wing tank. Thus, the minimum heating rate of 357W is equivalent to about 35 kW in a full-scale wing tank. References 2, 14, and 17 discuss heating concepts for use of high-freezing-point fuels in commercial airplanes, assuming about 50 kW for minimum effectiveness. The optimum efficiency of fuel heating depends on the heat source, the means of heat exchange, and the minimum acceptable holdup (ref. 11), since holdup may not be completely reducible to zero.

5.4 FLOW IMPROVED FUEL TESTS

As an alternative to recirculation and heating to improve fuel flowability essentially by increasing its temperature, it is possible to improve the flowability at low temperatures by using additives. The additives are believed to inhibit the formation of a solidified fuel matrix that has a tendency to trap still liquid fuel, preventing its flow. Table 8 lists the series of tests conducted to evaluate the flowability of the flow improved fuels.

5.4.1 Selection of Additives

Four different additives were obtained as courtesy samples from the Exxon Chemical Company through NASA. The limited series of tests were not intended to evaluate the additives themselves, nor did their use imply that the formulations were optimized for jet fuel improvement. The additives for the simulator tests were selected from initial pour point measurements with additive-modified LFPA-1 and LFPA-4 fuels. For LFPA-1, a commercial

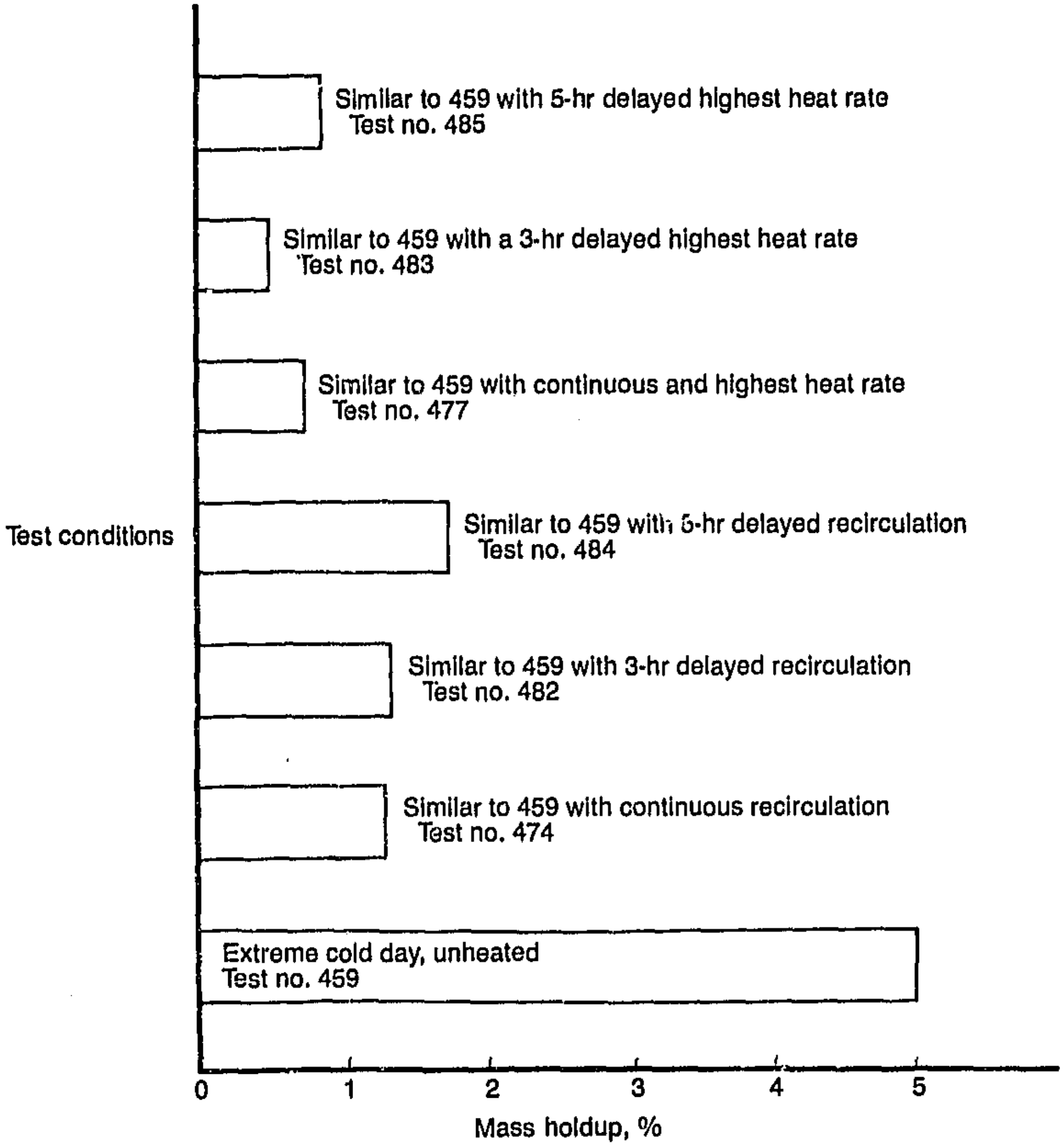

Figure 42. Comparison of Holdup Results From Continuous and Delayed Heating, Flight Simulation Tests, LFPA-4

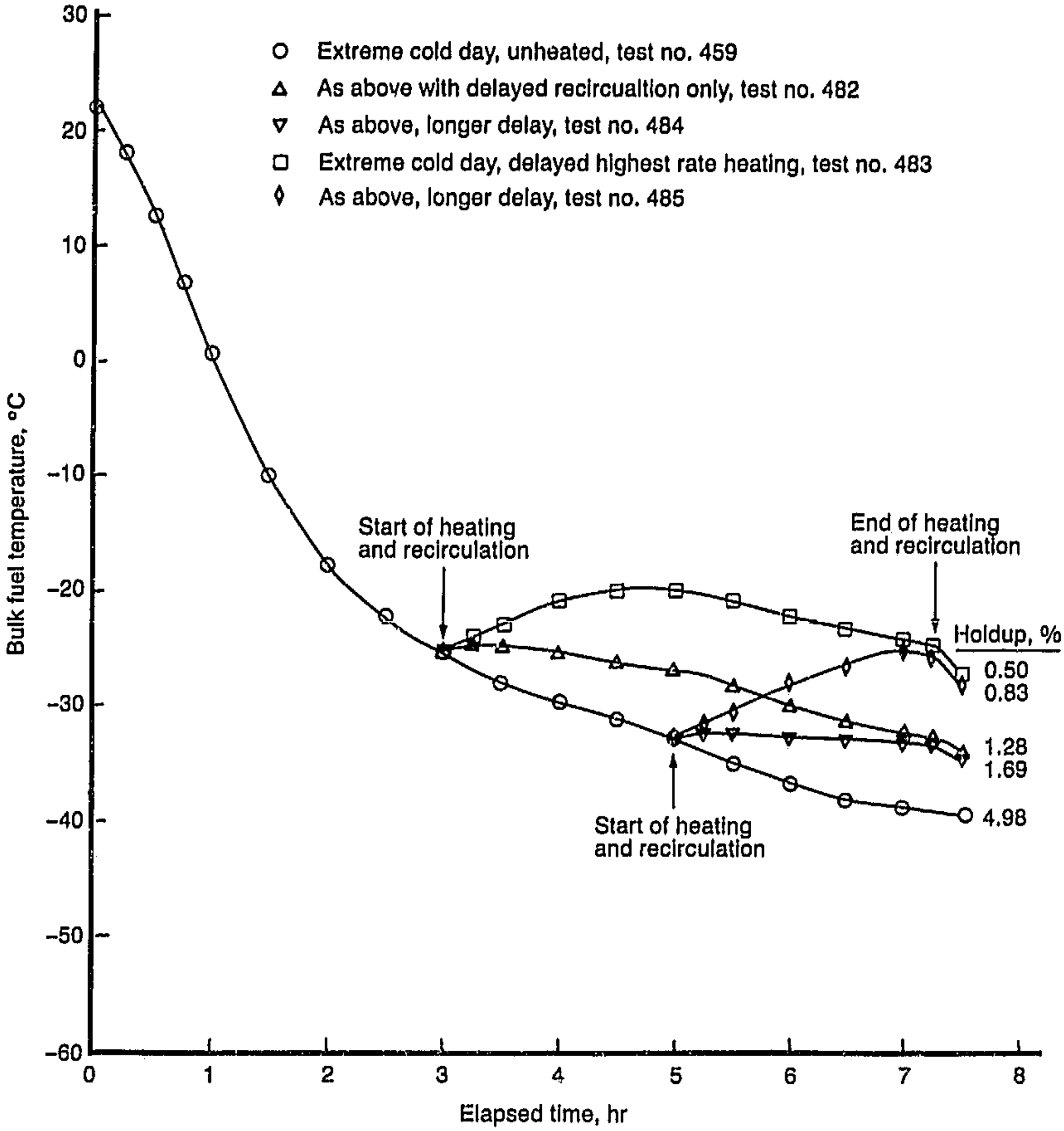

Figure 43. Bulk Fuel Temperature Histories in Delayed Heating, Flight Simulations With LFPA-4

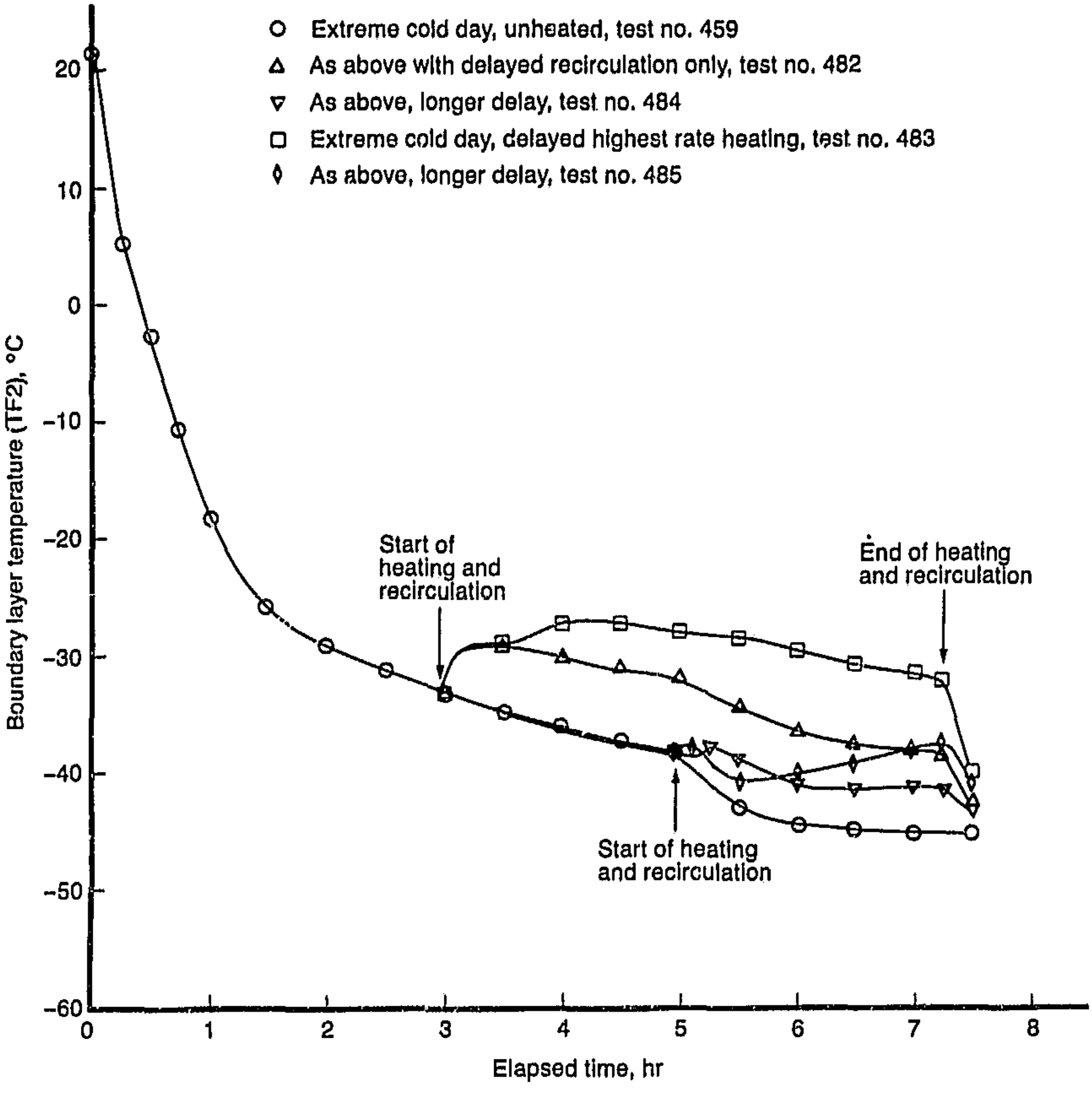

Figure 44. Critical Boundary Layer Temperature Histories in Delayed Heating, Flight Simulations With LFPA-4

Table 8. List of Tests With Flow-Improved Fuels

Fuel	Test no.	Test conditions	Chill time, hr.:min.	Holdup, %	Remarks
Modified LFPA-4 (1000 ppm No. 151 additive)	502	Static, skin temperatures at −51.1°C	1:00	0.80	
	503		2:00	1.67	
	504		3:00	4.32	
	505		3:45	7.62	
	510	Dynamic (slosh), tank 97%-full, skin temperatures at −51.1°C	3:30	3.22	
	511	Static, extreme cold day simulation	7:30	1.72	
	512	As above with intermediate heat rate, 900W	7:30	1.07 / 0.55	
	513	As above, recirculation only	7:30	0.80 / 0.54	
	514	Static, skin temperatures at −47°C	2:00	0.38	No holdup
	515	Static, skin temperatures at −49°C	4:00	4.10	
Modified LFPA-1 (1000 ppm Paradyne 25 additive)	506	Static, skin temperatures at −57°C	1:45	0.63	
	507		9:00	3.52	
	508		4:00	1.11	
	509		7:00	3.05	

Total number of tests: 14

additive, Paradyne 25, was chosen for further testing on the basis of a reduction of pour point by about 5°C at a 1000 ppm concentration. For LFPA-4, a high-wax fuel, modification was difficult. The selected additive, a proprietary blend no. 151, reduced pour point by about 2.5°C at a 1000 ppm concentration.

5.4.2 Modified Fuel Tests.

Static holdup tests were conducted with both fuels. Both additives were effective in improving the flowability (fig. 45). For test conditions in which unmodified LFPA-4 produced holdups greater than 2%, the presence of the flow improver additive reduced the holdup by about 32% on the average. With LFPA-1, this corresponding average reduction was 64%. This implies that the effectiveness of Paradyne 25 in LFPA-1 was twice that of no. 151 in LFPA-4 as far as the flowability improvement is concerned. In the initial pour point tests, the same relative improvement was noted, that is, the reduction in pour point (in Kelvin) for LFPA-4 was twice that of LFPA-1. Thus, from these rather limited number of tests, it appears that the flowability improvement as measured by holdup may be predictable from the pour point suppression.

Temperature profile histories for a modified and unmodified test with LFPA-4 are compared in Figure 46. The modified fuel test started with 3°C higher bulk temperatures, but the bulk temperatures were the same by the end of the two tests. The temperature gradients were different, however. The modified fuel appeared to have a smaller boundary layer, possibly due to better conduction (less wax buildup) near the bottom skin.

Static tests with modified LFPA-4 gave the same relative holdup reduction, even for a test with a reduced chilling rate. However, a test with the extreme cold day flight simulation gave a 65% reduction in holdup compared to the unmodified case. It may be that the effectiveness of the flow improver is related to the difference between the skin temperature and the fuel freezing point. For the flight simulation test, the skin temperatures were below the freezing point for only the last 2.7 hr of a 7.5-hr test and the difference did not exceed 5.4°C, whereas in other tests, skin temperatures were 8 to 10°C below the fuel freezing point for a greater portion of the test time.

Figure 47 presents the results of the modified fuel holdup tests with LFPA-4. A slosh test was performed with this fuel. Holdup was reduced 50% compared to the static results for the same modified fuel. As in the tests with the unmodified fuels, the holdup reduction was due to reduced heat transfer from the unwetted upper surface, causing higher bulk temperatures throughout the test. Two tests imposed external fuel heating on the modified fuel, using the extreme cold day simulation. The minimum heating rate reduced the modified fuel holdup by 41%. Higher rates of heating had no further influence on holdup.

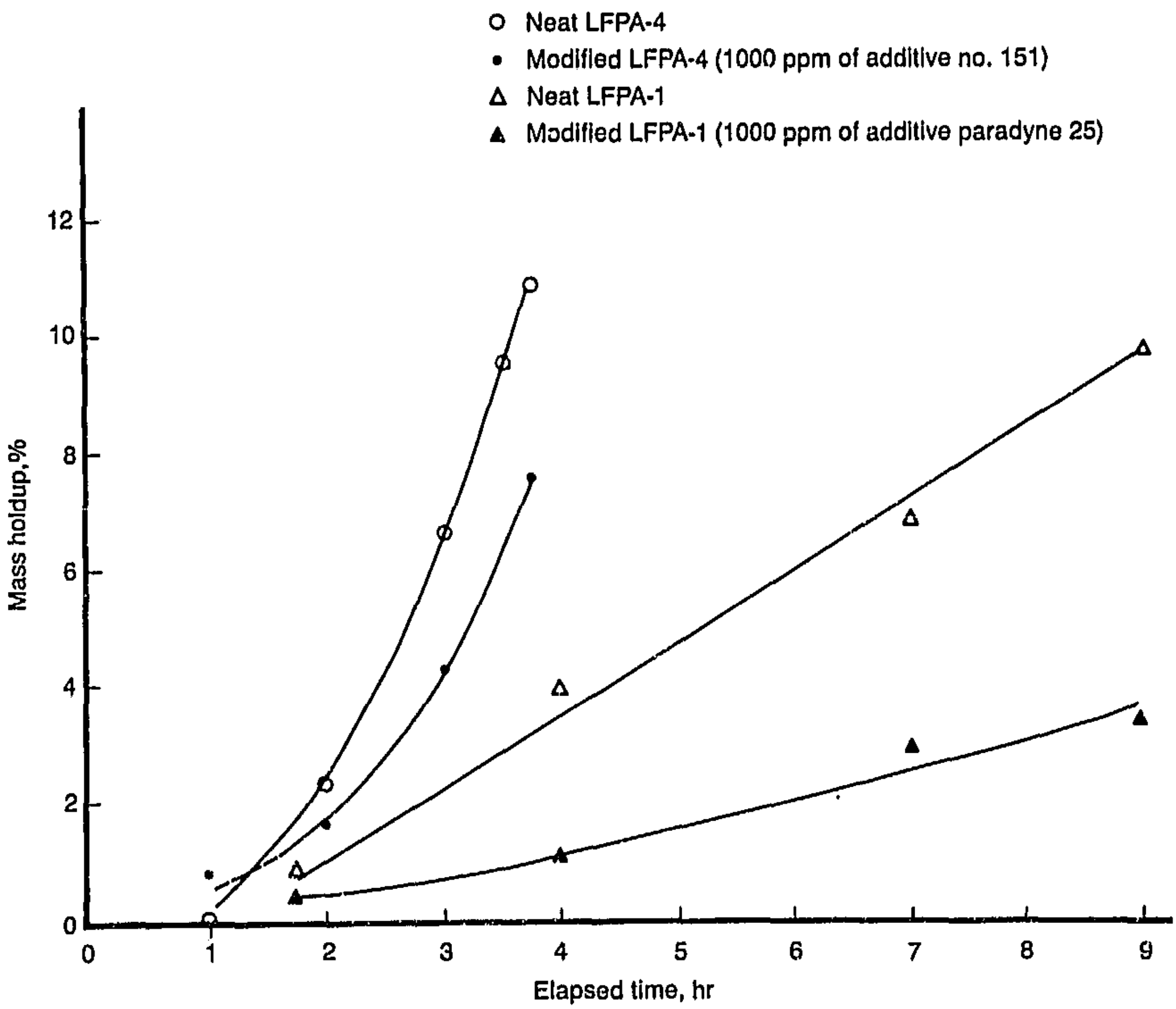

Figure 45. Holdup Reduction Due to Flow Improver Additives

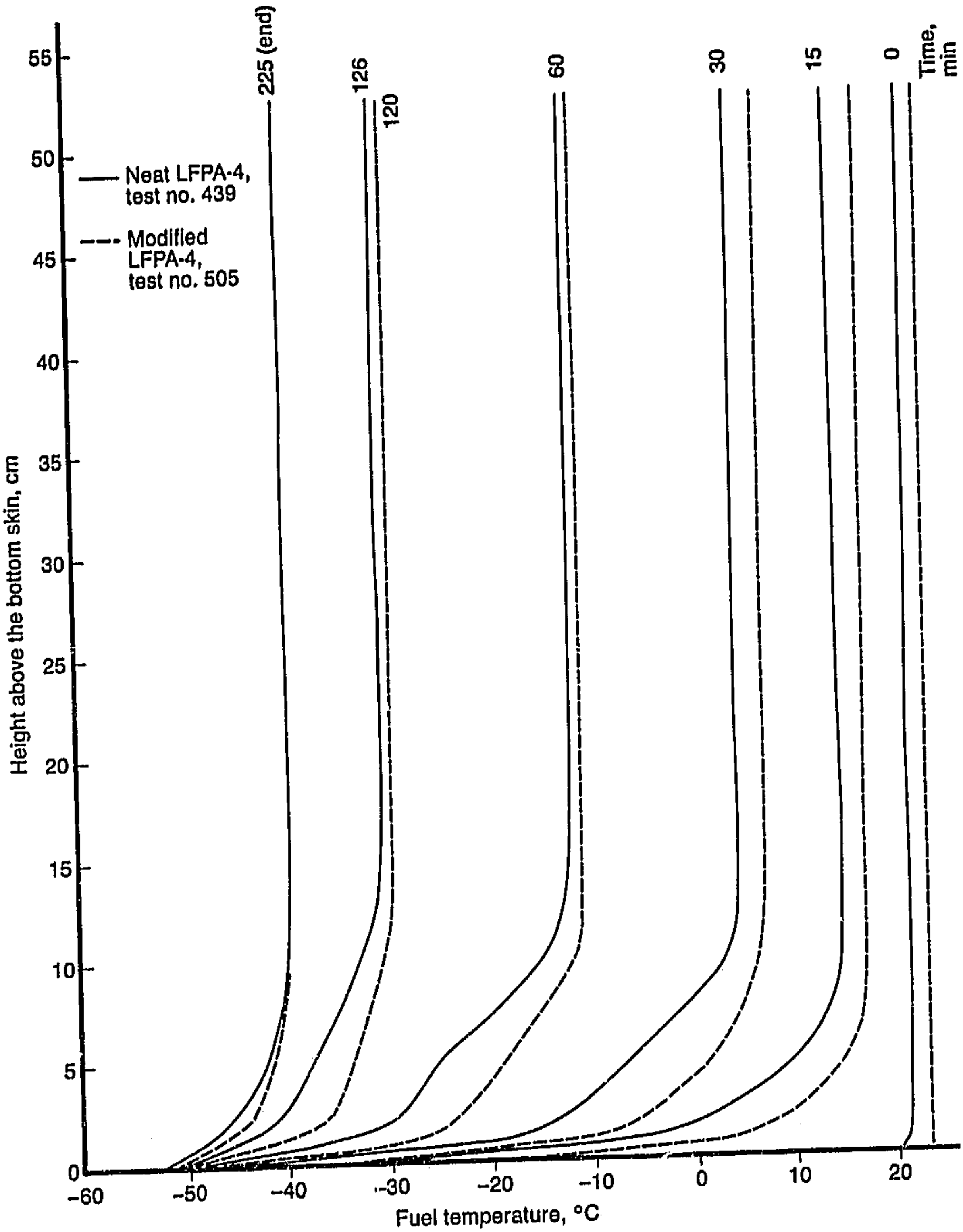

Figure 46. Temperature Profiles Under Identical Test Conditions With Neat and Modified LFPA-4

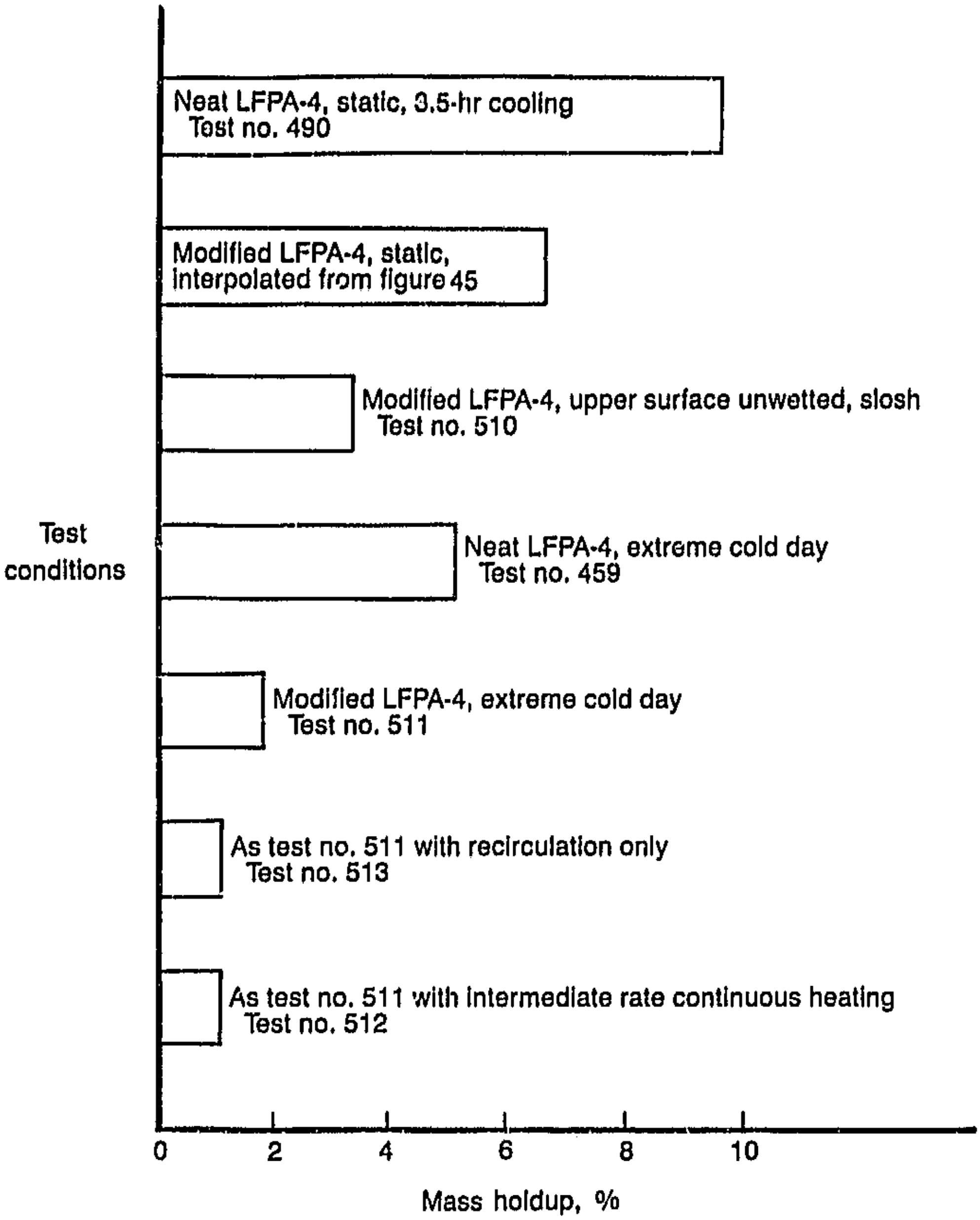

Figure 47. Comparison of Holdup Results From Modified LFPA-4 Tests With Different Chilling Rates, Dynamic Conditions and External Heating

6.0 SUMMARY OF RESULTS

A large array of tests conducted in a wing tank simulator provided extensive data useful in the study of aviation fuel flowability at low temperatures. From the data presented in the preceding section, the following results may be stated.

1. The flowability of fuel at low temperatures depends on its composition. Fuels with small differences between their freezing points exhibited widely differing flowability behavior as characterized by unpumpable fuel quantity after similar cooling conditions and times. In static tests with tank skin surfaces at 10°C below the fuel freezing point, mass holdup varied up to 13.5% depending on the fuel and the chill period.
2. The rate of cold fuel withdrawal has a slight but probably insignificant effect on the flowability.
3. Dynamic conditions such as vibrations or slosh imposed on the tank produce very little, if any, change in either the lower thermal boundary layer or the unpumpable fuel quantity.
4. The correlation of holdup with fuel temperature at a critical boundary layer location, 0.6 cm from the tank bottom surface, yielded a separate curve for each fuel. However, when the difference (freezing point - boundary layer temperature) was used instead, a clear pattern emerged. Three separate correlations appeared. The first was for three fuels with freezing point and pour points within 1°C and inferior flowability. The second was for two fuels with this difference greater than 5°C and improved flowability. The remaining fuel LFPA-1 with this difference equal to about 5°C had a unique correlation showing even better flowability.
5. Simulation of extreme cold day commercial flight histories by programming the time variations of the tank skin temperatures produced only small holdups in the range 1 to 5%. These were further reduced when the upper surface was unwetted. Moreover, when the warming phase at the end of flight was simulated, no holdup occurred.
6. External fuel heating and recirculation was an effective means of reducing the thermal boundary layer thickness as well as holdup. In the simulator a minimum heat input of about 360W net was generally sufficient for this purpose. In addition, the effectiveness of delayed heating is comparable to continuous heating. That is, if the heating is started when the bulk fuel temperature is within 5°C of the fuel freezing point, most holdup is eliminated just as in a continuously heated case.
7. Flow improver additives can significantly reduce holdup and improve flowability. However, their effectiveness may be less than the external heating method of improving flowability.

7.0 CONCLUDING REMARKS

The results of the wing simulator test program have considerably enhanced the data base on aviation turbine fuel flowability at low temperatures. Fuel composition, particularly wax or n-paraffin content, has the major influence on flowability as defined by the unpumpable holdup at given temperature or chilling time conditions. Freezing point is only a general guide to fuel behavior. Flowability is better characterized by the pour point or the difference between freezing and pour points. Fuels with larger differences have superior low temperature flowability properties.

The six test fuels were chosen to show compositional variations, but they all met current Jet A freezing point specifications. Tests simulating very low probability, extreme cold day flight conditions showed that these fuels could operate with less than 5% holdup, or unavailable fuel. Furthermore, even this small amount of unavailable fuel is recoverable during the descent, or warming phase, of the simulated flight. Dynamic conditions, such as vibrations, slosh, and the rate of pumpout, have minor effects, if any, on flowability. Fuel heating was shown to be an effective means of enhancing low temperature flowability, and only moderate rates of heating (such as from external fuel recirculation alone) may be sufficient for this purpose. Flow-improving additives also show promise, but more research is needed to optimize these additives for use with aviation turbine fuels.

In general, it may be concluded that jet fuels with moderately higher freezing points than present fuels, or fuels with higher fractions of waxy components, may be feasible for commercial flight use in conjunction with moderate heat input, flow-improving additives, or both.

8.0 REFERENCES

1. P. T. Ford and A. G. Robertson, "Jet Fuels Redefining the Low Temperature Requirements," Shell Aviation News, No. 441, July 1977, pp. 22-26.
2. R. Friedman, "High-Freezing-Point Fuels Used for Aviation Turbine Engines," ASME Paper 79-GT-141, March 1979.
3. D. V. Byrne, "An Experimental Study of Fuels Near or Below Their Freezing Point," Boeing Document D6-48572, 1979. (Available on request.)
4. F. J. Stockemer, "Experimental Study of Low Temperature Behavior of Aviation Turbine Fuels in a Wing Tank Model," NASA Contractor Report CR-159615, 1979.
5. R. Friedman and F. J. Stockemer, "Temperature and Flow Measurements on Near-Freezing Aviation Fuels in a Wing-Tank Model," ASME Paper 80-GT-63, 1980.
6. F. J. Stockemer, "Experimental Study of Fuel Heating at Low Temperatures in a Wing Tank Model," NASA Contractor Report CR-165391, 1981.
7. F. J. Stockemer and R. L. Deane, "Additional Experiments on Flowability Improvements of Aviation Fuels at Low Temperatures," NASA Contractor Report CR-167912, 1982.
8. P. M. McConnell, L. A. Massmann, G. N. Peterson, and F. F. Tolle, "Fuel/Engine/Airframe Trade Off Study: Operational Effects of Increased Freeze Point Fuels," U. S. Air Force Report AFWAL-TR-82-2067, 1982.
9. P. M. McConnell, L. A. Desmarais, F. F. Tolle, and C. L. Delaney, "Operational Effects of Increased Freeze Point Fuels in Military Airplanes," AIAA Paper 83-1139, 1983.
10. A. J. Pasion and I. Thomas, "Preliminary Analysis of Aircraft Fuel Systems for Use with Broadened Specifications Fuels," Boeing Document D6-44538, NASA Contractor Report CR-135198, 1977.
11. L. A. Desmarais and F. F. Tolle, "Fuel Freze Point Investigatioins," Boeing Document D180-28285-1, U. S. Air Force Report AFWAL-TR-84-2049, 1984.
12. R. Svehla, "In Flight Atmospheric and Fuel Tank Temperature Measurements," in "Assessment of Alternative Aircraft Fuels," NASA Conference Publication CP 2307, 1984, pp. 131-139.
13. W. H. Jasperson and G. D. Nastrom, "Temperature Histories of Commercial Flights at Severe Conditions from GASP Data," NASA Contractor Report CR-168247, 1983.
14. I. Thomas, "Broadened Jet Fuel Specifications: Their Effect Upon Commercial Airplane Design and Operation," Shell Aviation News, No. 450, 1978, pp. 32-35.
15. CRC Aviation Group on Low Temperature Flow Performance of Aviation Turbine Fuels, "Low Temperature Behavior of Fuels in Simulated Aircraft Tanks," Coordinating Research Council, Inc., Report No. 532, Atlanta, GA, 1983.
16. R. Friedman and F. J. Stockemer, "Heating Experiments for Flowability Improvement of Near Freezing Aviation Fuel," Journal of Aircraft, Vol. 21, 1984, pp. 250-255.
17. A. J. Pasion, "Design and Evaluation of Aircraft Heat Source Systems for Use with High Freezing Point Fuels," Boeing Document D6-48097, NASA Contractor Report CR-159569, 1979.

APPENDIX A
SUMMARY OF TESTS

This Appendix is a compilation of all useful tests conducted in this study. Tests that were discarded due to malfunctions or inappropriate test conditions are not included. The numbering scheme was intended to correspond to the work plan and started with 401 to facilitate continuous record keeping by NASA-LeRC. To minimize fuel changes, tests falling into different categories but using the same fuel were conducted consecutively. This resulted in test number sequence not being chronological. A few of the test numbers were not used or corresponded to deleted tests.

The compilation indicates test number, date, fuel used, test details, and holdup results with brief remarks. An explanation of some symbols used in the matrix is given below.

1. In column "constant skin temperatures," the programmed temperature is shown in parentheses below the X mark. The same temperature should be assumed for all following tests in the table until a different temperature is shown or unless it is a flight simulation.
2. In column "flight simulation," the symbols in circles have the following meaning:
   - a - Extreme cold day excluding the final warm up, Figure 25
   - a1 - Extreme cold day with prechilling
   - b - Extended cold day, Figure 25
   - b1 - Extended cold day with prechilling
   - c - Extreme cold day including final warm-up, Figure 25
   - d - Modified extreme cold day (5°C lower in the lowest temperature leg), Figure 25
   - e - Reference 12 flight test, Figure 35, both skins on upper skin profile
   - f - Reference 12 flight test, both skins on lower skin profile
   - g - Reference 12 flight test, both skins on separate profiles
   - g1 - Reference 12 flight test, both skins on separate profiles with prechilling
   - h - Reference 12 flight test upper skin modified schedule (with a warm-up phase between 2nd and 3rd hours in flight), Figure 35
3. In column "external heating," "i" designates intermediate rate of heat input (800-900W) and "h" designates highest rate of heat input (1200W).

Summary of Tests (Sheet 1 of 7)

TEST NO.	DATE	FUEL TYPE	TEST DETAILS: STATIC	CONSTANT SKIN TEMPERATURES	VIBRATION	SLOSH	UNWETTED UPPER SURFACE	FLIGHT SIMULATION	RECIRCULATION	EXTERNAL HEATING	FLOW-IMPROVER	CHILL TIME MINUTES	PUMPOUT TIME MINUTES	BULK FUEL TEMPERATURE AT PUMPOUT °C	% MASS HOLDUP	REMARKS
401	(1984) 4-6	LFPA-3	X	X (-52.8)								330	20	-44.1	12.27	Trapped liquid in a stringer bay. Up to 2 [illegible] thick frozen fuel above bottom stringers.
402	5-1	"	X	X								270	20	-43.2	8.34	Trapped liquid in one bay. Up to 1 cm thick frozen fuel above bottom stringers.
403	4-17	"	X	X								188	20	-40.7	4.80	Up to .3 cm thick frozen fuel above bottom stringers.
404	4-19	"	X	X								39	20	- 4.9	0.38	Practically no holdup; a few fuel crystals on stringers.
405	4-19	"	X	X								194	40	-40.4	3.97	Holdup appearance same as 403.
406	4-20	"	X	X								327	40	-44.1	11.86	Holdup appearance same as 401.
407	4-23	"	X	X								271	40	-43.3	4.32	Holdup appearance same as 402.
408	4-24	"	X	X								270	10	-43.3	9.43	Holdup appearance same as 402.
409	4-25	"	X	X								190	10	-40.7	4.91	Holdup appearance same as 403.
410	4-30	"	X	X								333	10	-43.8	13.06	Up to 3 cm thick frozen fuel above bottom stringers.
411	5-4	"		X	X							270	20	-43.2	10.31	Up to 1.5 cm thick frozen fuel above bottom stringers.
412	5-7	"		X	X							331	20	-43.9	11.97	Holdup appearance same as 401.
415	5-14	"	X					X (a)				450	20	-40.6	1.33	Very thin layer of frozen fuel on bottom surface. (415–417)
416	5-16	"	X					X (21)				450	20	-40.5	1.50	
417	5-17	"			X			X (a)				450	20	-41.0	1.19	

Summary of Tests (Sheet 2 of 7)

TEST NO.	DATE	FUEL TYPE	TEST DETAILS: STATIC	CONSTANT SKIN TEMPERATURES	VIBRATION	SLOSH	UNWETTED UPPER SURFACE	FLIGHT SIMULATION	RECIRCULATION	EXTERNAL HEATING	FLOW-IMPROVER	CHILL TIME MINUTES	PUMPOUT TIME MINUTES	BULK FUEL TEMPERATURE AT PUMPOUT °C	% MASS HOLDUP	REMARKS
418	(1984) 5-18	LFPA-3			X			X (a1)				450	20	-40.4	1.32	Very thin layer of frozen fuel on bottom
419	5-24	"	X					X (b)				640	20	-42.3	1.50	surface.
420	5-25	"			X			X (b)				640	20	-41.7	0.66 / 0.74	Holdup result corrected by weighing thawed fuel shown below.
421	5-29	"			X			X (b1)				640	20	-41.7	1.05	
422	5-9	"	X	X (-47.8)								270	20	-40.9	2.04	
423	5-10	"	X	X								330	20	-41.9	2.78	
424	5-11	"	X	X								190	20	-37.3	0.97	
425	5-30	"		X	X							330	20	-42.0	1.34	
426	5-31	"		X	X							270	20	-40.3	1.10	
427	6-1	"	X	X (-52.8)			X					330	20	-40.7	8.84	
428	6-4	"	X	X (-47.8)			X					330	20	-37.0	1.02	
429	6-5	"		X (-52.8)		X	X					330	20	-40.2	8.24	
430	6-6	"		X (-47.8)		X	X					330	20	-36.7	1.07	
431	6-6	"						X (c)				630	20	-36.3	0.16 / 0.00	There was no holdup. Upper result is due to measurement uncertainty.
434	6-12	LFPA-2	X	X (-54.7)								180	20	-41.4	2.61	The fuel left a film on window interior, making visual observations difficult.

Summary of Tests (Sheet 3 of 7)

TEST NO.	DATE	FUEL TYPE	TEST DETAILS: STATIC	CONSTANT SKIN TEMPERATURES	VIBRATION	SLOSH	UNWETTED UPPER SURFACE	FLIGHT SIMULATION	RECIRCULATION	EXTERNAL HEATING	FLOW-IMPROVER	CHILL TIME MINUTES	PUMPOUT TIME MINUTES	BULK FUEL TEMPERATURE AT PUMPOUT °C	% MASS HOLDUP	REMARKS
435	(1984) 6-13	LFPA-2	X	X								300	20	-45.9	6.17	The fuel left a film on window interior
436	6-15	"	X	X								390	20	-47.0	8.29	making visual observations difficult.
437	6-18	"	X	X								100	20	-28.9	0.25 / 0.00	No holdup seen. Upper number is measurement uncertainty.
438	6-19	LFPA-4	X	X (-51.1)								180	20	-37.4	6.72	Up to 1-cm-thick layer of frozen fuel on bottom stringers
439	6-21	"	X	X								225	20	-39.7	11.00	Up to 2-cm-thick layer of frozen fuel on bottom stringers.
440	6-21	"	X	X								55	20	-12.5	0.14 / 0.00	There was no holdup. Upper result is uncertainty in measurements.
441	6-22	"	X	X								120	20	-31.9	2.37	No frozen fuel on stringers.
442	6-25	LFP-9	X	X (-55.0)								180	20	-40.1	4.62	The holdup had smooth, glassy texture.
443	6-26	"	X	X								300	20	-44.8	13.50	About 2-cms-thick frozen fuel on bottom stringers.
444	6-27	"	X	X								240	20	-43.2	9.16	About 0.7-cm-thick frozen fuel on bottom stringers.
445	6-28	"	X	X								80	20	-25.4	0.90	A thin layer of frozen fuel on bottom surface.
446	7-16	LFP-11	X	X (-57.0)								180	20	-40.9	1.95	Windows covered with film, visual observation difficult.
447	7-12	"	X	X								300	20	-45.9	5.83	Up to 0.7-cm-thick holdup on bottom stringers. Frozen fuel appeared very grainy.
448	7-13	"	X	X								420	20	-48.1	7.59	Up to 1-cm-thick holdup on bottom stringers with grainy texture.
449	7-17	"	X	X								105	20	-28.9	0.39	Small holdup, very thin layer of frozen fuel on bottom surface.

Summary of Tests (Sheet 4 of 7)

TEST No	DATE	FUEL TYPE	TEST DETAILS: STATIC	CONSTANT SKIN TEMPERATURES	VIBRATION	SLOSH	UNWETTED UPPER SURFACE	FLIGHT SIMULATION	RECIRCULATION	EXTERNAL HEATING	FLOW-IMPROVER	CHILL TIME MINUTES	PUMPOUT TIME MINUTES	BULK FUEL TEMPERATURE AT PUMPOUT °C	% MASS HOLDUP	REMARKS
450	(1984) 8-27	LFPA-3	X	X (-52.8)			X					330	20	-41.0	8.29	No trapped liquid visible, about 0.3 cm thick frozen fuel on bottom stringers.
451	8-29	"		X		X	X					330	20	-41.6	8.54	Same holdup as 450.
452	8-15	LFPA-1	X	X (-57.1)								240	20	-46.8	3.98	No frozen fuel on bottom stringers. Slightly grainy appearance.
453	8-16	"	X	X								420	20	-50.0	6.93	Some frozen fuel on top of bottom stringers.
454	8-17	"	X	X								105	20	-32.7	0.93	Slight holdup was visible.
455	8-20	"	X	X								540	20	-50.3	9.86	1.2-cm-thick layer of frozen fuel on bottom stringers.
456	8-21	"	X	X (-49.0)								240	20	-40.1	0.41	Almost no holdup.
457	8-9	LFPA-4	X	X (-49.0)								240	20	-38.5	5.83	A thin layer of frozen fuel on bottom stringers.
458	8-22	LFPA-1	X					X ⓐ				450	20	-40.0	0.69 / 0.33	Very small holdup. Lower number based on thawed fuel weighing.
459	9-13	LFPA-4	X					X ⓐ				450	20	-39.7	4.98	Up to 0.2-cm-thick frozen fuel on top of bottom stringers.
460	8-23	LFPA-1	X					X ⓓ				450	20	-43.1	0.47	No holdup was visible.
461	8-30	LFPA-3	X					X ⓓ				450	20	-42.8	6.05	Up to 0.4-cm-thick frozen fuel on bottom stringers.
462	7-25	LFP-11	X					X ⓔ				410	20	-31.4	0.38	Almost no holdup. Heavy film on windows.
463	7-26	"	X					X ⓕ				410	20	-28.8	0.36	Almost no holdup. A brown patch observed on the bottom surface.
464	7-27	"	X					X ⓖ				410	20	-30.6	0.15 / 0.23	No visible holdup, small quantity of liquid at bottom. Lower result from thawed fuel.

Summary of Tests (Sheet 5 of 7)

TEST NO.	DATE	FUEL TYPE	TEST DETAILS: STATIC	CONSTANT SKIN TEMPERATURES	VIBRATION	SLOSH	UNWETTED UPPER SURFACE	FLIGHT SIMULATION	RECIRCULATION	EXTERNAL HEATING	FLOW-IMPROVER	CHILL TIME MINUTES	PUMPOUT TIME MINUTES	BULK FUEL TEMPERATURE AT PUMPOUT °C	% MASS HOLDUP	REMARKS
455	(1984) 7-31	LFPA-4	X					X (g)				410	20	-31.3	0.44	
466	8-3	"	X				X	X (g)				410	20	-26.2	0.40	Almost no holdup. About 0.4 kg thawed
467	8-6	"				X	X	X (c)				410	20	-26.4	0.58	fuel obtained in each test. Small differences seen are due to measurement
468	8-7	"				X	X	X (e)				410	20	-27.8	0.10 / 0.23	uncertainties.
469	8-8	"	X					X (h)				410	20	-28.8	0.30	
474	9-10	"	X					X (a)	X			450	20	-33.4	1.25	Small holdup on the bottom surface.
476	9-14	"	X					X (a)	X	X i		450	20	-29.8	1.07	Thin layer of frozen fuel at the bottom.
477	9-5	"	X					X (a)	X	X h		450	20	-26.8	0.67	Very thin layer of frozen fuel on the bottom.
478	10-3	LFPA-1	X					X (a)	X			450	20	-33.6	0.39	Small holdup, some frozen fuel crystals on stringers and bottom of tank.
479	10-4	"	X					X (a)	X			450	20	-33.6	0.49	Small holdup similar to 478.
480	10-9	"	X					X (a)	X			450	20	-33.6	0.48	Small holdup similar to 478.
482	9-25	LFPA-4	X					X (a)	X			450	20	-33.8	1.28	Same holdup as 474.
483	9-26	"	X					X (a)	X	X h		450	20	-27.0	0.50	Very small holdup on bottom.
484	9-24	"	X					X (a)	X			450	20	-34.5	1.69	Some frozen fuel at the bottom and walls of stringers.
485	9-19	"	X					X (a)	X	X h		450	20	-28.0	0.83	Very small holdup at the bottom.

Summary of Tests (Sheet 6 of 7)

TEST NO.	DATE	FUEL TYPE	TEST DETAILS: STATIC	CONSTANT SKIN TEMPERATURES	VIBRATION	SLOSH	UNWETTED UPPER SURFACE	FLIGHT SIMULATION	RECIRCULATION	EXTERNAL HEATING	FLOW-IMPROVER	CHILL TIME MINUTES	PUMPOUT TIME MINUTES	BULK FUEL TEMPERATURE AT PUMPOUT °C	% MASS HOLDUP	REMARKS
486	(1984) 10-10	LFPA-1	X	X (-56.0)								360	20	-48.5	2.50	Frozen fuel coarse in appearance, mostly on bottom surface.
487	10-11	"	X	X					X	X h		360	20	-33.2	0.78	Small holdup, mostly a thin layer of
488	10-12	"	X	X					X			360	20	-41.6	0.95	frozen fuel at bottom.
489	10-15	"	X	X (-56.0)					X	X i		360	20	-34.8	0.97	Scattered fuel crystals and a thin, clear layer at the bottom.
490	9-27	LFPA-4	X	X (-51.1)								210	20	-39.4	9.58	Up to 1-cm-thick frozen fuel layer on top of bottom stringers.
491	9-28	"	X	X					X	X h		210	20	-29.0	1.28	Thin layer of frozen fuel at bottom and on stringers.
492	10-18	"	X	X					X			210	20	-33.7	1.73	Small holdups similar to previous cases.
493	10-19	"	X	X					X	X i		210	20	-29.0	1.40	
494	10-24	"	X									210	20	-39.7	8.58	About .8-cm-thick frozen fuel on top of bottom stringers.
495	10-25	"	X						X	X h		210	20	-28.7	1.07	
496	10-29	"	X	X					X	X i		210	20	-33.9	2.00	Small holdups similar to previous cases.
497	10-22	"		X	X				X	X i		210	20	-30.2	1.50	
498	10-23	"		X		X	X		X	X i		210	20	-22.9	0.40	
499	11-7	"	X					X (91)				410	20	-30.0	0.86 / 0.17	Almost no holdup. Lower number based on thawed fuel quantity.
502	11-8	LFPA-4	X	X (-51.1)							X	60	20	-14.0	0.80	Very small holdup with bubbly appearance.

Summary of Tests (Sheet 7 of 7)

TEST NO.	DATE	FUEL TYPE	TEST DETAILS												REMARKS
			STATIC	CONSTANT SKIN TEMPERATURES	VIBRATION	SLOSH	UNWETTED UPPER SURFACE	FLIGHT SIMULATION	RECIRCULATION	EXTERNAL HEATING	FLOW-IMPROVER	CHILL TIME MINUTES	PUMPOUT TIME MINUTES	BULK FUEL TEMPERATURE AT PUMPOUT °C	% MASS HOLDUP	
503	(1984) 11-9	LFPA-4	X	X							X	120	20	-31.6	1.67	Thin layer of frozen fuel at bottom and on stringer walls.
504	11-14	"	X	X (-51.1)							X	180	20	-37.7	4.32	Up to .3-cm-thick layer on bottom stringers.
505	11-13	"	X	X							X	225	20	-39.8	7.62	Up to 0.7-cm-thick layer on top of bottom stringers.
506	12-10	LFPA-1	X	X (-56.0)							X	105	20	-27.7	0.63	Very small holdup at bottom.
507	12-11	"	X	X							X	540	20	-49.7	3.52	Small to moderate holdup similar to previous cases. (507–509)
508	12-12	"	X	X							X	240	20	-44.6	1.11	
509	12-13	"	X	X							X	420	20	-49.2	3.05	
510	11-15	LFPA-4		X		X	X				X	180	20	-35.9	3.22	Thin film and lumps on stringers, most holdup at bottom.
511	11-16	"	X					X @			X	450	20	-38.9	1.72	Grainy texture, light holdup.
512	11-19	"	X					X @	X	X i	X	450	20	-25.1	1.07 / 0.55	No visible holdup. Lower number based on thawed fuel quantity.
513	11-20	"	X					X @	X		X	450	20	-29.9	0.89	Small holdup, mainly thin layer at bottom.
514	11-27	"	X	X (-47.6)							X	120	20	-27.3	0.38	Almost no holdup, very thin layer at bottom.
515	11-28	"	X	X (-49.0)							X	240	40	-39.2	4.10	Frozen fuel at bottom and on stringers.Gravity drain instead of pumpout due to pump failure.

APPENDIX B

Comparision of Holdup Results Using Two Methods of Measurements

The following pages list holdup results using two methods of measurements. In the first method, the fuel quantities at the start of a test, before the pumpout, and after the pumpout in the simulator test tank were determined using a weigh tank and load cell arrangement. These measurements were recorded by the data monitoring system. The second method involved extracting the thawed fuel by gravity drain following an overnight warming of test tank after a test, and manually weighing it on a precision scale. To calculate the holdup percentage, the fuel quantity in the test tank before the pumpout was still obtained from the load cell measurements. The second method was initiated with test 411 and followed thereafter for each test.

Comparison of holdup measurements

Test no.	Date (1984)	Holdup measured by load cell		Holdup measured by weighing thawed fuel	
		kg	%	kg	%
411	5-4	17.77	10.31	17.67	10.26
412	5-7	20.59	11.97	20.38	11.85
415	5-14	2.29	1.33	1.83	1.06
416	5-16	2.60	1.50	2.17	1.25
417	5-17	2.04	1.19	1.84	1.07
418	5-18	2.27	1.32	1.83	1.06
419	5-24	2.59	1.50	2.06	1.19
420	5-26	1.14	0.66	1.27	0.74
421	5-29	1.80	1.05	1.40	0.82
422	5-9	3.51	2.04	2.96	1.72
423	5-10	4.79	2.78	3.91	2.27
424	5-11	1.67	0.97	1.48	0.86
425	5-30	2.31	1.34	2.27	1.32
426	5-31	1.90	1.10	1.85	1.07
427	6-1	10.27	8.84	10.05	8.65
428	6-4	1.17	1.02	0.86	0.75
429	6-5	9.48	8.24	9.33	8.11
430	6-6	1.23	1.07	0.99	0.86
431	6-8	0.27	0.16	0	0
434	6-12	4.53	2.61	4.22	2.43
435	6-13	10.76	6.17	10.36	5.94
436	6-15	14.52	8.29	14.41	8.23
437	6-18	0.44	0.25	0	0
438	6-19	11.60	6.72	11.44	6.63
439	6-21	19.22	11.00	19.03	10.89
440	6-21	0.24	0.14	0	0
441	6-22	4.09	2.37	4.18	2.42
442	6-25	8.18	4.62	8.03	4.53
443	6-26	24.00	13.50	23.07	12.97
444	6-27	16.34	9.16	15.69	8.80
445	6-28	1.55	0.90	1.21	0.70
446	7-16	3.49	1.95	3.32	1.86
447	7-12	10.5	5.83	10.21	5.67
448	7-13	13.68	7.59	13.55	7.52
449	7-17	0.69	0.39	0.54	0.30
450	8-27	13.13	8.29	11.96	7.55
451	8-29	13.52	8.54	13.73	8.67
452	8-15	6.94	3.98	6.81	3.90
453	8-16	12.06	6.93	11.60	6.66
454	8-17	1.60	0.33	1.39	0.81
455	8-20	17.30	9.86	16.76	9.55
456	8-21	0.72	0.41	0.53	0.30
457	8-9	9.99	5.83	9.82	5.73
458	8-22	1.19	0.69	0.56	0.33
459	9-13	8.57	5.00	8.63	5.04
460	8-23	0.81	0.47	0.60	0.35
461	8-30	10.43	6.05	10.23	5.97
462	7-25	0.68	0.38	0.42	0.27
463	7-26	0.64	0.36	0.49	0.28

Comparison of holdup measurements

Test no.	Date (1984)	Holdup measured by load cell		Holdup measured by weighing thawed fuel	
		kg	%	kg	%
464	7-27	0.26	0.15	0.39	0.23
465	7-31	0.75	0.44	0.64	0.38
466	8-3	0.59	0.40	0.42	0.28
467	8-6	0.84	0.58	0.42	0.29
468	8-7	0.16	0.10	0.37	0.23
469	8-8	0.50	0.30	0.43	0.26
474	9-10	2.13	1.25	2.10	1.23
476	9-14	1.82	1.07	1.60	0.94
477	9-5	(3.44	1.89)*	1.22	0.67
478	10-3	(1.54	0.89)*	0.67	0.39
479	10-4	0.84	0.49	0.61	0.35
480	10-9	0.82	0.48	0.64	0.38
482	9-25	2.19	1.28	1.82	1.06
483	9-26	0.85	0.50	0.87	0.51
484	9-24	2.90	1.69	2.49	1.45
485	9-19	1.43	0.83	0.87	0.51
486	10-10	4.38	2.50	3.49	2.00
487	10-11	1.36	0.78	1.20	0.69
488	10-12	1.66	0.95	1.40	0.8
489	10-15	1.70	0.97	1.23	0.70
490	9-27	16.44	9.58	16.42	9.57
491	9-28	2.16	1.28	2.63	1.56
492	10-18	2.96	1.73	2.67	1.56
493	10-19	2.38	1.40	1.82	1.07
494	10-24	14.80	8.58	14.15	8.20
495	10-25	1.81	1.07	1.69	1.00
496	10-29	3.42	2.00	3.21	1.88
497	10-22	2.54	1.50	2.00	1.18
498	10-23	0.64	0.40	0.86	0.54
499	11-7	1.36	0.86	0.26	0.17
502	11-8	1.34	0.80	0.73	0.43
503	11-9	2.86	1.67	2.32	1.36
504	11-14	7.45	4.32	6.92	4.01
505	11-13	13.1	7.62	12.53	7.29
506	12-10	1.09	0.63	0.61	0.35
507	12-11	6.18	3.52	5.97	3.40
508	12-12	1.94	1.11	1.66	0.95
509	12-13	5.35	3.05	4.95	2.82
510	11-15	5.1	3.22	5.52	3.49
511	11-16	3.0	1.72	2.73	1.57
512	11-19	1.83	1.07	0.94	0.55
513	11-20	1.53	0.89	0.93	0.55
514	11-27	0.66	0.38	0.48	0.27
515	11-28	7.86	4.10	6.70	3.50

*For these tests, the difference in holdup between the two methods exceeded the experimental uncertainty. The load cell measurements were discarded, and instead, the results of second method were reported and used in discussions.

1. Report No.	2. Government Accession No.	3. Recipient's Catalog No.
NASA CR-174938		

4. Title and Subtitle	5. Report Date
Detailed Studies of Aviation Fuel Flowability	JUNE, 1985
	6. Performing Organization Code
7. Author(s)	8. Performing Organization Report No.
H. K. Mehta and R. S. Armstrong	D6-52990
9. Performing Organization Name and Address	10. Work Unit No.
Boeing Commercial Airplane Company P.O. Box 3707 Seattle, WA 98124	11. Contract or Grant No. NAS 3-24081
	13. Type of Report and Period Covered Final Report
12. Sponsoring Agency Name and Address National Aeronautics and Space Administration Washington, DC 20546	14. Sponsoring Agency Code 505-40-22

15. Supplementary Notes

Final Report. Project Manager, Robert Friedman, Aeropropulsion Facilities and Experiments Division, Cleveland, Ohio 44135.

16. Abstract

Six Jet A fuels, with varying compositions, were tested for low temperature flowability in a 190-liter simulator tank that modeled a section of a wing tank of a wide-body commercial airplane. The insulated tank was chilled by circulating coolant through the upper and lower surfaces. Flowability was determined as a function of fuel temperature by holdup, the fraction of unflowable fuel remaining in the tank after otherwise complete withdrawal. In static tests with subfreezing tank conditions, holdup varied with temperature and fuel composition. However, a general correlation of two or three classes of fuel type was obtained by plotting holdup as a function of the difference between freezing point and boundary-layer temperature, measured 0.6 cm above the bottom tank surface. Dynamic conditions of vibrations and slosh or rate of fuel withdrawal had very minor effects on holdup. Tests with cooling scheduled to represent extreme, cold-day flights showed, at most, slight holdup for any combination of fuel type or dynamic conditions. Tests that superimposed external fuel heating and recirculation during the cooldown period indicated reduced holdup by modification of the low-temperature boundary layer. Fuel heating was just as effective when initiated during the later times of the tests as when applied continuously. The use of flow-improving additives showed promise in holdup reduction, but the selected additives were not necessarily optimized for jet fuel improvement.

17. Key Words (Suggested by Author(s))	18. Distribution Statement
Fuels Aircraft Fuels Jet Fuels Fuel Freezing Point Aircraft Fuel Systems Flow Improvers	Unclassified - Unlimited STAR Category 28

19. Security Classif. (of this report)	20. Security Classif. (of this page)	21. No. of Pages	22. Price
Unclassified	Unclassified	89	

FORM 00005

For sale by the National Technical Information Service, Springfield, Virginia 22161